Quaternary Geomorphology, Stratigraphy, and Paleoclimate of the central Southern Alps, South Island, New Zealand

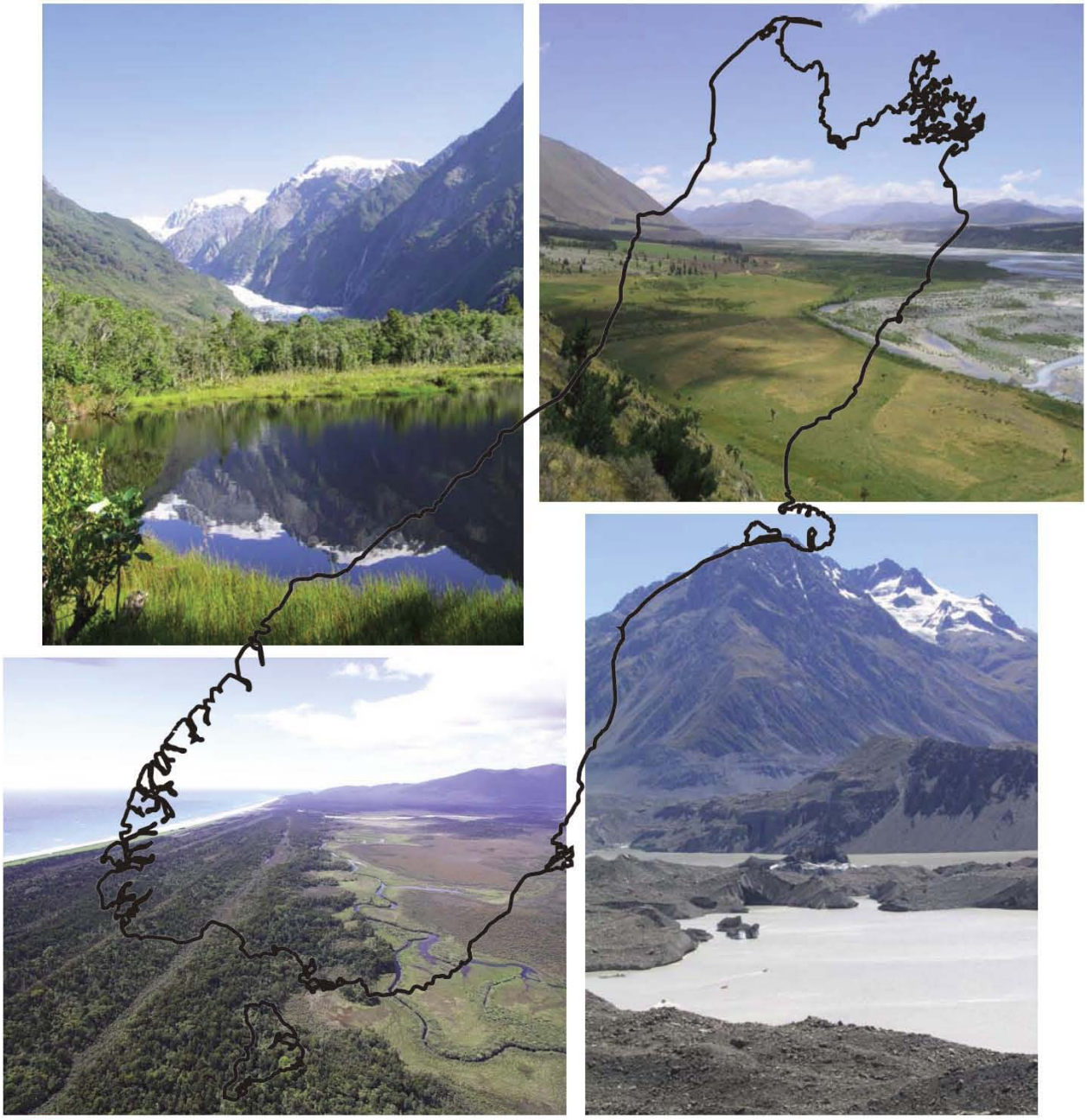

INQUA 2007 Post Conference Field Trip

Authors: Peter Almond, David Barrell, Olivia Hyatt, Henrik Rother, James Shulmeister & Marcus Vandergoes

Editor & Compiler: Olivia Hyatt

ISBN 978-0-86476-189-7

Published by Lincoln University
PO Box 84, Lincoln 7647,
Canterbury,
New Zealand

Authors and Leaders: Peter C. Almond, *Agriculture and Life Sciences Division, Lincoln University, Canterbury, NZ.*
David J.A. Barrell, *GNS Science, Dunedin, NZ.*
Olivia M. Hyatt, *Department of Geological Sciences, University of Canterbury, Christchurch, NZ.*
Henrik Rother, *ANSTO, Institute for Environmental Research, Menai, NSW, Australia.*
James Shulmeister, *Department of Geological Sciences, University of Canterbury, Christchurch, NZ.*
Marcus J. Vandergoes, *GNS Science, Lower Hutt, NZ.*

Organisers: Peter C. Almond.
Fiona L. Shanhun, *Agriculture and Life Sciences Division, Lincoln University, Canterbury, NZ.*

Editor & Compiler: Olivia M. Hyatt.

Cover images, Jamie Shulmeister, Olivia Hyatt and Andrew Wells

Contents

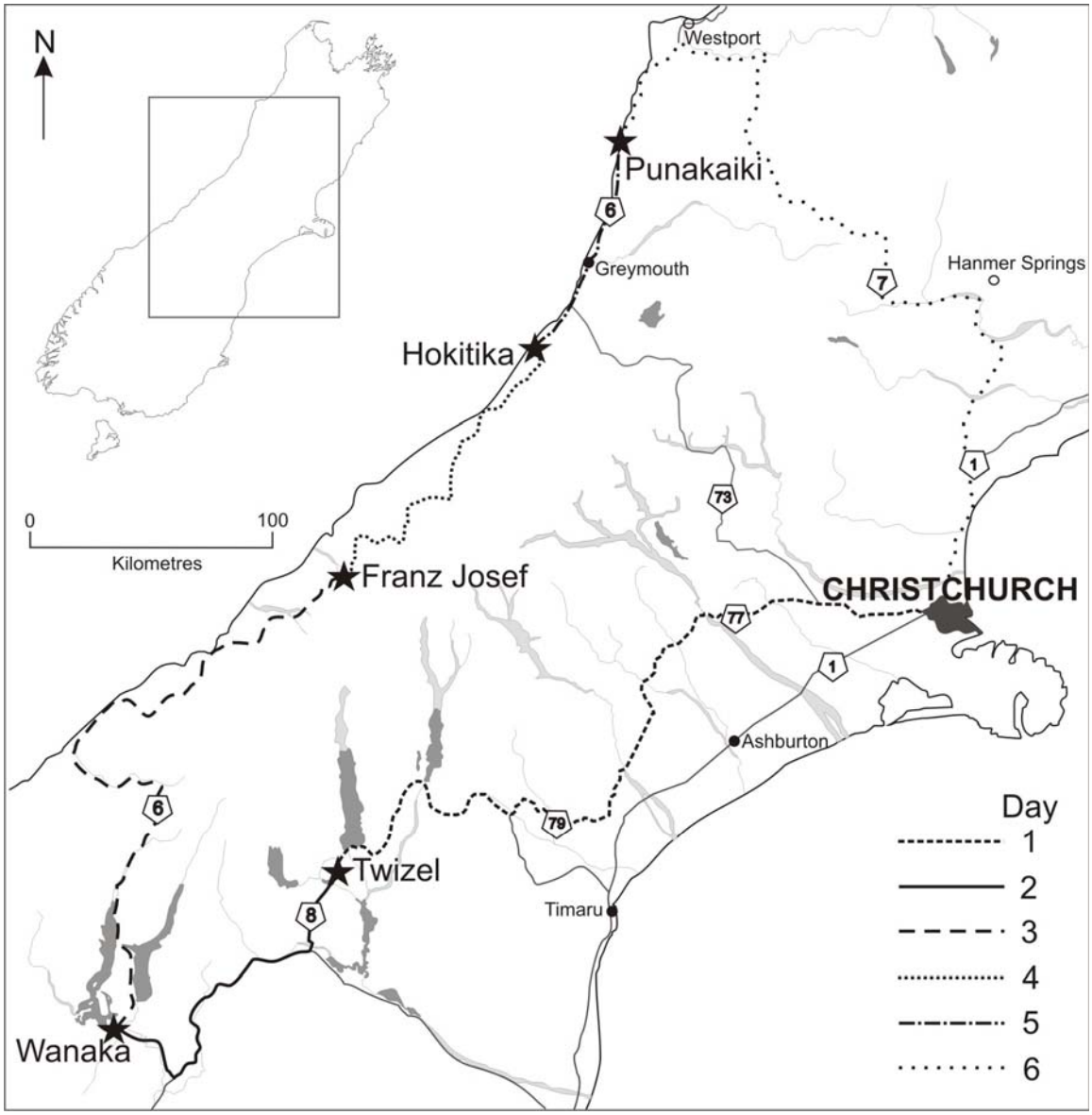

Introduction (Almond and Barrell)

New Zealand's Southern Alps and South America's Andes provide the two locations where mountain chains are high enough to intercept the roaring forties above permanent snow line. Consequently a full suite of glacial erosion and sedimentary features are preserved, ranging in age from 19th century "Little Ice Age" to mid Pleistocene. We will see spectacular examples of glacial landforms upon which a wide range of analytical procedures have been applied, and all set in some of the most spectacular alpine scenery in the world. To the east of the Alps repeated glacial advances have excavated 9 large finger lakes with well exposed terminal and lateral moraine belts and broad plains of coalescing outwash fans. Drainage from these continues off shore into the Bounty Trough with thick glacial sediment sequences interbedding with interglacial carbonate oozes. The generally dry nature of the inland basins has restricted vegetation cover, resulting in spectacular exposure of the glacial landscape. To the west glacial landforms are preserved on a narrow piedmont between the range bounding Alpine Fault in the SE and the Tasman Sea in the NW. On parts of the piedmont that are uplifting a succession of glacial landforms have been truncated by interglacial coastal erosion, and glacial deposits interfinger with marine deposits. In areas without tectonic uplift unravelling the stratigraphy has proved much more difficult. Despite Westland having some of the highest rainfalls in the world, loess has been produced from outwash surfaces and now its soil and tephra stratigraphy are an important chronological and correlation tool. Participants will see key sites upon which a variety of stratigraphic and geochronological techniques have been applied and will participate in on going debate concerning the interpretation of New Zealand's glacial record.

On our first day we leave Christchurch and travel inland to the eastern front range of the Southern Alps, venturing into the Rakaia valley. Here we will see spectacular examples of glacial landforms, glacial sedimentology, and post glacial valley modification. After leaving the Rakaia Valley we follow the foot of ranges southwards to the McKenzie Basin, a tectonic depression adjacent to the highest peaks in

the Southern Alps. Twizel is our stop for the night. Day 2, we backtrack slightly and head up the southern flank of Lake Pukaki, one of the large finger lakes described above, to Mt Cook village, seeing glacial features ranging from Last Glacial Maximum to latest Holocene in age, as well as present-day glaciers. From Mt Cook village we retrace our steps to Twizel and continue south to the driest and most continental region of New Zealand, Central Otago. We stay on the shores of Lake Wanaka for the night of Day 2. Day 3 takes us from the dry climates of Central Otago to the wet, forest cloaked landscape of the West Coast via the Haast Pass over the Southern Alps. This day involves soils, Holocene coastal geomorphology, marine terraces and late glacial moraines. The day ends in the township of Franz Josef. Day 4 starts with a plane flight for those with the inclination or a trip up to see the Franz Josef glacier. Afterwards we travel to Okarito Bog, the site of a splendid pollen record spanning the complete last glacial cycle, then head north to Hokitika. On the way we stop to discuss last glacial maximum moraines in the Poerua valley, and the effects of a recent large landslide on the landscape and people of the valley. The area around Hokitika is the focus of the next day when we review the classic glacial geomorphology of the Hokitika-Taramakau systems. The final part of the day takes us to Punakaiki on the western flanks of the Paparoa Range. On day 6 we continue north, stopping briefly near Westport to discuss a well studied peat section on a marine terrace of Cape Foulwind, then head through the Buller Gorge to the Inangahua Valley. We then turn south again to re-cross the Southern Alps over the Lewis Pass. Our final stop of the tour before Christchurch is in the Hope Valley.

The central part of South Island of New Zealand is, for the most part, thinly populated. Population is concentrated in the city of Christchurch, and to a much lesser extent in Timaru. Elsewhere, the lowland areas are rural with scattered townships servicing the agriculture or tourism industries. The central South Island landscape is dominated by mountains, but includes cultivated plains, terraces and downlands, grassed or forested hills and ranges. The region is crossed by the Alpine Fault, a major active fault on which most of the ongoing movement between the Australian Plate (to the northwest) and the Pacific Plate (to the southeast) is concentrated.

The plate boundary developed in the early Miocene. Since then, right-lateral horizontal movement on the Alpine Fault has offset older basement rocks in the South Island by 480 km (e.g. Turnbull 2000; Forsyth 2001; Nathan, Rattenbury et al. 2002; Rattenbury, Townsend et al. 2006; e.g. Cox and Barrell in press 2007). Northwest of the Alpine Fault, basement rock consists of well-indurated Paleozoic to Mesozoic sedimentary, metamorphic and plutonic rocks that were originally part of the Gondwanaland supercontinent (Fig. 1). Southeast of the Alpine Fault, the basement rock is predominantly of a classic 'greywacke' type, dominated by indurated, fractured, grey sandstones but including a diverse range of interbbedded mudstones (argillite), sandstones, minor conglomerates and volcanogenic sediments. These rocks, largely comprising the Torlesse Terrane but including Caples Terrane towards the southwest, were deposited and accreted to Gondwanaland during the Carboniferous to Early Cretaceous. Parts of this terrane have been metamorphosed into semischist or schist, particularly in the area southwest of the Waitaki valley. Non-marine Cretaceous sedimentary rocks and mid-Cretaceous volcanic and shallow intrusive rocks occur in the Canterbury foothills and in places beneath the Canterbury Plains.

Basement rocks on both sides of the Alpine Fault were largely covered with a blanket of predominantly marine Late Cretaceous to Pliocene sedimentary rocks, with localised occurrences of volcanic rocks. Development of the plate boundary during the late Cenozoic was accompanied by widespread faulting and folding that deformed the basement and overlying cover, and resulted in uplift and the formation of mountains. The Late Cretaceous to Pliocene sequence was mostly eroded from the uplifted areas but has been preserved beneath inland basins, Canterbury Plains and offshore. Localised basaltic volcanism occurred in the Timaru and Geraldine area in the Late Pliocene.

During the Quaternary, geological processes and the evolution of landscapes were greatly influenced by global, cycles of warmer (interglacial) and colder (glacial) climate operating on 100,000 and 40,000 year time scales. There are isolated remnants of uplifted coastal and shallow marine interglacial sediments in South Westland. Widespread accelerated erosion on mountain slopes during glaciations overwhelmed rivers with sediment resulting in synchronous aggradation of most rivers draining the axial ranges. The aggrading rivers formed broad alluvial fans that provided large source areas for loess. Tephrastratigraphy and dating has shown aggradation gravels and loess packages to be broadly coeval. The most recent major cold period (Last Glacial Maximum or LGM) began about 30 000 years ago and ended abruptly about 18 000 years ago with the rapid retreat of glaciers. Climates warmed towards interglacial conditions, apart from a short interlude somewhere between 11 400 and 14 000 years ago when some glaciers re-advanced. Glaciers now occur only near the highest parts of the Southern Alps, and in the last few thousand years have undergone many episodes of minor advance and retreat (e.g. see Alloway et al. 2007; for overview and references). Sediment deposition in coastal and offshore areas has been influenced by large fluctuations in sea level due to glacial/interglacial climate cycles. Sea level was at least 120 m below present during the LGM, but later rose very rapidly, reaching its present level about 7 000 years ago. Cliff erosion is widespread along the modern coastline.

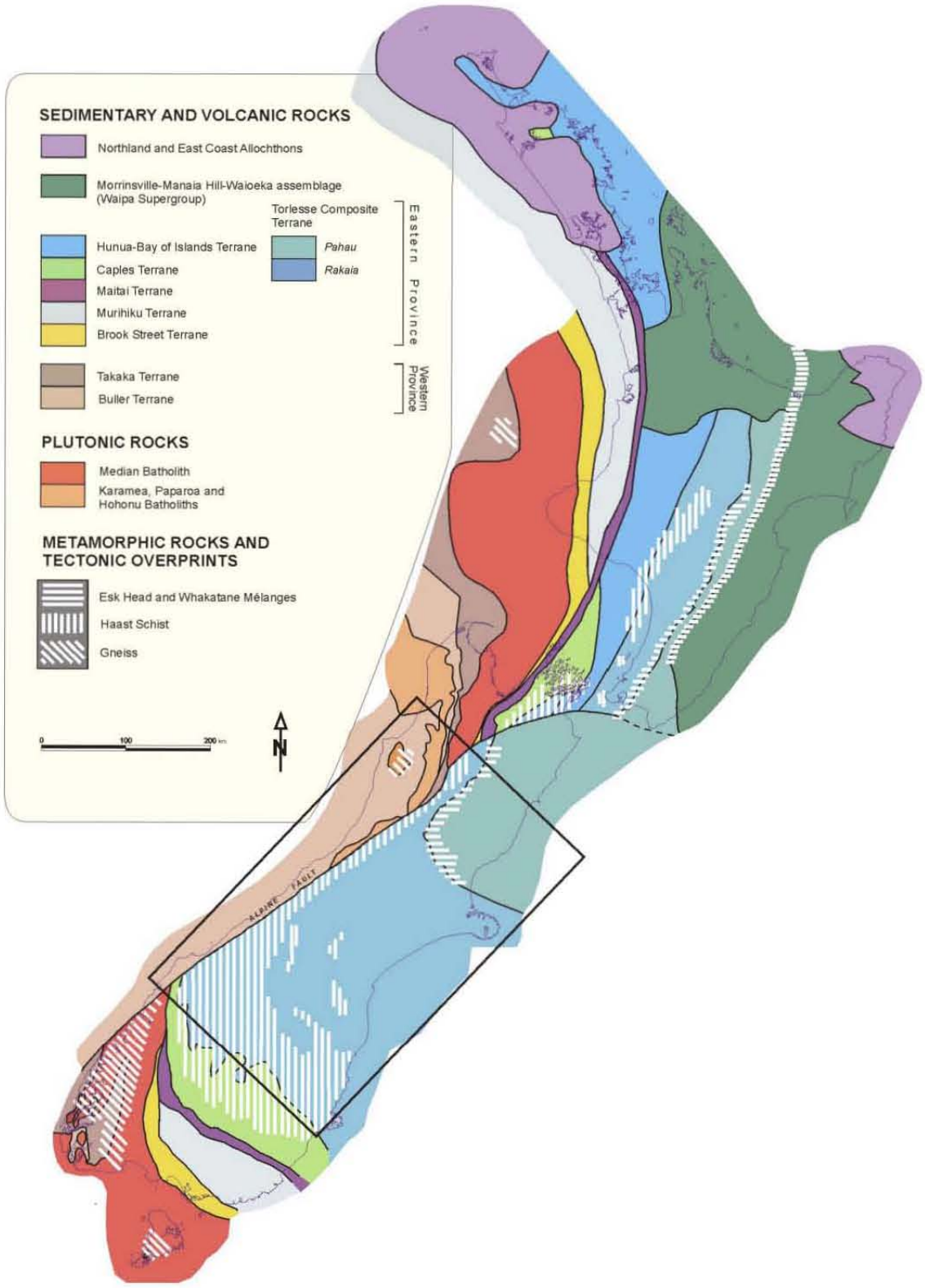

Figure 1. Pre-Cenozoic basement rocks of New Zealand, subdivided into tectonostratigraphic terranes; the extent of the Northland and East Coast allochthons is also shown. Late Cretaceous to Cenozoic sedimentary and volcanic cover rocks and Quaternary sediments are omitted. The Central South Island region is indicated by the rectangle. (Adapted from Mortimer, 2004).

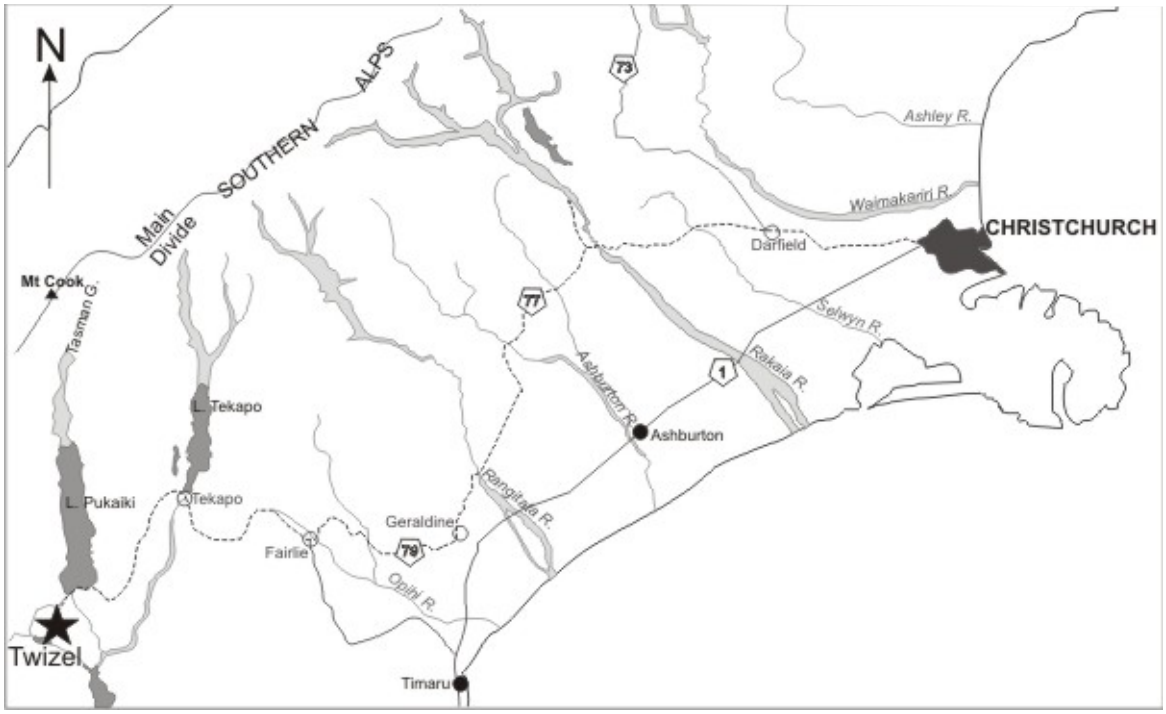

DAY 1. Christchurch to Twizel, with stops in the Rakaia Valley and Mackenzie Basin (Shumeister, Hyatt and Barrell)

Travel west inland from Christchurch on highway 73 to Darfield then turn onto Bangor Road. Turn left onto highway 77 and follow for about 7km.

Christchurch to Glentunnel

From Christchurch up to the Rakaia Gorge we will drive across the Canterbury Plains. The Canterbury Plains are the product of the coalesced alluvial fans of the major glacially fed rivers that debouche from the Southern Alps. The major rivers contributing to the Plains are from north to south, the Waimakariri, the Rakaia and the Rangitata. Extensive glaciation occurred in the headwaters of each of these systems. Smaller rivers such as the Selwyn occupy the inter fan troughs between the coalescing fans. These smaller rivers had variable but limited amounts of glaciation in their headwaters as they do not extend as far into the main ranges.

The plains themselves are roughly 175 km x 50 km in extent and trend NNE to SSW. The gravels of the plains extend a further 40-50 km offshore (Fig 2). Offshore and along the coastal section of the plains, the fan gravels are interfingered at depth by wedges of fine sediments of marine and estuarine provenance, separating the gravels neatly into both sea-level and consequently isotope-stage-defined packages (e.g. Browne and Naish, 2003). Onshore the fine sediment wedges peter out within a few kilometres of the coast and undifferentiated fan gravels up to 1km thick underlie the plains. Christchurch city itself straddles this transition. Much of the downtown and eastern suburbs are constructed on a Holocene progradation wedge termed the Christchurch Formation (Formation names follow Brown and Wilson, 1988) and are composed of a mix of fluvial, aeolian, back barrier swamp and estuarine sediments. Inland a series of floodplain and river terrace surfaces are visible. Holocene gravels of the Springston Formation create the lower terraces and modern floodplains along the tracks of the major rivers (the Waimakariri and Rakaia) and predominate in the near-coastal reaches. Further inland the rivers are incised within the last glacial aggradation fan of OIS 2. Traditionally, geologists have subdivided these aggradation deposits into a younger set (Burnham Formation) and an older set (Windwhistle Formation) (e.g. Suggate 1963, 1965, 1973; Wilson 1989). The two cannot to be differentiated in the subsurface in water wells (Brown and Wilson 1988). Previous workers generally correlated the surface of the Windwhistle Formation with the glacial episode during Marine Oxygen Isotope Stage (MIS) 4, and the Burnham Formation with MIS 2. Regional-scale reassessment of the mapping of these formations (e.g. Cox & Barrell 2007 – in press), including the characteristics of soils developed on them, has found that much of what has previously been mapped as Windwhistle Formation is not significantly different in age from Burnham Formation. On the Canterbury Plains surface, with few exceptions, Windwhistle deposits are becoming generally regarded as an early phase of deposition within the Last Glacial Maximum (LGM).

Critical to understanding the relationship between the terraces surfaces on the plains and the fluvial and glacial systems that created them is the convergence of the Holocene Springston Formation with the glacial aggradation gravels of the Burnham/Windwhistle Formation. What this demonstrates is that fan slopes were significantly steeper during glacial times and it represents the effects of greater sediment supply and changed base-levels when glaciers reached the edge of the plains (Leckie 1996). This will be quite easily observable from our first geological stop – at the Gorge Road outlook over the Rakaia.

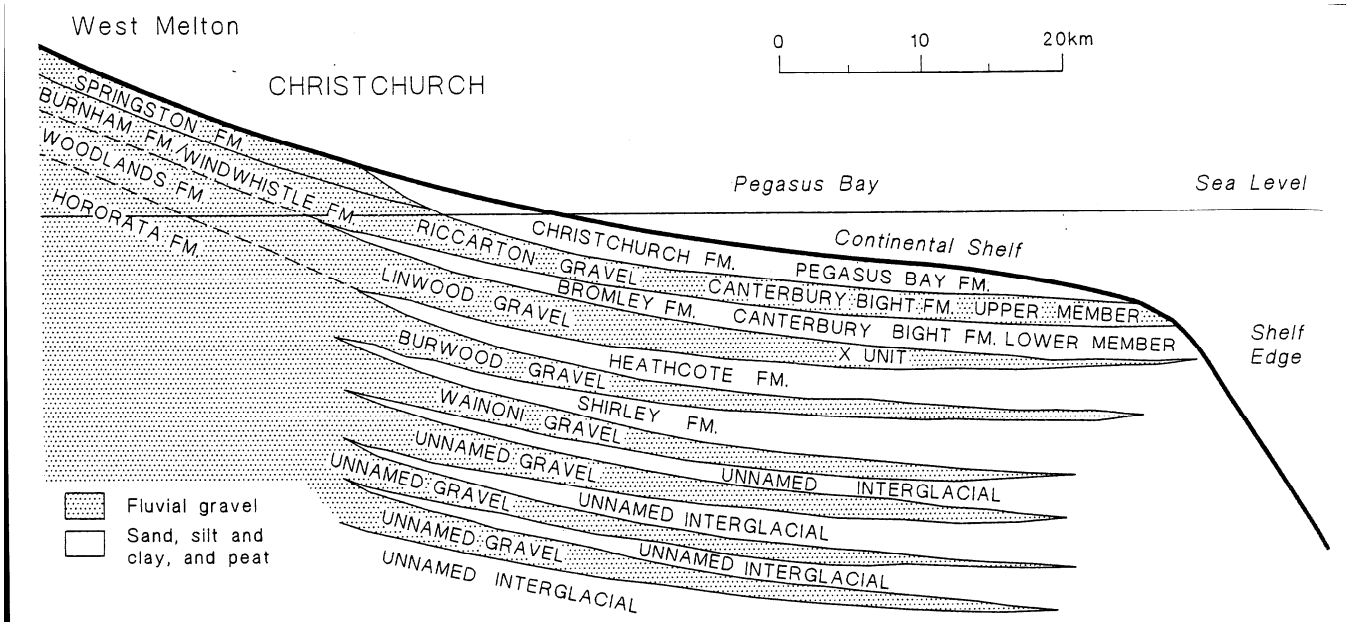

Fig 2. Gravel formations of the Canterbury Plain (from Brown and Weeber, 1992). Note that there are seven distinct wedges visible in the coastal and marine sections of the record separated from each other by fine sediments. Inland no such separation of the gravels occurs. *Copyright and courtesey of GNS Science.*

From Glentunnel follow highway 77 west.

Glentunnel to Rakaia Gorge

Beyond Glentunnel we pass down a narrow valley between a basalt ridge to the south and the foothills of the Southern Alps to the north which are comprised mainly of greywackes. The northern flanks of the basalt ridge are underlain by Cenozoic shallow water marine sediments. At the Glentunnel end there is no direct evidence of glaciation. By the Glenroy end there is clearer evidence of ice overrun. No terminal position is apparent. In between, the valley floor is flat and underlain by lake sediments. At least 20 m of lake sediments are preserved but are unfossiliferous. The age of the lake is currently unknown and its origin may be pro-glacial, or perhaps the result of ponding due to coalescing alluvial fans.

After Glenroy we are well within the limits of maximum Rakaia glaciation. The glacial sequence of the Rakaia was defined by Soons (1963) and Soons and Gullentops (1973), on the basis of relationships between outwash gravels and moraine sequences. Put simply, younger glaciations nest within larger older glaciations. Each glacial advance is marked by a terrace riser with moraine extending immediately downstream of the riser, giving way to outwash gravels further down valley. A complex pattern of avulsing drainage systems and interglacial incision complicates observing the relationships but we start on rolling hills of the Hororata Formation before stepping down to the Woodlands Formation and then down to Tui Creek. The Hororata Formation is a catch all for all pre-OIS 6 advances. No terminus is identified and other than low rolling relief it is unremarkable. All the younger advances have at least one recognizable terminal position.

Turn off highway 77 on the left down a short unmarked gravel road as the road starts to descend steeply.

Stop 1-1. Outlook of the Canterbury Plains, Rakaia River terraces and Rakaia Gorge

Introduction to the Rakaia Valley

The Middle Rakaia Valley (MRV) is situated in the foothills of the Canterbury High Country on the eastern side of the Southern Alps, South Island, New Zealand. The Rakaia River is one of the largest braided river systems in New Zealand, flowing 120 km eastward to the Pacific Ocean. The river flow averages 221 cumecs; high flows over 800 cumecs are common and in exceptional floods flow can exceed 3500 cumecs. Its has a catchment of 2626 km^2 in the main ranges of the Southern Alps (43ºS) above the gorge. The catchment is made up of three main branches, Rakaia, Mathias and Wilberforce, with smaller northern tributaries of the Avoca and Harper Rivers. The upper Rakaia has many small, dwindling glaciers. The two largest, the Ramsay and Lyell occupy the upper catchment of the Rakakia River.

The most striking aspects of the stopping point are the extensive suite of terraces visible (Fig 3) and the exceptional overview of a classic braidplain. There are several important points to notice about the terraces.

Firstly, if you look down valley you will see that the modern floodplain converges with the terraces some distance down valley. This reflects the lower gradient of the interglaciation floodplain as compared to the glacial aggradation surfaces.

Secondly, along the lines of the terrace risers opposite you may notice some very small scale hummocky topography. These are the ‘terminal moraine’ remnants. Unlike further downstream (and up valley) where extensive areas of ice-smoothed ground occurs, ice modification along these margins was very minor and represents ice abutting its own outwash fan. During glacial advances these margins were continuously reworked so all that we see

Fig 3. The difference a day makes. The Rakaia Valley from the Gorge Road lookout. At left 8th January 2004 (187 cumecs) at right 9th January 2004 (3651 cumecs)

preserved are briefly held maximum limits.

Thirdly, the terrace surfaces are young but older sediments may be buried under them. In this case the brighter orange gravels underneath the grey gravels (Fig . 4) were mapped by Soons as Woodlands (OIS 6: >130,000 years) gravels under Bayfield (<20,000 years) gravels. We have luminescence dated some lake sediments about 500 m upstream that we correlate with the orange gravels and indeed these yields OIS 6 ages. The attribution of the younger gravels to Bayfield advances is secure.

The Rakaia Valley was heavily glaciated in its upper and middle reaches during glacial phases in the late Quaternary. Some glacial terminal limits are well known (e.g. von Haast, 1871; Speight, 1933) with the key mapping work carried out by Soons (1963; Soons and Gullentops, 1973) in the region of the Rakaia Gorge (Table 1 and Fig 5). The larger (earlier) glaciations such as the Woodlands extended about ~75 km from the Rakaia Headwaters and advanced some kilometres on to the Canterbury Plains beyond the gorge, while smaller but still extensive advances such as the Acheron advance extended ~60 km from the headwater but were confined within the "Middle Rakaia Valley" upstream of the gorge.

This Middle Rakaia Valley contains extensive outcrops of poorly documented glacial and proglacial sediments. Though the existence of these sediments, notably 'lake beds', has been known for some considerable time (Speight, 1926), there were no stratigraphic or sedimentary descriptions for most of these units/beds and their ages were conjectural. These sediments have been and continue to be the focus of study in the valley.

Geology and tectonic setting

The MRV upstream of the gorge to the catchments is predominately composed of greywackes of the Permian-Triassic Torlesse Terrane. The Torlesse is composed of sandstones and argillites with some conglomerates, breccias and chert. The mid-Cretaceous Mount Somers Volcanics Group comprises much of the gorge and Rockwood Range at the mouth of the MRV. These rocks, largely andesites, rhyolites and ignimbrites, were erupted onto Torlesse Terrane rocks along the foothills of Mid Canterbury. Tertiary coal beds, limestones and clastic sediments occur as outliers within the MRV, the Rakaia Gorge and within the Acheron River.

Glacial Advance	Age
Acheron	deglaciation
Bayfields	LGM
Tui Creek	OIS 4
Woodlands	OIS 6
Hororata	Older

Table 1. Glacial systems of the Rakaia and their inferred ages (following Soons and Gullentops, 1973). Our work will reclassify the Tui Creek as OIS3/2 and reduce Bayfields to post the LGM maximum but will confirm the other ages.

Fig 4. Photograph of terraces from the Gorge Road outlook, looking west, with the Mount Hutt Range in the background.

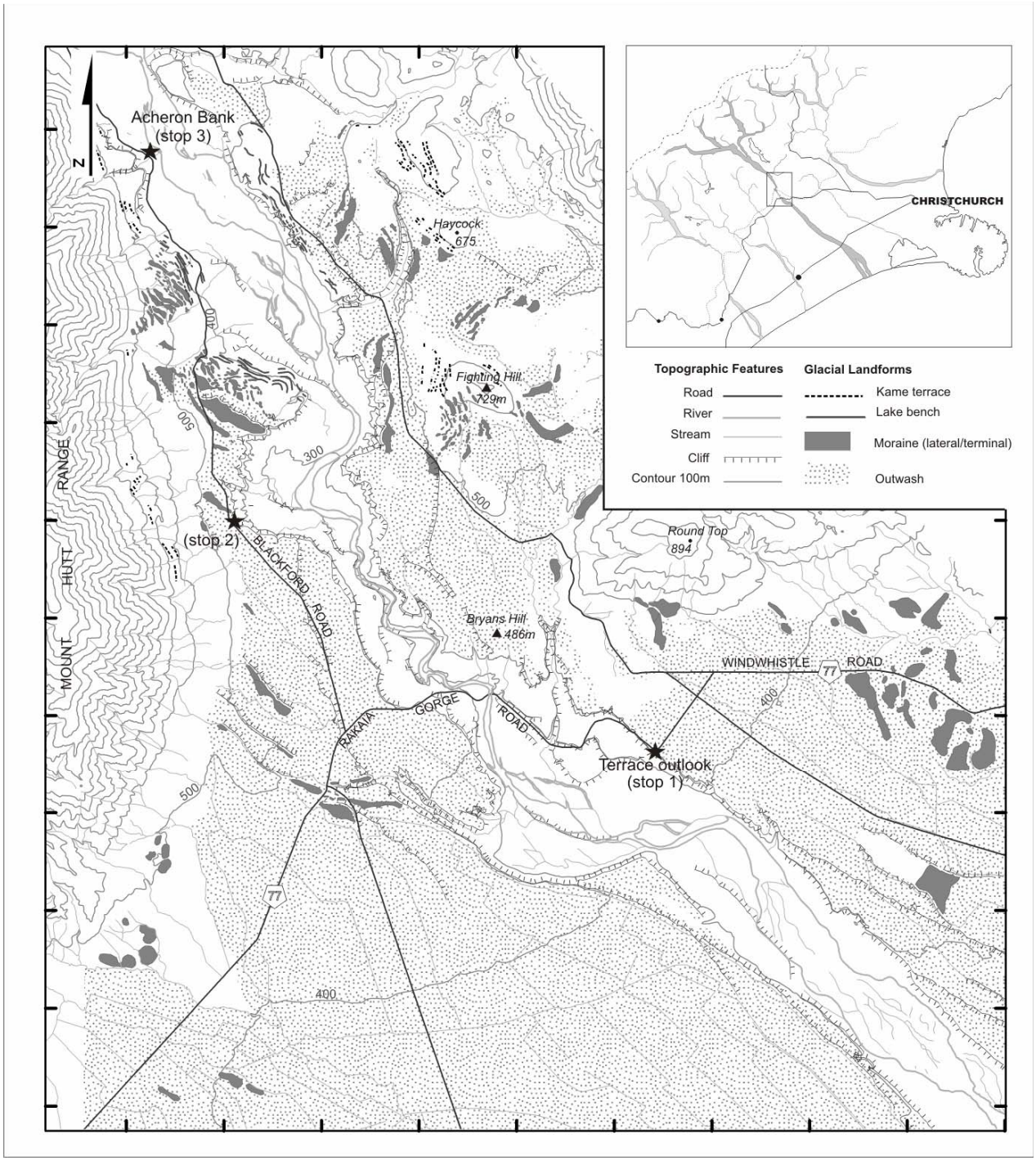

Fig 5. Simplified geomorphological map of the Middle Rakaia Valley.

The area is very active tectonically. The Porters Pass Fault crosses the MRV near the southeastern end of Lake Coleridge and disappears beneath the floodplain of the Rakaia River. A thrust fault outcrops in the gorge with substantial throw on Quaternary deposits but no discernible surface expression. There are some important structural unknowns in the valley which have been uncovered through recent investigations into the glacial sediments and will be discussed in the field.

Turn back onto highway 77 and continue west down into the Rakaia Gorge then ascend terraces on western side of the gorge. Turn right down *Blackford Road about 3km from the gorge bridge. Follow the road for about 5km.*

Stop 1-2. Bayfield Terminal Moraine

The Bayfield terminal moraine (intersection with Blackford Road, NZMS260, sheet K35: 960463) protrudes up to 8 metres above the surrounding outwash surface (Fig 6). The moraine is barely 20 m wide and penetrates to a depth of only a few metres. In short, it is a very small feature. This moraine marks the down valley maximum for the Bayfield advances and was inferred to represent the LGM limit of ice in the Rakaia based on a correlation to a dated lake sequence in a splay valley (Dry Acheron) (Soons and Burrows, 1978). The Tui Creek limits, 2 km further down valley, have recently been dated by us to the global LGM using surface exposure dating and the Bayfield advances are now dated to c. 16 ka (Shulmeister et al., unpub data).

Fig 6. Bayfield terminal moraine at Blackford Station with deer fence posts (c. 2m) for scale.

The Bayfield terminal moraine still represents the down valley limit of a significant re-advance. The scale of this re-advance can be measured from the very extensive aggradation surfaces associated with the terminal moraine. Bayfield outwash gravels underlie the moraine to a maximum depth of about 80 m (Fig 7). If the traditional model of outwash-moraine pairing is used, the very extensive Burnham Formation gravels, which are traceable to within a few kilometres of the coast, represent the aggradation surface associated with this moraine. This highlights the remarkable disjunct between the scale of terminal moraines and the events they represent. Clearly, either these types of valley glaciers did not produce large terminal moraines (at least in these settings), or the preservation potential of such moraines is very low. We believe that both statements are true and that the absence of large moraines is a function of the concentrated drainage associated with these strongly valley-confined glacier reaches AND high levels of year round fluvial activity associated with low elevation of the glacier terminus (c.450 m AMSL), and the extensive ablation zone of an extended Rakaia glacier.

The traditional form of glacial mapping in New Zealand has been based on linking terminal moraine sequences with outwash gravels/terrace surfaces (e.g. Gage, 1958 & Suggate 1965). This is very similar to the classic approach taken in Europe early in the Twentieth century though at least one surviving member of this original mapping group insists that they took no direct lead from Europe.

Fig 7. Aggradation gravels under the Bayfields moraines. These gravels are typically 60-80m thick at this location and thin down valley. They terminate abruptly a few hundred metres up valley from the youngest Bayfields position.

Continue to drive up Blackford Road, which turns into a gravel road (Double Hill Run Road), continue until Hutt Stream Ford.

As we drive up valley to the next stop, note the large fans on the left along the base of the Mount Hutt Range. Many have abandoned terraces that were active during the deglacial times and prograded into a proglacial lake. Across the river, lake benches are present above the cliffs and represent lake levels of the last proglacial lake in the valley.

Stop 1-3. Acheron Bank

Acheron Bank is located on the east side of the Rakaia River, adjacent to the confluence of the Rakaia and Acheron Rivers (K35/945552 and K35/956544), about 15km upstream of the Rakaia Gorge Bridge. The bank/cliff is actively being undercut by the Rakaia River producing a spectacular profile of sediments over 100 meters high in the middle of the outcrop decreasing to 40 m laterally, with over 1 km of continuous exposure. Acheron Bank is one of many large exposures outcropping along the Rakaia River, which extend from the Rakaia Gorge up to Acheron Bank.

Access to the outcrop is difficult and a complete face description has only been obtained from the extreme northern (Fig 8) end where log (Fig 9) and the following description is taken from (at K35/945552). The outcrop has large horizontal and vertical variability in unit thicknesses and extent. Luminescence samples have been recovered from units 2, 3 and 5 and are shown on Fig 9.

Unit 1: 0-20 m: Largely composed of sub-rounded pebble to cobble, matrix supported, weakly compacted diamicton, with some deformed silt beds and an increase in stratification and percentage of clast towards the top of the unit. This unit is notably less deformed at the down valley end.

Unit 2: 20-35m: Sub-mm to dm scale bedded silts with rare clasts up to boulder size. There are impact structures around the boulders and some pebbles and thin beds of matrix

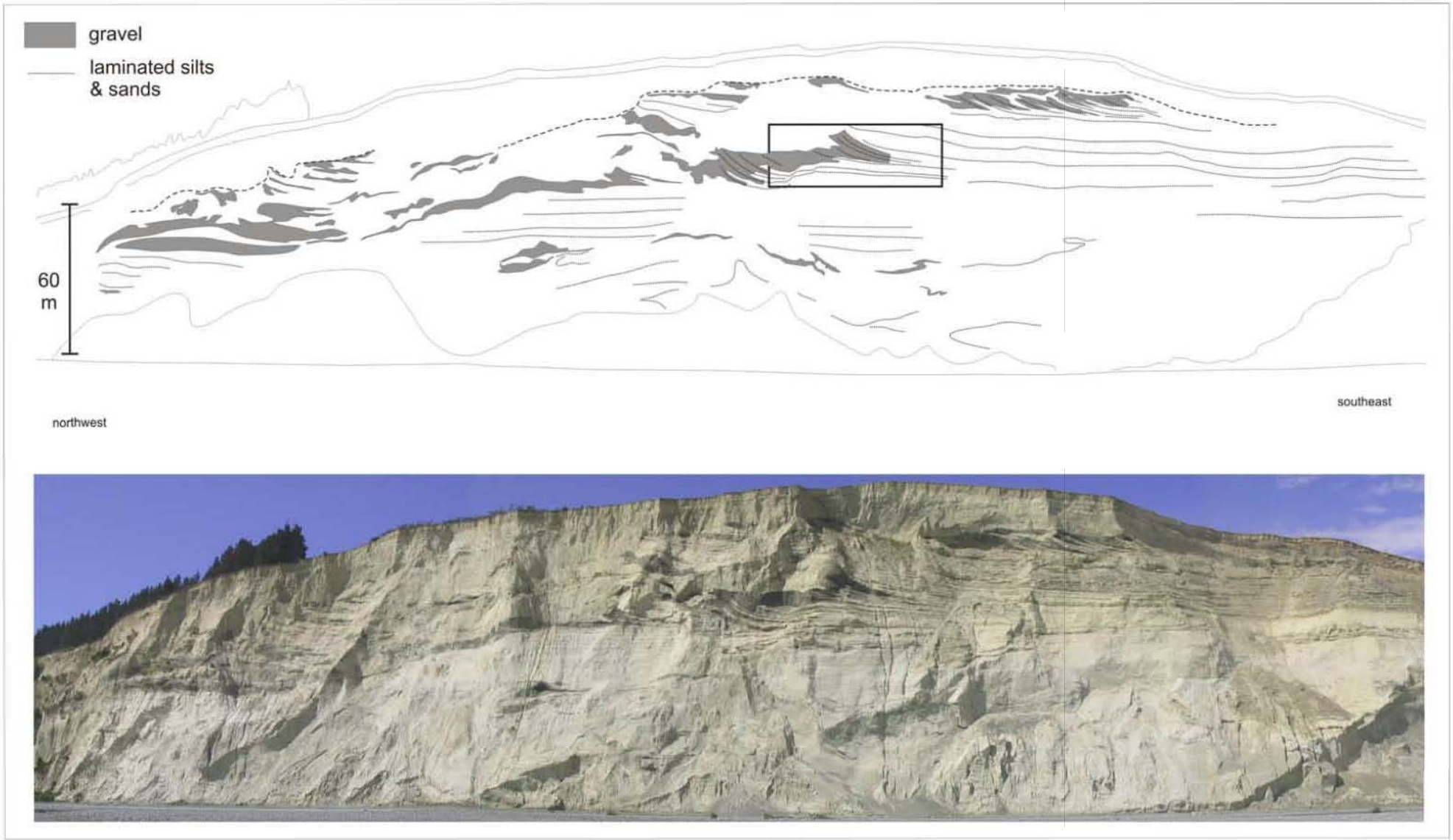

Fig 8. Photo and sketch of Acheron Bank, with approximate locations of the log (Fig 9) and 3D diagram (Fig 10).

supported intrabeds of fine gravels also occur. The basal c. 1m of the unit comprises contorted silts with flame, and ball and pillow structures. The basal contact is sharp and forms a shallow trough in the underlying diamicton. Above the basal sub-unit is a 0.3 m thick matrix supported angular gravel. Above this lamination dominates.

Unit 3: 35-55m: Metre scale interbedded angular clast supported even openwork gravel alternating with occasional matrix supported sub-rounded gravels (diamicton), rare sorted coarse sand and granule beds and incorporating patches of laminated silts. In section the unit is chaotic but from a distance the coarse scale bedding is apparent. The bedding dips down valley at low but varying angles. The lower part of this unit comprises clast supported to openwork gravel with gravel drapes extending laterally into sands and silts.

Unit 4: 55-60m: Sub-rounded matrix supported pebble to cobbles, weakly stratified diamiction, with rare boulders and cm to m scale patches of chaotically disturbed silts. The upper contact of the unit is marked by a distinct boulder pavement with large greywacke boulders up to 1m in diameter

Unit 5: 60-64m: Comprises 1.5-4 m of massive yellow brown silts with rare gravel particles.

The basal unit is interpreted as a glacio-lacustrine deposit. The lower part of the unit at the northern end and all the unit at the southern end lacks compaction and is a glacially derived mass flow into a pro-glacial lake. On the northern up-ice side the unit has been subsequently deformed by ice push and over-riding ice. In the top few metres there is evidence of direct ice contact with glacio-tectonised gravel fans present. These mark deposition from ice into shallow water followed by ice-over run of the fans. This appears to be the stratigraphic representation of a De Geer moraine (e.g. Larsen et al., 1991).

In the northern part of the face, the base of unit 2 is a trough bed that incises the basal glacio-lacustrine deposit and represents a mass flow deposit with a slurry fill of lacustrine silts.
The main body of Unit 2 represents lake beds with occasional debris flows into the lake and frequent dumping of ice rafted material. Drop stones are present, but are relatively rare. Given the lateral extent and thickness this was probably a proglacial lake in a relatively distal position. The luminescence age dates this to an early part of the penultimate ice age. It indicates an ice retreat from the ice-overrun at the top of Unit 1.

Unit 3 appears to reflect the approach of a new ice margin. Just as at the top of Unit 1, there are angular fan gravels that are glacio-tectonised and overridden from the north in a series of step-ups. Where logged at the western end, the unit is highly chaotic with a mix of sediments that reflect proximal proglacial outwash, mass movement deposits dumped from the ice face and melt-out ponds. Observation of the main part of this sequence demonstrates very well organized gravel fans grading laterally into well sorted sand beds. These indicate direct alluvial deposition from an ice front into shallow water, followed by ice push and over-run (Fig 10). Silt beds (pond fill) at the northern end yielded an OIS 4 age (Fig 9).
.
Unit 4 is a stratified diamicton. It was not possible to examine the face in detail due to lack of access, but it appears similar to the mass flow deposits of Unit 1 except for the boulder pavement on top. The units true lateral extent is not well known. The persistent preservation of stratification in diamicts is characteristic of so-called 'tills' in these New Zealand valley settings (e.g. Speight, 1940; Gage, 1965). We believe that the till attribution is incorrect in the Rakaia and likely to be incorrect elsewhere. This will

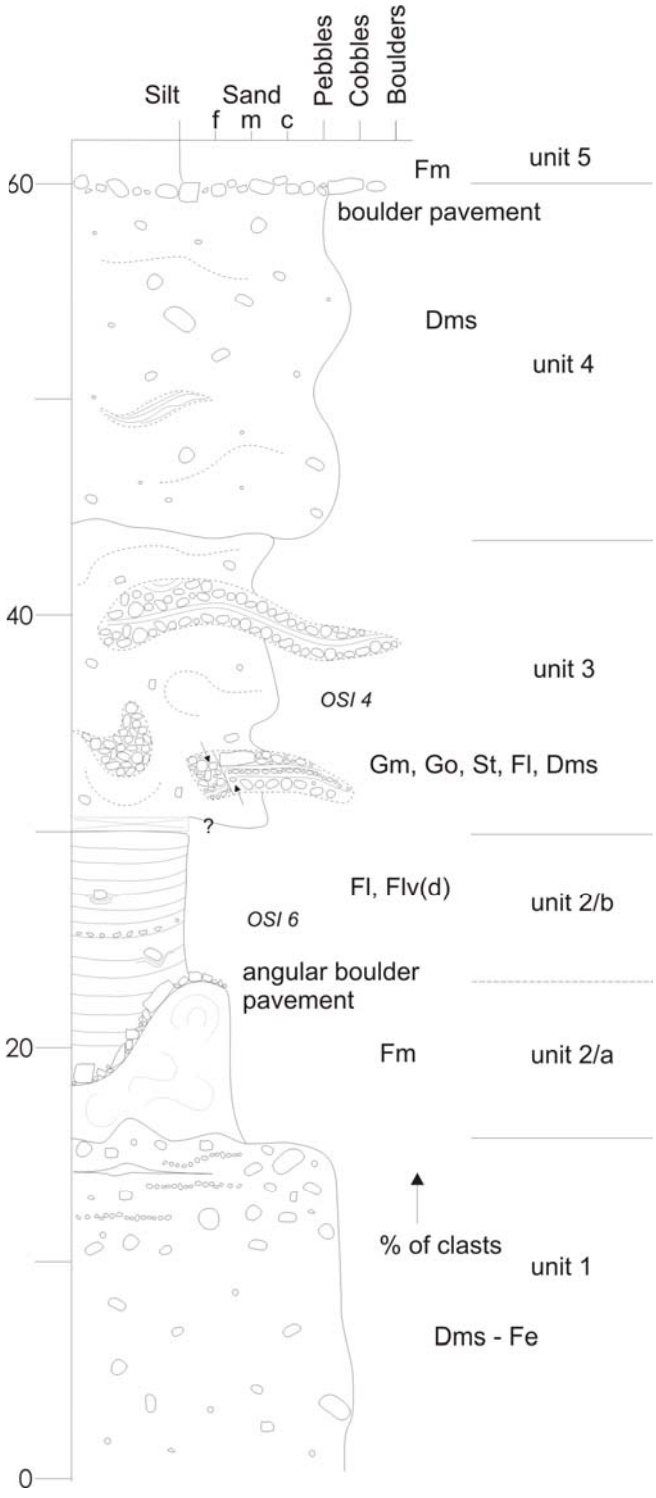

Fig 9. Log of northern end of Acheron Bank (see Fig 8).

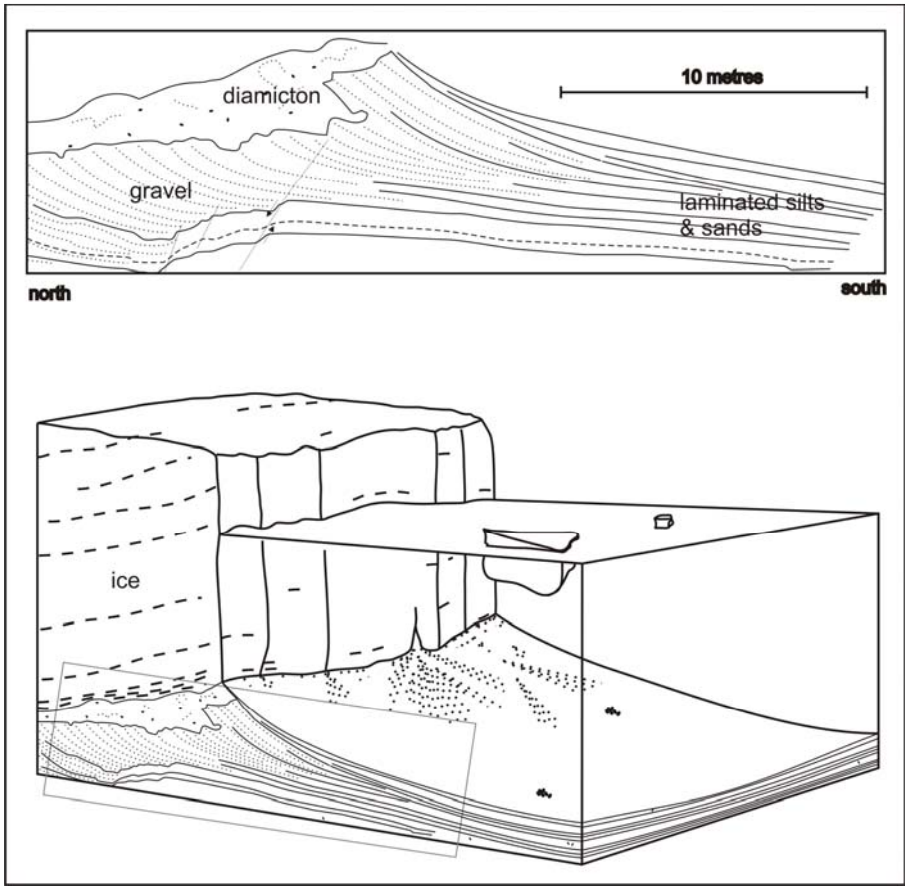

Fig 10. At bottom, ice contact sub-aqueous fan or 'De Geer moraine'. The stratigraphic outcrop at Acheron Bank (top, for location of sketch see Fig. 7) is interpreted as an ice contact fan of a Be Geer type. Adapted from Benn, 1996.

be discussed in the field. Unit 4 was laid down in an ice proximal but pro-glacial setting. This indicates a retreat from the terminal position of Unit 3. Given that the youngest (Acheron/Bayfields – OIS1-2) advances barely reached this elevation, it is likely to relate to an OIS 3 or OIS 4 advance. Unit 5 is a post glacial loess deposit which is laid down on ice carved surfaces and lake benches.

The key points of interest from this outcrop are twofold. Firstly there is the unexpected survival of thick sedimentary deposits over 10 km up ice from LGM terminal positions. This is particularly remarkable for Acheron Bank which is in a central location in the valley and should have been eroded by subsequent advances. It appears as though this outcrop and those between Acheron Bank and the gorge have survived because they occupy an over-deepened trough from an earlier, larger, glacial system.

Secondly, the stratigraphic exposure of 'De Geer' like proglacial micro-deltaic features marks distinct phases of ice advance through this location. The luminescence ages on these advances are somewhat surprising falling with mid-OIS 5 for the lower series and early OIS 3 for the upper. If correct, they imply full (or near full) glaciation of the Rakaia in interstadials and even during interglacial. The implications will be discussed in the field.

Rakaia to Geraldine

After leaving the Rakaia Valley we will follow the edge of the foothills south, crossing a series of fans and alluvial plains associated with braided rivers. The first major braided rivers we cross are the branches (North and South) of the Ashburton. These rivers carried substantial outwash flows during the LGM, originating from distributary lobes of the Rakaia (in the north) and the Rangitata (in the south) glaciers, as well as outwash from local valley glaciers in the adjacent ranges. A spectacular complex of LGM moraines is preserved in inland basins in the South Ashburton & Rangitata catchments. What are arguably the best preserved LGM glacial landforms in New Zealand lie in the vicinity of a series of shallow lakes (L. Heron in the north and L. Clearwater in the South). The floor of this basin (at c. 700m) is higher than the valley floors of either the Rangitata or Rakaia. Consequently, the lobes that pushed into this basin stagnated at the end of the last ice age, no major drainage occupied the basin, and a spectacular sequence of recessional features was left stranded. The sequence was described by Mabin (1980, 1984; also see Oliver & Keene 1990) and is now being re-evaluated by students from the University of Canterbury.

Ice was confined to the inland basins during the LGM but earlier advances were much larger. The largest advances over-ran the hill tops on the up gorge side and high level outwash terraces are preserved near Mt Somers, although there are few obvious terminal positions. The terraces evident to the west of the highway near Mt Somers have been uplifted relative to the plains by active reverse faults/

folds running parallel to the range-front (Cox & Barrell 2007 – in press; Barrell et al 1996). This fault/fold zone has caused up to 10 m of vertical deformation of LGM outwash surface, implying that the average rate of tectonic uplift of the range-front is approximately 0.5 mm/year.

The road from Mt Somers towards Geraldine crosses LGM aggradation plains of vast extent, sourced from the South Ashburton and Rangitata catchments. Holocene deposits are confined to the immediate vicinity of the river channels and inter-fan streams such as the Hinds River. Nearing Geraldine, we cross composite LGM and Holocene fans of minor rivers draining the frontal range. In some locations, notably within several kilometres of the incised valleys of the Rangitata and Rakaia Rivers, alluvial silt mobilized from the river bed during frequent föhn north-westerly gales is actively accumulating as Holocene loess on adjacent terraces. Generally the Holocene loess sheet is less than 1 m thick, but exceptionally reaches 4 m near Barrhill, on the south bank of the Rakaia River channel, 25 km downstream of the Rakaia Gorge bridge (e.g. Berger et al. 1996).

Geraldine to Lake Tekapo

West of Geraldine we pass into hill and downland country, into which river and stream valleys are broadly incised. The geology is dominated by Cretaceous to Neogene, weak sedimentary rocks, with underlying basement of Mesozoic greywacke and some low-grade schist (semischist) exposed in the ranges. Medium to high-level alluvial gravel terraces occur throughout the landscape, in places forming extensive dissected plateaux. The gravel is generally weathered and is probably of mid-Quaternary age (i.e. much older than MIS 6) and the highest remnants may well be of early Quaternary age. The tectonic regime appears to be one of very broad, very slow uplift. The rounded form of the rolling country (downs) is due to extensive and thick accumulations of silty loess. The loess has been blown from aggrading floodplains, probably during cold climate phases, the most recent of which was the LGM (e.g. Berger et al. 2001b).

Fairlie lies in the broad, north-south trending, Cannington synclinal depression (Langdale & Stern 1998). The Opihi River has cut a spectacular antecedent slot gorge across the eastern margin of the syncline. Nested fans, ranging in age from Holocene back to at least mid-Quaternary lies along the flanks of the ranges, while an extensive LGM alluvial aggradation plain occupies much of the basin floor. These deposits include outwash from cirque and minor-valley glaciers that formed on the higher ranges, especially the Two Thumb Range, to the north, during the LGM and in earlier glacial episodes.

As we proceed west of Fairlie into the Opihi River headwaters, note the generally incised and terraced landscape. Erosion is the dominant process. Note the contrast as we cross Burkes Pass and descend into the Mackenzie Basin. The Mackenzie Basin contains a complex of broad aggradation fans – deposition is the predominant process. A simple explanation is that much of the Mackenzie Basin catchment is sourced in the high-relief, high precipitation zone at the Main Divide of the Southern Alps. This has produced abundant sediment through time, and contrasts the sediment-poor area east of Burkes Pass that is fed only by local drainage from lower mountains in a drier area.

LGM outwash surfaces, flanked by LGM to Holocene alluvial fans, are the main feature of the Mackenzie Basin west of Burkes Pass. Nearing Tekapo, we cross remnants of pre-LGM outwash terraces and moraines, before reaching the complex of LGM moraines upon which Lake Tekapo township and which impound post-glacial Lake Tekapo.

Lake Tekapo to Twizel

From Tekapo, we have three options for completing the journey to Twizel, time and weather permitting.

1) Panoramic view from Mt John (Fig 7): we may ferry the party up onto Mt John via the support van. In good conditions, the view across the LGM terminal and post-Termination retreat moraines is unparalleled. Mt John is an ice-sculpted knob of greywacke rock. A veneer of pre-LGM gravel is preserved in places on the knob. Scarps and rents around the perimeter of Mt John's crest attest to gravitational collapse of the greywacke slopes following retreat of the LGM ice.
2) The Tekapo-Pukaki lateral moraine sequence. We may divert west off the highway and proceed down Braemar Rd to Lake Pukaki. The road crosses an extensive area of subdued moraine forms, mapped as the Wolds Formation, and thought to be at least as old as MIS 8. East of the road is the spectacular fault-line escarpment of the Irishman Creek Fault, upthrown to the east by up to 200 m on Wolds glacial deposits. In places, Pliocene sediments are exposed in the hanging wall. Late Quaternary tectonic scarps up to several metres high cross LGM to Holocene surfaces. Some large landslides can be seen on the escarpment face, and may well be earthquake-generated. West of Irishman Stream, the road climbs up the Wolds lateral moraine complex of the ice-age Pukaki Glacier, and from its crest, excellent views are afforded of the Pukaki glacial trough, and its pre-LGM through to LGM lateral moraines. There is a narrow belt of moderately subdued moraine, locally known as Balmoral Formation, probably of MIS 4 or MIS 6 age. We then cross the LGM latero-terminal moraine complex, with many individual moraine ridges flanked or cut by multiple meltwater outwash fans. Mid-way down the complex, there is a subtle transition to LGM retreat moraines, with numerous kame and meltwater surfaces, and stream gullies draining directly down the evacuated post-Termination glacier trough.
3) The Tekapo-Pukaki terminal moraine sequence. A suite of these landforms is crossed by State Highway 8 southwest of Tekapo township. Balmoral and Wolds moraines and outwash (as described above) are notably subdued, especially the Wolds surfaces, even though the loess on them is rarely thicker than 2 m (Maizels 1989). South

of the hydroelectric canal, broad rises and falls in the height of the Wolds terrace to the east of the road are not morainic but are broad tectonic anticlines and synclines that deform the Wolds surface, but affect the Balmoral surfaces to a much lesser extent, and do not appear to affect LGM surfaces (Cox & Barrell 2007 – in press). Note the huge, weathered boulders on the Balmoral moraines west of the highway after crossing Irishman Stream. Beyond the greywacke ridge of Mt Mary at Simon's Pass, the highway traverses the Balmoral and LGM outwash and moraines that impound Lake Pukaki. We proceed across Pukaki Dam and down the LGM outwash plains to Twizel.

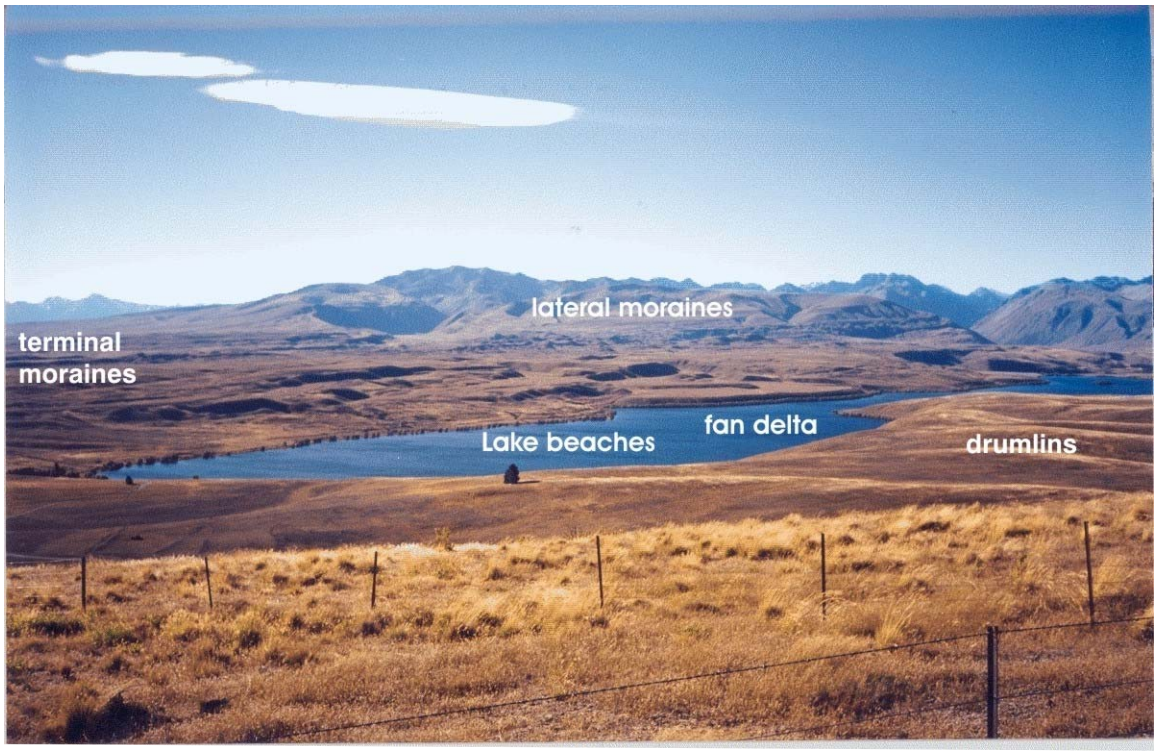

Fig 11. Photograph of Lake Alexandrea from Mt John, looking northwest.

Day 2, Twizel to Wanaka (Barrell and Shulmeister)

We begin by travelling north from Twizel to the Lake Pukaki dam, where we will examine LGM outwash and ice-contact deposits near the dam spillway. We will then proceed north on State Highway 80 along the western shore of the lake and the Tasman valley to Aoraki/Mt Cook village, and then to the glaciers. There is a light 15 minute walk across Holocene moraines to the Mueller Glacier lookout. We then return down-valley, pausing to note the Late-Glacial moraines of the Birch Hill advance.

We proceed south across LGM outwash plains past Twizel and Ruataniwha Dam, which occupies the former channel of the Ohau River. The low hills to the right of the highway mark the active Ostler Fault. We will examine the fault scarp, and glaciogenic deposits, at Lake Ohau Road. We continue the journey across LGM surfaces, with minor LGM to Holocene fans, to the Ahuriri River and Omarama, before proceeding up the Ahuriri LGM outwash plain, and then up the Longslip catchment and over Lindis Pass. We descend through the Lindis catchment to the upper Clutha valley at Tiaras. We then travel southwest to Bendigo, where we will examine moraine, formed by the Clutha Glacier in the mid-Quaternary. We then travel up the Clutha valley, across a complex of river terraces, fans and pre-LGM moraines, before reaching the LGM moraines at Wanaka.

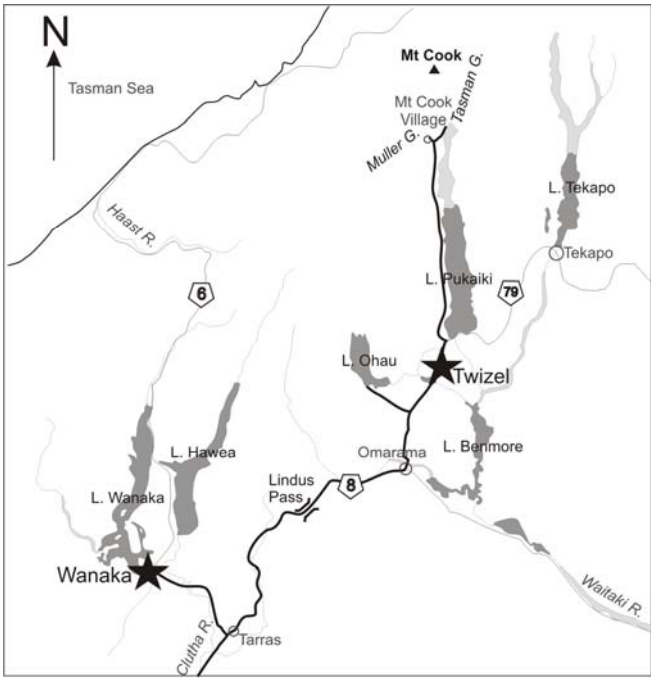

Mackenzie Basin

The Mackenzie Basin is a large tectonic depression, aligned NE-SW, some 90 km long and 10 to 30 km wide. It is bounded to the east by ranges and to the west by the Southern Alps (Fig. 12). Late Cenozoic sediments are preserved beneath parts of the Mackenzie Basin, and are exposed where uplifted along Quaternary faults. Lakes Ohau, Pukaki and Tekapo occupy glacial troughs last occupied by ice during the last glacial maximum (LGM). Table 2 sets out the local Quaternary stratigraphic names. Moraines surround the lakes and extensive outwash plains extend around the basin floor, while alluvial fans have built out from the surrounding ranges (Speight 1963). Drainage from the lakes exits the basin through the Benmore gorge (now drowned for hydro-electric generation), which marks the start of the Waitaki valley. As in other parts of the Southern Alps, there is a dramatic precipitation gradient, from extreme humidity in the west to sub-humid or semi-arid conditions further east (e.g. Henderson & Thompson 1989), due to the interaction between the Southern Alps and the mid-latitude westerly wind zone. Mean annual precipitation is about 10,000 mm/y at the crest of the Southern Alps (known as the Main Divide), but reduces exponentially to about 4,500 mm/y at the Mueller Glacier terminus and to about 600 mm/y at the Lake Pukaki outlet.

Glacial Deposit	Assigned Climatic Event	Assigned Oxygen Isotope (MIS) Stage and (Age)	Comments
Holocene till/outwash	"Neoglacial"	1 (0 – 5 ka)	Supported by 14C dates
Birch Hill Formation	Late Glacial	1 – 2 (10 – 12 ka)	Supported by 10Be dates
Tekapo Formation	Late Otira Glacial	2 (16 – 18 ka)	Supported by 14C/10Be dates
Mt John Formation		2 (18 – 24 ka)	Supported by 10Be dates
Balmoral 2 Formation	? Early Otira Glacial	4 (59 – 71 ka)	Correlation with MIS 4 uncertain
	Kaihinu Interglacial	5	None recognised
Balmoral 1 Formation	? Waimea Glacial	6 (128 – 186 ka)	Correlation with MIS 6 uncertain
	Karoro Interglacial	7	None recognised
Wolds Formation	? Waimaunga Glacial	8 (245 – 303 ka)	Correlation with MIS 8 uncertain. May include deposits from more than one glacial event

Table 2. Glacial stratigraphy of Mackenzie Basin – Mt Cook area. "Interglacial" phases are shaded. MIS 8 may be a minimum age for some or all of Wolds Formation.

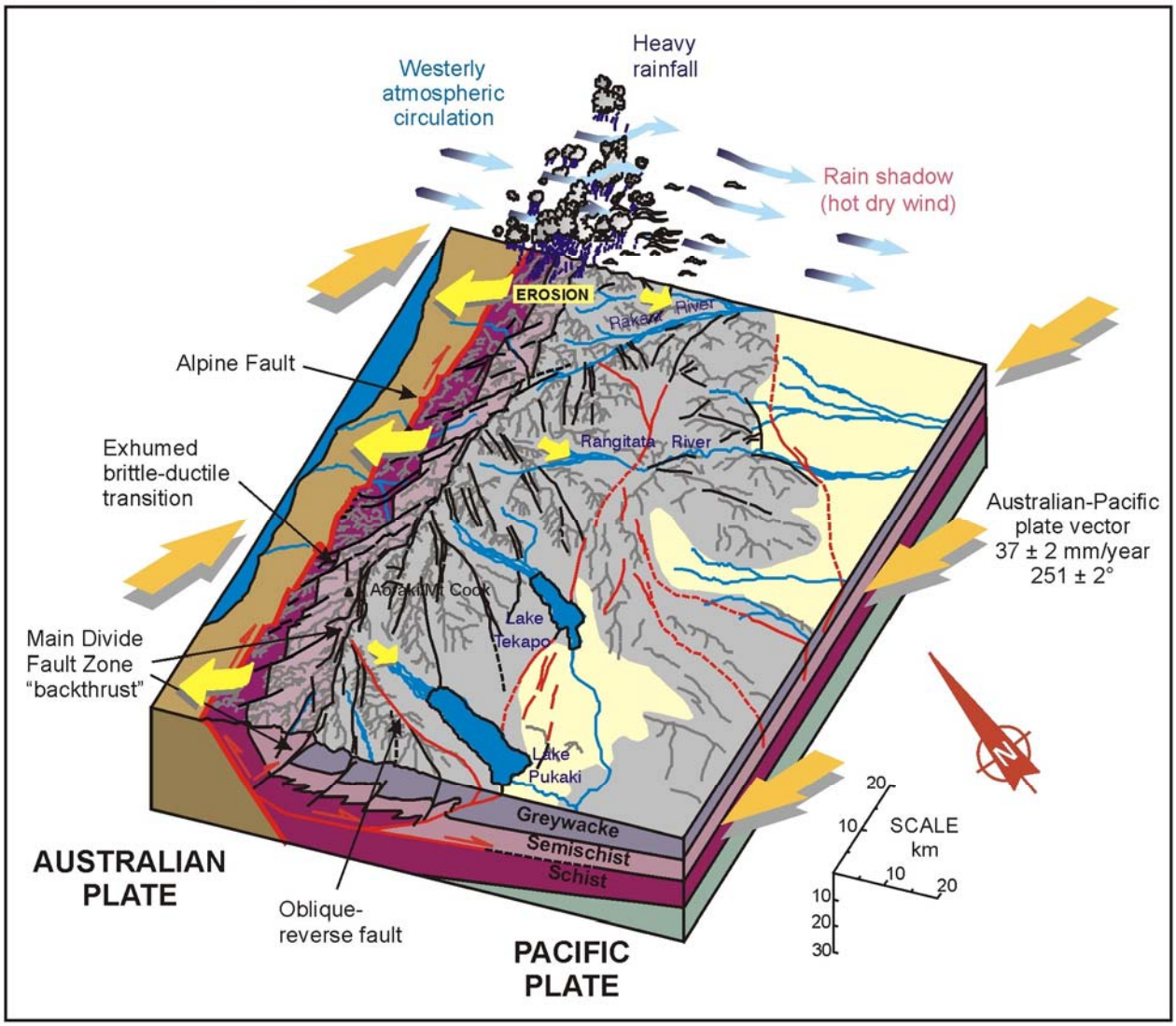

Fig 12. Schematic block diagram summarising the tectonic and geomorphic setting of the Southern Alps (after Cox & Barrell 2007 – in press). The map areas of Quaternary deposits are shown in yellow, and known active faults are red.

Pollen diagrams from Duncan Stream 10 km northwest of the Lake Pukaki outlet record an early Holocene vegetation dominated by *Phyllocladus alpinus* (mountain toatoa, a small, hardy tree) between 8,000 and 5,000 ^{14}C y BP, followed by increasing dominance of *Halocarpus bidwillii* (bog pine), *Aciphylla* (speargrass, commonly called 'spaniard') and grassland (McGlone and Moar 1998), as well as the appearance of layers of charcoal. This is attributed to a change in climate that led to more droughty conditions, and greater frequency of natural fires. At the time of arrival of humans in New Zealand, about 1250 AD, vegetation near the western range-front south of Lake Ohau comprised a cover of *Halocarpus* scrub, but at 600 – 800 ^{14}C y BP rapidly changed to grassland, probably in response to anthropogenic fires (McGlone & Moar 1998).

Stop 2-1. Lake Pukaki outlet (H38: 819645)

A track leading south from State Highway 8 at H38: 815646 down to the Pukaki River channel below the Pukaki Dam passes through late LGM moraine ridges, and crosses an LGM outwash surface downstream of a prominent moraine ridge, attributed to the locally-named Tekapo advance. From the river channel, the nature of deposits under these landforms can be seen. Points to note are the thick rounded outwash gravel underneath the outwash plain which extends upstream beneath the diamicton associated with the moraine ridge, the chaotic silt-dominated nature of the diamicton, and the 20° lake-ward dipping contact of the diamicton and outwash. The geological events here are: (i) aggradation of LGM outwash gravel in front of the Pukaki glacier; (ii) sufficient withdrawal of ice to allow silty lacustrine sedimentation in front of the glacier, and; (iii) ice re-advance that picked up and chaotically re-deposited the silty lake sediment as a diamict (Hart 1996; Mager & Fitzsimons 2007), out and over the earlier formed outwash deposits.

This exposure may well contain the best understood glacial stratigraphy in New Zealand, as a result of investigations for, and the excavation of, foundations for the Pukaki Dam (Read 1976; also see McGlone 1996). It was demonstrated that this diamicton was the 'last throw of the dice' for the LGM at Pukaki. Towards the lake, the diamicton was overlain (prior to removal by excavation) by ice-marginal, exquisitely bedded, sands (known to the dam workers as the "Fancy Sands"), in turn overlain by still-water lake sediments comprising dark plastic silty clay, known as

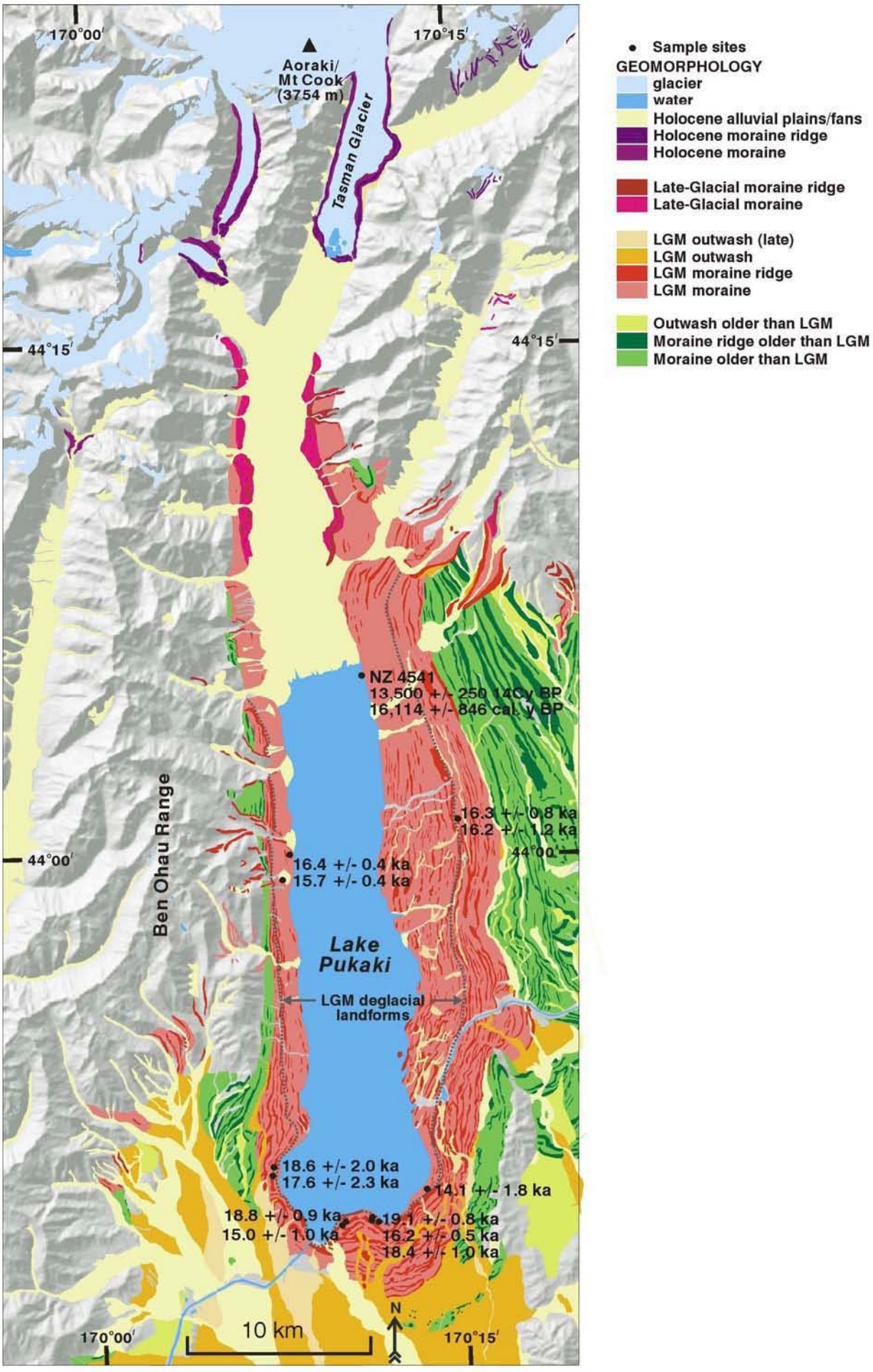

Fig 13. Glacial geomorphology map of the Lake Pukaki area, with Beryllium-10 ages for 12 moraine boulders, and a Carbon-14 age for an organic silt (after Schaefer et al. 2006).

"Pukaki Pug". A radiocarbon-dated wood sample from about 4 m above the base of the Pukaki Pug (NZ-1651; Read 1976) has an age of 13,551 ± 478 calendar years BP age, and is a minimum for ice withdrawal from the terminal area and the initiation of Lake Pukaki. So, this diamicton exposed at this site, and the associated moraine ridge, represent the last advance of Pukaki Glacier before the local Termination at the end of the LGM.

Surface Exposure Dating using Beryllium-10 is improving our understanding of LGM glacial history at Pukaki (Schaefer et al. 2006). The last-advance moraine ridge at the outlet can be traced with some confidence around the lake basin (Fig. 13), marking the change to deglacial (i.e. ice-recessional) landforms. ^{10}Be ages from moraine boulders outside (i.e. older than) the last-advance ridge average 17.8 ± 1.4 ka, whereas the ages of boulders on or inside this ridge average 16.2 ± 0.9 ka (Fig. 14).

Support for these results comes from a site 30 km up-valley from the outlet (Fig. 13), approximately 400 m below the Tekapo lateral moraine crest and 35 m above the 1950 lake level (i.e. now submerged; see paragraph below), where an organic layer in clay, ponded behind a deglacial meltwater channel, returned a ^{14}C age of 13,500 ± 250 years BP (NZ-4541; Moar, 1980; Suggate, 1990). This corresponds to a calibrated ^{14}C calendar age of 16,114 ± 846 years BP.

It is important to appreciate just how much change has occurred at Lake Pukaki since it was artificially raised for hydroelectric water storage. When full, the lake stands 55 m higher than its original level. There is a flight of post-glacial lake beaches on the moraines surrounding Lake Pukaki, but these are now submerged. It is instructive, therefore, to realise that the modern shorelines and clifflines of Lake Pukaki are very, very young. The original lake was raised about 15 m in 1951 to provide storage for hydro-electric power generation dams downstream in the Waitaki valley, and was raised by a further 40 m in 1979 (Read 1976, Irwin and Pickrill 1983). The shoreline development that we see is the effect of less than 30 years of shoreline processes under a widely fluctuating water level.

Stop 2-2. Mount Cook – Holocene moraines of Mueller Glacier (H36: 762170)

The Alpine Memorial on the Mueller moraines provides a wonderful view of the Mueller glacier trough, Mt Sefton, the Hooker Valley and Mt Cook (on a good day). The Hooker and Mueller glaciers, like other glaciers in Aoraki/ Mt Cook National Park, have been in rapid retreat since about 1980, although downwasting (reduction in height) of the glaciers had begun by early 20th Century following the c. 1890 peak of the last of the glacial advances of the "Little Ice Age" (Hochstein et al. 1995). The peak of the "Little Ice Age" advances has been dated to c. 1725 AD using lichenometry (Winkler, 2000; 2004; Lowell et al. 2005).

The 19th-20th century termini of the Mueller, Hooker and Tasman glaciers lie at the inner margin of nested suites of terminal moraines. Glacial down-wasting and retreat during the 20th century, and continuing to the present day, has partially exposed the stratigraphy in the inner margins of the lateral moraines, and in a few locations the glacial

Fig 14. During a fine day on the LGM moraines at Lake Pukaki, Joerg Schaefer makes notes atop the greywacke mega-boulder from which SED sample Kiwi 407 (16.2 ± 0.5 ^{10}Be y BP; Schaefer et al. 2006) was collected, while Bob Finkel reviews the surroundings.

deposits within the moraines comprise successive layers of till, with radiocarbon-datable wood and buried soils locally preserved on the inter-layer contacts (e.g. Gellatly et al.. 1988; Burrows 1989). The stratigraphy and dating indicate that the moraine complexes were constructed by vertical accretion during a succession of glacial advances since approximately 5 ka, the so-called Neoglaciation (Porter 2000). Just outboard of the main Holocene moraine complex of the Mueller Glacier, Foliage Hill (H36: 758167) has well-developed soils and weathering rinds on greywacke clasts, suggesting that the hill is the remnant of moraine formed in a glacial advance that ended at c. 7.2 ka (Birkeland 1982, Gellatly 1984), although Porter (2000) cautions that this age estimate is very ill-constrained.

Note the character and setting of the lake that is forming within the Mueller lateral and terminal moraines. As the trip returns south alongside Lake Pukaki, imagine the same scene scaled up many times, and moved back in time to 14 – 16 ka. The present-day rapid ice retreat and formation of lakes at the Aoraki/Mt Cook National Park glacier termini is an excellent small-scale analogue for the glacial withdrawal at the termination of the LGM.

The other feature to note is the concentric area of raised ground upon which Mt Cook village and the Hermitage Hotel are constructed. It has been suggested that it is a moraine remnant, but it is more likely, given its position and form, to be the debris pile of a sizeable rock avalanche event(s), derived from the mountain slope behind.

Stop 2-3. Tasman Glacier viewing point

The Tasman Glacier is the largest valley glacier in New Zealand at c. 28 km long. The main accumulation area lies above 2400m, while the glacier snout lies near 730 m AMSL. The viewing point over the Tasman is a c. 20 minute (moderately vigorous) walk from the carpark. The viewing point provides excellent up valley views over the Tasman melt-water lake (Fig. 15) and the lower reaches of the glacier itself. The salient features of this glacier are the extensive debris cover on the lower reaches and the presence of the large, and rapidly enlarging, melt-water

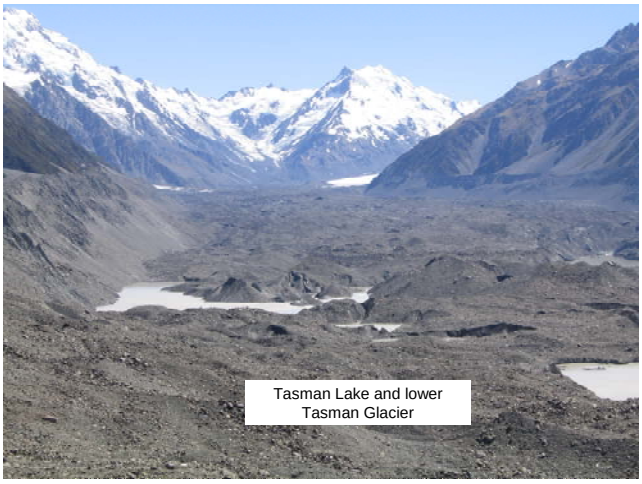

Fig 15. View up Tasman Valley from the lookout point. The glacier is heavily covered in debris. Note the evidence for substantial down wasting from the lateral moraines. The Tasman Lake has only recently extended into this region. Photo J. Shulmeister.

lake (Tasman Lake) at the terminus. These phenomena are closely related and the lake is very young.

Recent work includes that of Kirkbride and Warren, Hochstein et al. (1995) and Roehl (2003, 2005). Kirkbride (1993), Warren, and Kirkbride (1998) and Kirkbride and Warren (1999) examined the relationship between downwasting and ice-contact lake enlargement (Fig. 16). The pattern of retreat (Hochstein et al., 1995) may be summarised as relatively slow downwasting (c. 55 m) and little change in terminal position from the late 19th Century until about 1971. In 1971, the glacier surface extended all the way to the terminal moraine. Several moulins were present on the glacier. By 1982, the meltwater ponds were expanding rapidly and had depths of 20-50m. A small lake occurred at the outlet of the Tasman River with another pond hugging the eastern wall of the moraine. The lakes were milky in colour indicating connection with the main glacial drainage. By 1993, the ponds had coalesced to form Tasman Lake, which at that time was about 1 km^2 in area. A leadline survey showed much of the lake to exceed 100 m in depth and over 130 m in the vicinity of the ice front. Since 1993, the lake has continued to expand rapidly and now occupies much of the lower 3 km of the glacier trough behind the terminal moraine complex. Kirkbride and Warren (1999) predicted that up 10 km of retreat may occur with rapid calving of ice into the Lake. This is likely to cause debuttressing of the valley sides and an increased risk of landslides. Tasman Lake is a possible analog environment for some of the glacio-lacustrine sediments seen in outcrop in Rakaia Valley and other New Zealand valleys.

The downwasting has been asymmetrically distributed across the glacier. By the mid-nineties it had thinned by 185 m, 10 km up ice whereas a transect 2 km from the snout showed only 115 m of thinning. This has resulted in very low gradients in the lower reaches of the glacier (0.0097) and a decline in velocity from c. 13 m per year at the 10 km transect to only 1.3 m per year at the 2 km transect (Kirkbride and Warren, 1999). This differential reflects debris cover on the lower reaches of the glacier which has partly insulated the lower parts from ablation. The lower reaches of the glacier are out of equilibrium and the ice is virtually stagnant, which has contributed to the rapid growth of the terminal lake. Accelerated flows further up glacier have resulted in a net upward vector for the glacier surface in the lower reaches, with attendant increases in ablation further enhancing the debris cover. Consequently, the debris covered zone has been extending upstream over the last 100 years.

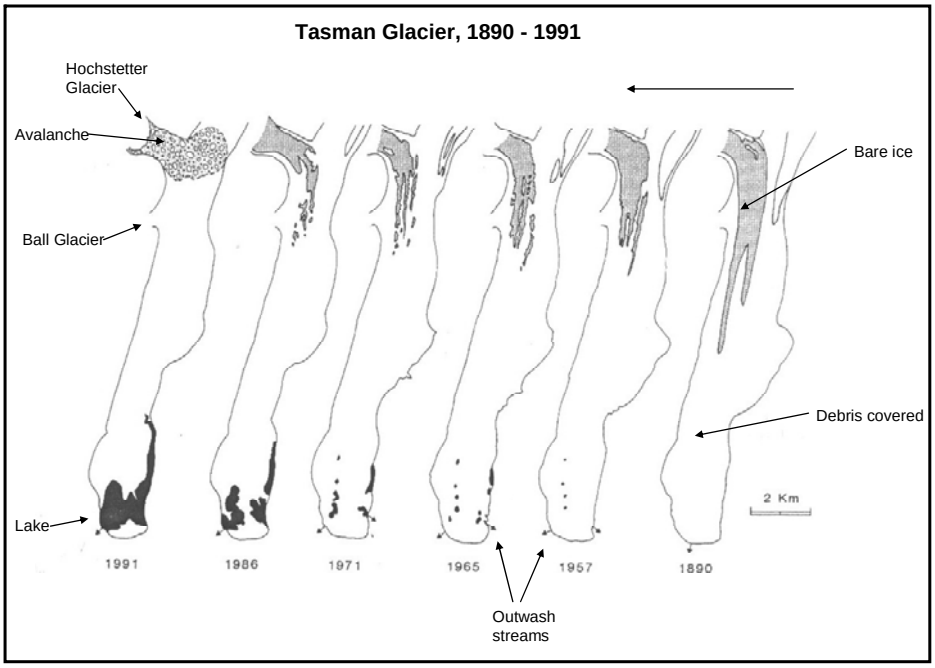

Fig 16. The development of Tasman Lake from 1890 to 1991 (modified from Kirkbride, 1993).

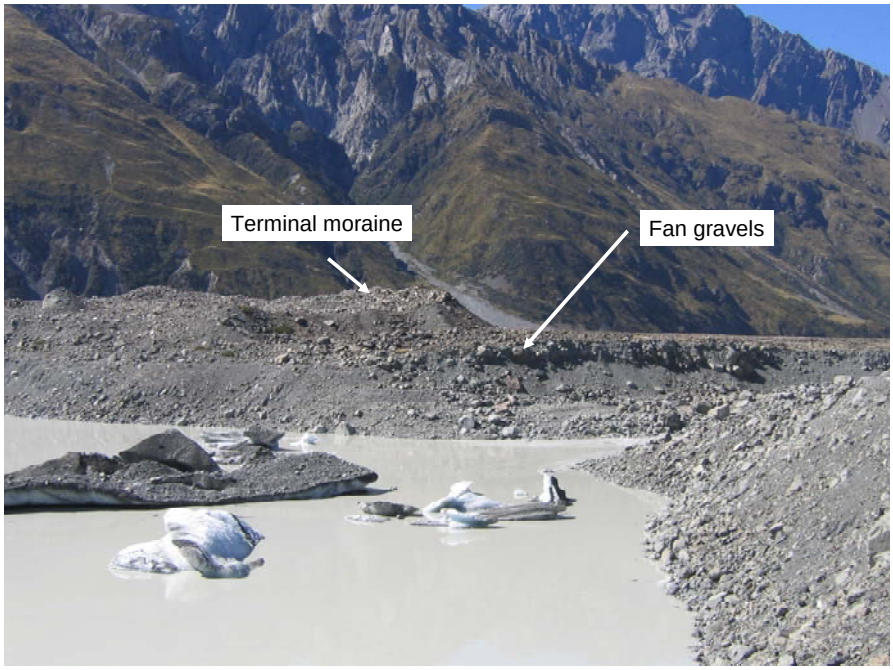

Fig 17. Terminal moraine and outwash gravel contact at mouth of Tasman Lake. Note that the fan surface projects under the moraine. Photo J. Shulmeister.

The other feature of note is the Tasman alluvial fan (outwash). The fan head system is demonstrated in Fig 17 above. The notable points about this fan head system are: 1) The terminal moraine in front of the glacier is very thin (only c. 5-15 m high) and narrow (only a few tens of metres wide). When viewed from down valley it s very evident that the terminal moraine in front is much lower than the lateral moraines. 2) The terminal moraines have no vertical persistence. The moraine is deposited directed on proximal fan materials and the moraine does not even reach down to the modern lake elevation. 3) Since the lake depth exceeds 100 m, the fan gravels are thick and persistent. They also fine very rapidly away from the terminal moraine. The fan surface (a sandur) extends from the Tasman Glacier to Lake Pukaki. The lake is confined by the outwash fan and not by the terminal moraine. The modern Lake Tasman is a possible analog environment for some of the glacio-lacustrine sediments seen in outcrop in Rakaia Valley and other New Zealand valleys.

The small size of the terminal moraine at the front of the glacier reflects the low preservation potential of moraines in a fan head system like this. The advancing glacier would recycle terminal moraine through the fan system and the surviving moraine is the product of only a brief period at the end of the last ice advance.

The present river channel is incised about 8 m into the 'Little Ice Age' outwash plain. This downcutting reflects the 20thC withdrawal of ice, formation of the lake and consequent cessation of supply of coarse sediment to the outwash plain. In the active channel of the Tasman River, close to the terminal area, the gravel is very coarse, with a mean intermediate-axis clast size of 105 mm. Clast size reduces progressively downstream, and at the Tasman River delta at the head of Lake Pukaki, the mean clast intermediate-axis is only 25 mm (Browne & Barrell, 2002).

As the trip returns south alongside Lake Pukaki, imagine the same scene scaled up many times, and moved back in time to 14 – 16 ka. The present-day rapid ice retreat and formation of lakes at the Aoraki/Mt Cook National Park glacier termini is an excellent small-scale analogue for the glacial withdrawal at the termination of the LGM.

Stop 2-4. Freds Stream – SH80 (H37: 774042)

The road runs through extensive hummocky ablation moraine of the Birch Hill glacial advance. On the north side of Freds Stream, a well-defined lateral moraine ridge marking the maximum height of the Birch Hill glacial ice can be seen on the opposite side of the Tasman valley about 150 m above the valley floor. The Birch Hill advance is attributed to a Late-Glacial interval of cool climate, within the period of ca. 11 to 14 ka (e.g. Speight 1963; Porter 1975; Birkeland 1982; Alloway et al. 2007).

Stop 2-5. Ostler Fault scarp at Lake Ohau Road (H39: 705463)

As the trip proceeds southwest along State Highway 8 from Ruataniwha Dam, note the c. 150 m high Ostler fault-line scarp 2 km NW of the road, with some landslides on the scarp face. The flat surface at the scarp crest is Table Hill, and is probably an early Balmoral, or possibly a Wolds, outwash surface (Mansergh & Read 1973; Read 1984). Further to the southwest, the fault forms a 20 - 30 m high scarp crossing a broad Mt John outwash channel extending from the LGM Ohau Glacier (Fig. 18). The trip proceeds west along Lake Ohau Road, crossing this scarp 300 to 500 m west of the highway. Note the presence of multiple small scarps in front of the main fault. The long-term average vertical slip rate is about 1 mm/year, judged by ca. 20 m of vertical separation across ca. 20 ka landforms (Davis et al. 2005).

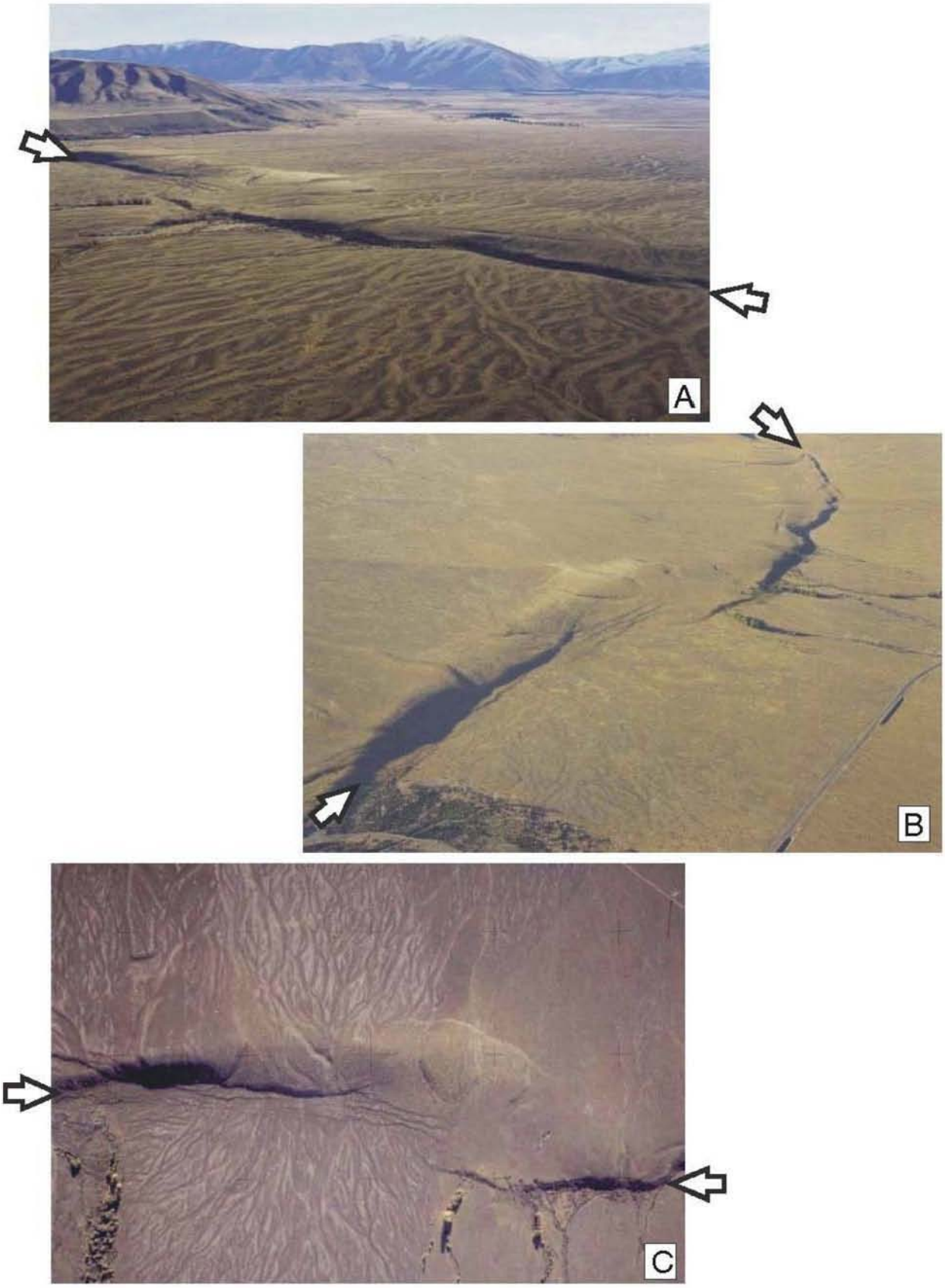

Fig 18. Complex surface deformation at the Ostler Fault, Lake Ohau Road. The LGM outwash plain (Mt John age) records the surface deformation that has occurred in several pre-historic major earthquakes over the past ca. 20 ka. Although displacements have broken out at distinct locations, there are also broad folds, up to 100 m wide, on the upthrown, hanging wall, side. Note the en-echelon step of this low-angle, purely dip-slip, thrust fault. Photo A looks west, B looks north and C looks northwest. Note the magnificent preservation of paleo-channels on this ca. 20 ka landform (From Van Dissen et al. 2003a).

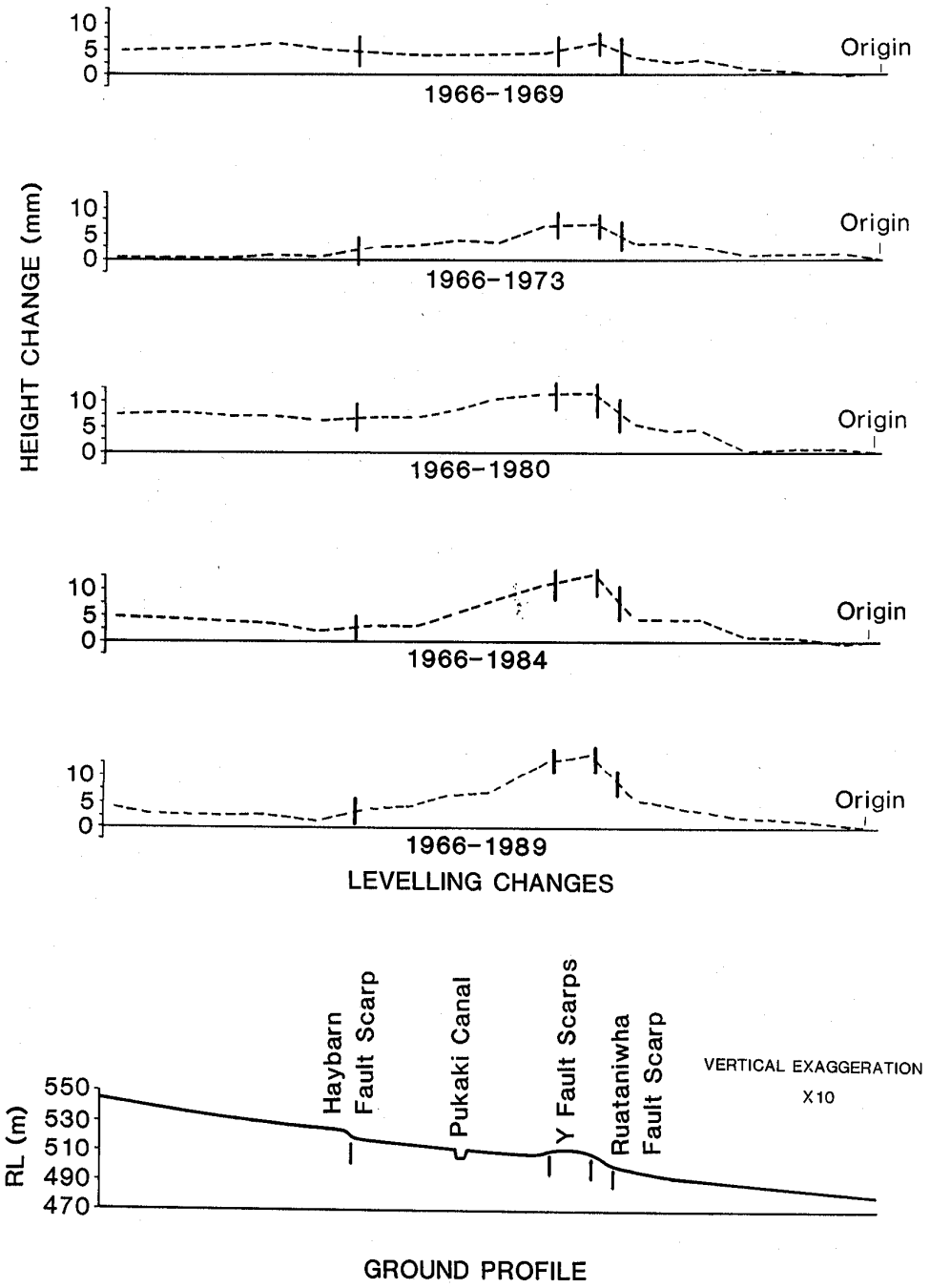

Fig 19. Differential aseismic deformation across the Ostler Fault Zone between 1966 and 1989 (from Blick et al. 1989).

The Ostler Fault is as good an example of Late Quaternary fault deformation as can be seen in New Zealand, because it affects relatively old landforms (LGM, ca. 20 ka). Although the Alpine Fault has a vertical slip rate that is an order of magnitude greater, it lies in a very active, high-precipitation landscape, with very young landforms that have not existed long enough to accumulate much deformation. In addition, the trace of the Alpine Fault is cloaked in rain forest for much of the length.

In the upper Twizel River (Duncan Stream), the Ostler Fault has ruptured, causing ground surface offset, at least three times in the past 10,000 years, with the most recent rupture about 3,600 years ago. At Lake Ruataniwha, the fault does not appear to have ruptured within at least the last 550 years (Van Dissen et al. 1993). Ministry for the Environment planning guidelines classify it as a Recurrence Interval Class II active fault, with an average duration of between 2,000 and 3,500 years for the recurrence of large earthquakes (MfE 2003; Van Dissen et al. 2003b) .

Back towards Twizel, immediately north of Ruataniwha reservoir, the Ostler Fault scarp is approximately the same height on the Mt John outwash surface as it is on the ca. 4,000 year younger Tekapo outwash surface. Clearly, no deformation occurred during that period, and shows that deformation occurs in discrete events, probably associated with large earthquakes. However, this is curiously at odds with the fact that the Ostler Fault is the only fault known in New Zealand to display present-day aseismic creep. Across the fault zone north of Lake Ruataniwha, levelling profiles detected upward buckling of the ground surface across the

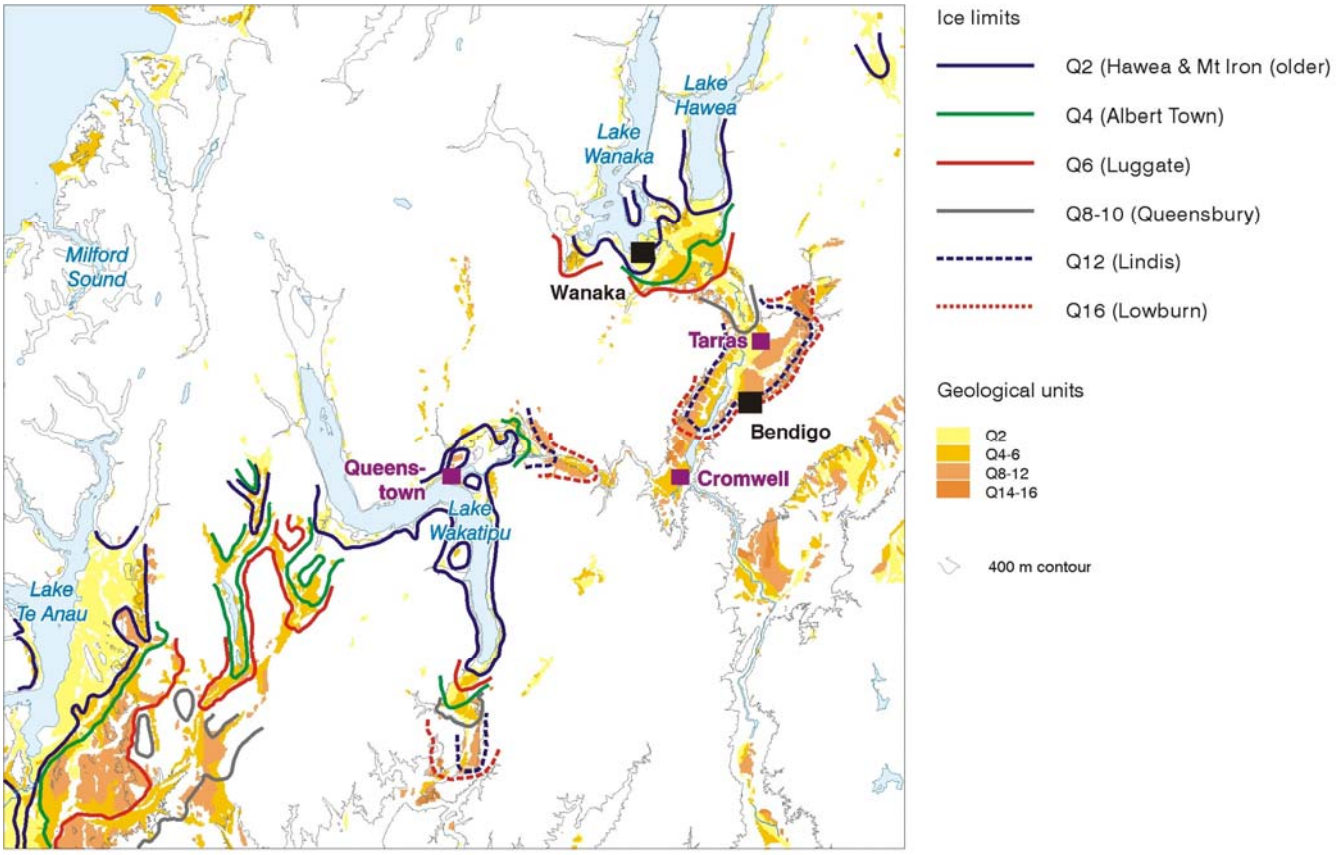

Fig 20. Ice limits of the main Central Otago catchments (from Turnbull 2000).

fault during the period 1966-1989 (Blick et al. 1989) (Fig. 19). This short-term rate of deformation is similar to the long-term average 1 mm/year vertical slip rate of the fault (Blick et al. 1989, Van Dissen et al. 1993). The differential tilting was sufficient that the turbines at Ohau-A hydroelectric power station, which straddles the tilt zone, have been placed on adjustable mounts. We do not the results of any post-1989 surveys, so cannot say whether the deformation is continuing at present. The origin of the creep is not known. The many possibilities include that it may be precursory to a major earthquake, or conversely that it might be emergent deformation resulting from a moderate-sized recent (e.g. last few hundred years) earthquake on the fault that was not quite strong enough to rupture the ground surface during the seismic event.

Stop 2-6. Ohau moraine/outwash complex (H38: 630507)

An array of LGM outwash plains and moraines are crossed by Lake Ohau Road. The outermost 'Mt John' moraines range in form from sharp bouldery ridges to more subdued, broad moraine topography that may have been partly over-ridden by ice. A gravel pit on Lake Ohau Road (H38: 628506) exposes the deposits within the more subdued moraines and shows a dominance of rounded outwash gravel, with no indications of angular detritus. We will drive to the shore of Lake Ohau, crossing an inner suite of nested moraines and outwash plains associated with the late LGM Tekapo advance.

As the trip returns to State Highway 8, note the backtilt of the Mt John outwash surface within 500 m of the upthrown side of the Ostler fault scarp, and in the same area, "islands" of slightly higher outwash surfaces that were elevated by fault rupture event(s) during deposition of the Mt John LGM outwash deposits.

Stop 2-7. Bendigo moraines, Clutha valley (G41: 224795)

The site of former 1860's gold rush town Bendigo lies on remnants of some of the oldest moraines in the Clutha catchment. The stop lies on an ice-sculpted rock bench with remnants of moraine, formed during the Lowburn advance (Fig. 20). An age of MIS 16 is tentatively inferred for this glacial episode (McSaveney et al. 1992; Turnbull 2000). Spectacular calcium carbonate accumulations (caliche) are found in places in the Lowburn Formation deposits. To the north is the extensive outwash/moraine complex of the Bendigo and The Bend terraces, mapped as Lindis Formation (McKellar 1960) and inferred to be of MIS 12 age (McSaveney et al. 1992; Turnbull 2000). The lower terraces and plains of the Clutha include outwash surfaces correlated with the Luggate (inferred MIS 6), Albert Town (inferred MIS 4) and LGM Mt Iron (earlier) and Hawea (later) advances. Note the extensive and locally nested fans at the foot of the Pisa Range on the west side of the Clutha River. Some of the older fans show buckling or offset associated with the active Pisa Fault Zone (Beanland & Berryman 1989).

The key point to appreciate from the view north is the vast extent of the Clutha Glacier during some previous glacial episodes, compared to its much smaller LGM ice extent. This contrast will become increasingly evident as we

proceed north up the Clutha valley to the LGM moraine complex at Wanaka.

A possible explanation that has been debated amongst geologists is that perhaps the Clutha used to have a more extensive larger alpine catchment. The very large Landsborough catchment, near Haast Pass, drains westward into the Haast River. Could it be that in the mid-Quaternary, it drained southeast to the Clutha, and provided sufficient ice catchment during glaciations to deliver ice as far south as the Bendigo – Cromwell area of the upper Clutha?

Day 3, Wanaka to Franz Josef (Almond)

Leaving Wanaka, we follow State Highway 6 to Hawea Township, then along the western shore of Lake Hawea. The road then traverses the eastern shore of Lake Wanaka, and continues on to Haast Pass, over the Southern Alps, following the Makarora River. From the pass the route follows the Haast River to Haast Township (136 km from Wanaka) on the piedmont plain of the West Coast. From Haast the highway parallels the Tasman Sea coast, crossing numerous large rivers contained within moraine-walled valleys, past the township of Fox Glacier (254 km) and on to Franz Josef (275 km).

From Wanaka to Haast a major change in vegetation occurs; from grassland/shrub association with varying components of indigenous and introduced species in the east, to a dense beech (Nothofagus) forest with some conifers (Podocarps) in the west. The persistence of large areas of unlogged forest in South Westland is a direct or indirect effect of high rainfall and steep topography. The limited desirability of most of the land for agriculture, and the isolation of the region (and importantly the distance from timber markets), saved much of the forest. Only the young and relatively fertile floodplains and part of the coastal strip have been cleared. Much of the area is now part of the South Westland World Heritage Area.

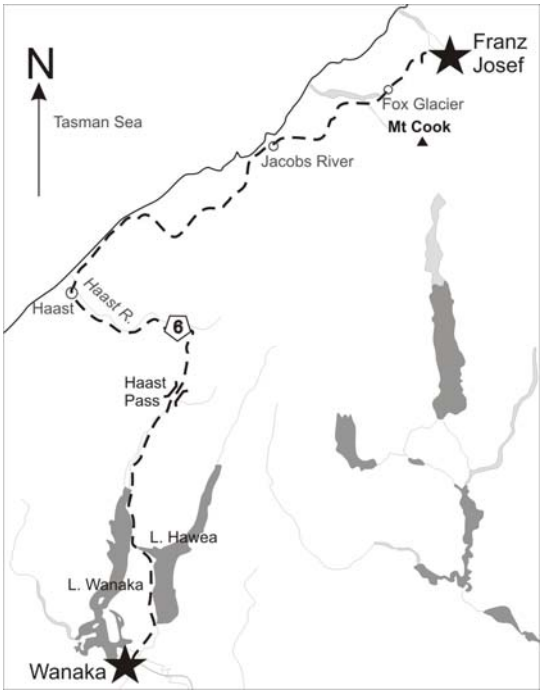

Stop 3-1 Haast sand dune geomorphology, forest succession, soil chronosequence and palaeoseismic record

The coastal plain from Jackson Bay to the Waita River, and the coastlines of bays associated with glaciated valleys further south are characterised by striking sequences of transverse dunes and inter-dune swamps. The area has been relatively little-modified by agriculture and the dunes

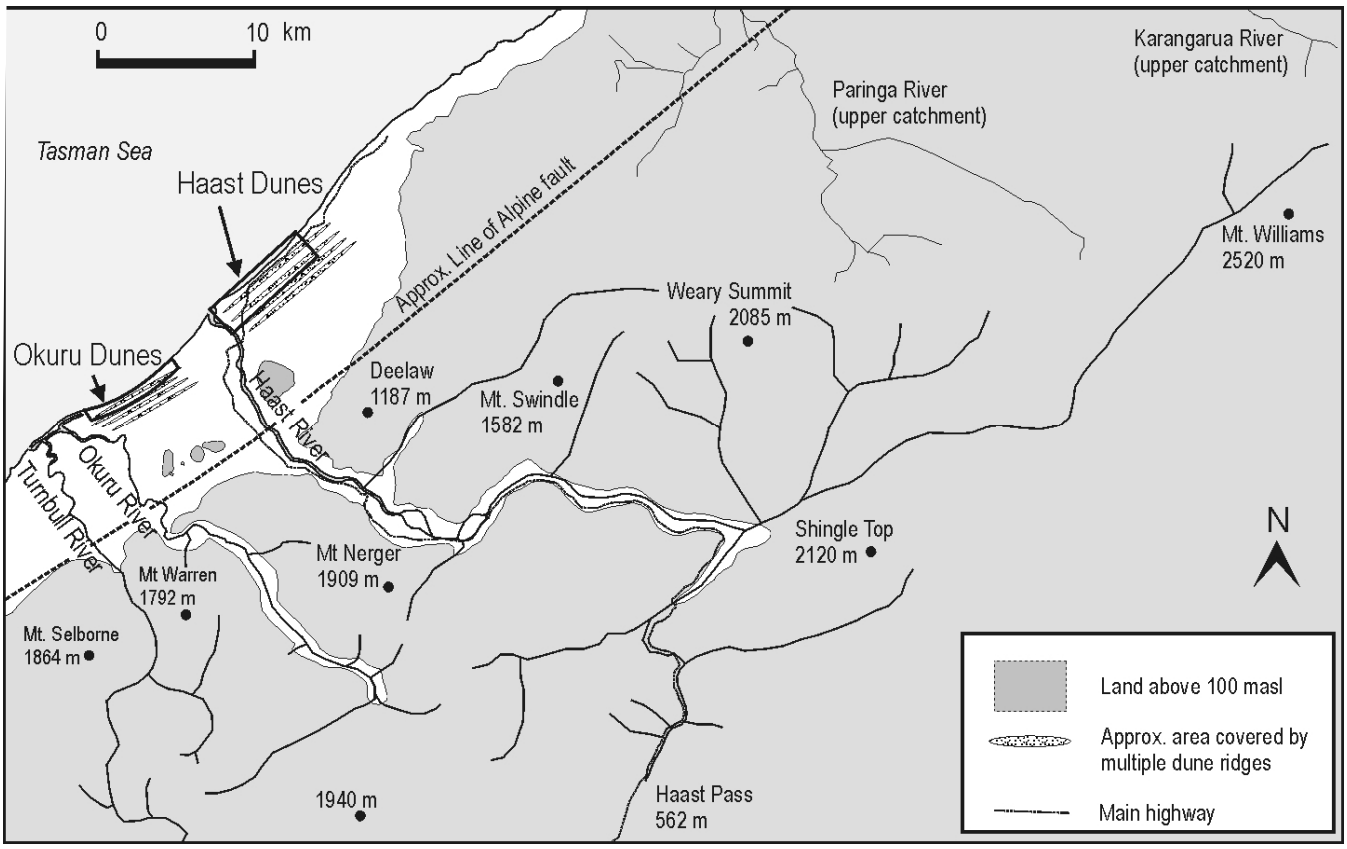

Fig 21. Location of the Haast and Okuru dune systems showing the Haast and Okuru Rivers and the location of the Alpine Fault (Modified from Wells and Goff, 2006).

remain largely covered by dense conifer-dominated forest including the podocarps rimu (*Dacrydium cupressinum)*, kahikatea (*Dacrycarpus dacrydioides)*, miro (*Prumnopitys ferruginea)*, *and* totara (*Podocarpus hallii)*. The interdune swamp vegetation includes a marginal shrub ecotone grading into flaxes, rushes, sedges, ferns and open water. The dune sequence points to episodic coastal progradation driven by influxes of sediment brought rapidly to the coast by the large rivers flowing from the Southern Alps. The sediment pulses have been postulated to have resulted either from periods of intense storminess punctuated by periods of relative quiescence, or from large earthquakes on the Alpine Fault. Recent work using the ages of trees on the dunes to determine the timing of dune building has elucidated an astonishing story of episodic, rapid coastal progradation driven by Alpine Fault earthquakes.

Wells and Goff (2006) used increment borers to take cores from at least 20 trees on each ridge-swale pair along transects across dune systems at Okuru and Haast (Fig. 21). Trees were sampled from dune crest, dune face (both seaward and landward) and inter-dune areas. A range of tree sizes were sampled including the largest trees at the sample sites. Tree ages were determined by counting annual growth rings from sanded cores. Age class distributions were then analysed to identify cohorts representing pulses of forest regeneration.

The analysis of tree ages identified four major pulses of forest recruitment. The spatial analysis of the associated cohorts of trees showed that successive cohorts established on land surfaces formed or made inhabitable by accretion of a new dune (Fig. 22). After a new dune formed, trees were able to establish on the seaward face of the youngest pre-existing dune, on the landward face of the new dune, and in the intervening inter-dune area. The fact that there was no systematic gradation in tree ages between the seaward face of the pre-existing dune and the landward face of the new dune indicates that dune accretion was very rapid.

The palaeoseismic record of the Alpine Fault, determined from dendrochronology, forest ages, radiocarbon dating of landslide and river aggradation deposits, and fault trenching, identifies four large earthquakes in the last 600 years. Those earthquakes occurred at AD 1826, AD 1717, AD 1615 ± 5, and AD 1460 ± 25 (Adams 1980; Cooper and Norris 1990; Wells et al. 1998; Yetton et al. 1998; Wells et al. 2001; Cullen et al. 2003). Allowing for a ca 28 year period between dune stabilisation and the time for establishment of trees and growth to coring height, (1 m) (Wells and Goff 2006), dune building happened between AD 1820-1850, AD 1700-1730, AD 1600-1630, and AD 1464-1495. The close correspondence between earthquake timing and dune building strongly supports a causal link.
The catchments of the Haast and Okuru Rivers lie within the steep, schistose mountains east of the Alpine Fault. The Landsborough River, which runs north for 50 km parallel to the axis of the Southern Alps, is a major tributary of the Haast. Sediment from widespread landsliding caused by shaking from the ca M8 earthquakes (based on fault rupture length) at the times given above would have made its way quickly to the coast, and been moved northwards by long-shore drift. Under current conditions the Haast River, has one of the highest sediment yields in the world, at about 12,736 t $km^{-2}yr^{-1}$ (Griffiths 1979). After an earthquake, the massive sediment flux is likely to overwhelm the transport

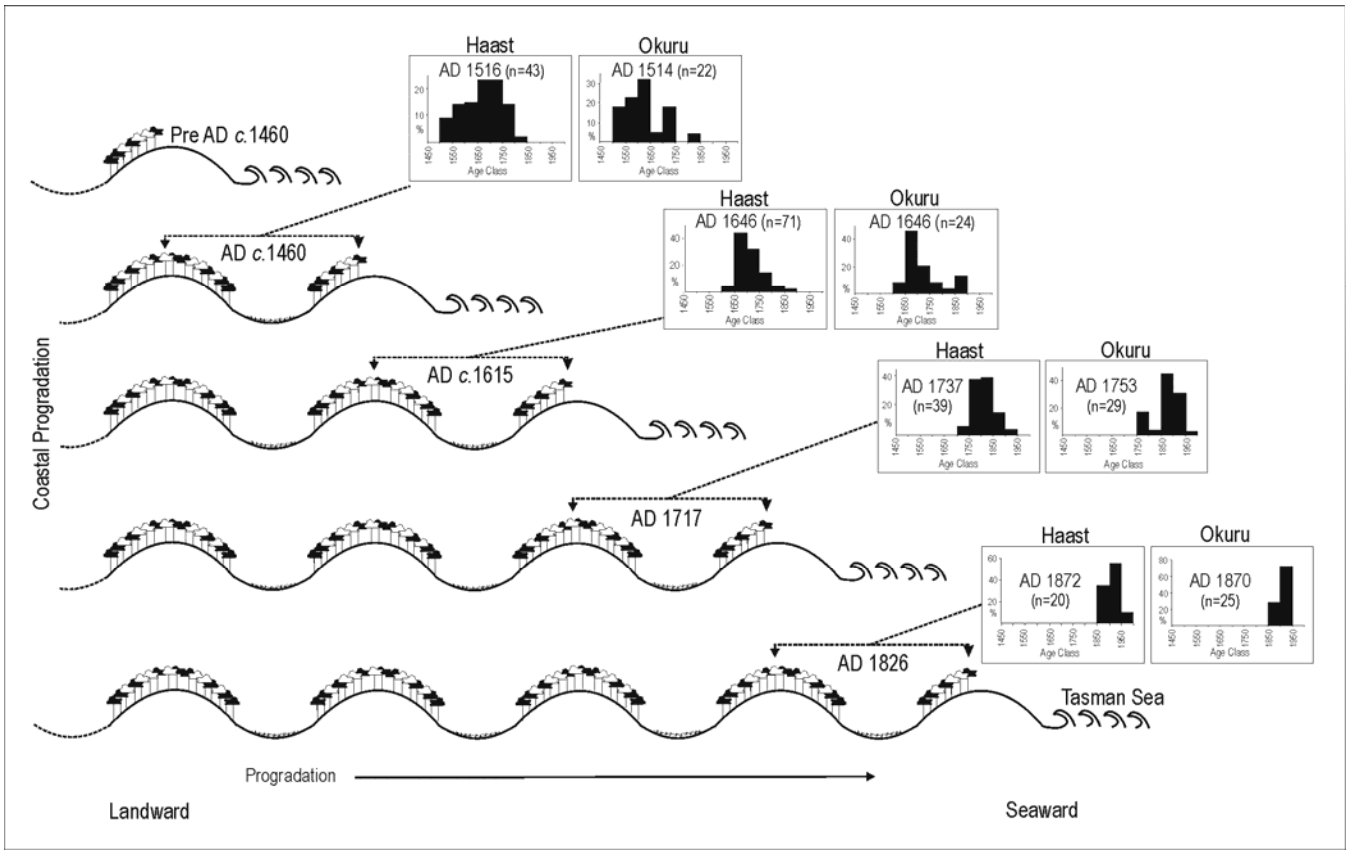

Fig 22. Distribution of tree ages across dune sequences at Haast and Okuru (see Fig. 21). Cohorts of trees establish on the landward side of the recently formed dune, the seaward face of the immediately older dune, and in the swale in between (Modified from Wells and Goff, 2006).

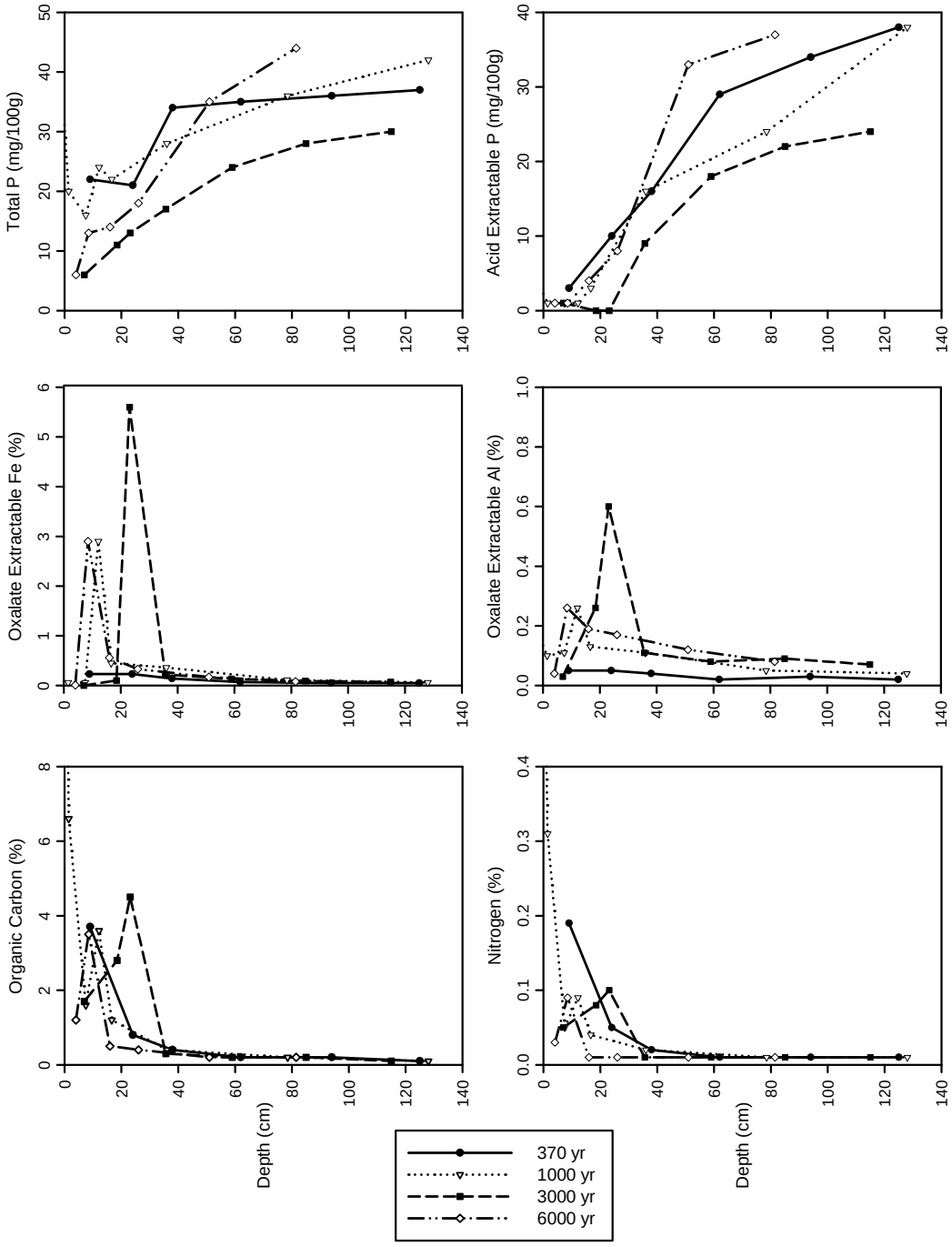

Fig 23. Soil chemical data from the Haast dune sequence.

capacity of the coastal system, causing progradation, and with it, large sand sources that allow transverse dunes to be formed by the persistent south-westerly winds. The picture evolving from the dunes near Haast complements findings from other studies of forest age and structure, lake sediments, and geomorphology, that suggest the present landscape, dynamic as it is, is relatively quiescent compared to the turmoil that follows Alpine Fault earthquakes. Serious consideration is being given to the readiness of West Coast communities for the next Alpine Fault earthquake, and their resilience in the face of the post-earthquake effects.

The Haast Dunes Soil Chronosequence

Within the context of very high erosion rates in the Southern Alps and high sediment yields to the lowland piedmont of Westland, episodic events occurring with different characteristic recurrence interval have produced arrays of geomorphic surfaces of different age. Storms occurring on annual to decadal timescales produce landslides and debris flows that form widespread erosional scars and runout deposits in the mountains (Hovius et al. 1997). Earthquakes on the Alpine Fault produce large landslide scars and runout deposits, river aggradation terraces and fan aggradation at centennial timescales, and climate change has produced sets of aggradation terraces and moraines at centennial to millennial timescales. These

age-sequences of landforms and the generally unmodified nature of the Westland landscape have presented many opportunities for studies of natural forest and ecological succession, and soil development (Stevens 1968a and b; Ross et al. 1977; Wardle 1980; Smith and Lee 1984; Sowden 1986; Tonkin and Basher 1990; Richardson et al. 2004). Studies of the effect of time on soil development where all other soil forming factors are essentially invariant are called soil chronosequences. The general pathway of soil morphological development for the high rainfall, strong leaching regime of Westland, elucidated by soil chronosequence studies, is as follows:

Recent Soils (Entisols, Regosols) with only an A horizon over a C horizon evolve typically within a few hundred years to Brown Soils (Inceptisols[1], Cambisols[2]), which have surface organic horizons, over an A horizon, which overlies a yellow-brown B horizon showing evidence of chemical weathering and soil structural development. With increasing time Brown Soils evolve to Podzols (Spodosols[1], Podzols[2]), in which acidification of the upper part of the soil in the presence of organic ligands derived from surface organic horizons leads to translocation of metal ions from surface to subsurface horizons. The morphological imprint of this process is the formation of a bleached upper eluvial (E) horizon, and a bright reddish brown illuvial (Bs) horizon, often associated with a dark brown organic rich (Bh) horizon. The rate of soil development increases with increasing rainfall (Tonkin and Basher 1990).

The Haast sand dunes have great potential for a soil chronosequence study because the ages of the dunes are well constrained at the young end of the sequence when soil development is rapid, the topographic factor remains constant across all dunes, and the soil parent material is expected to be homogeneous. Fig. 23 presents soil chemical data from soil pits dug on dunes about 50 m, 350, 940, and 1500 m in from the road. The pits were opened up in 1985 as part of a land resource assessment programme for South Westland. Dune ages are estimated to be 370 yr, 1000 yr, 3000 yr and 6000 yr respectively.

The data (Fig. 23) show trends consistent with other soil chronosequences in Westland (Tonkin and Basher 1990). Carbon content in topsoils increases across the two younger soils then decreases in the older soil as a result of increasing infertility. As topsoil C content decreases in the older soils, subsoil C content increases as a result of translocation of C complexed to metal ions. This is demonstrated by the large peaks in oxalate extractable Fe and Al in the 3000 yr old soil. The C trends are mirrored by nitrogen depth profiles.

The progressive weathering of the soils is well demonstrated by the total phosphorus curves. The 370 yr and 1000 yr old soils show a similar amount and depth distribution of P. The older soils are depleted in P, the 3000 yr old soil apparently more than the 6000 yr old soil. Ecosystem behaviour is strongly controlled by P availability; after P reserves are depleted, total biomass begins to decline in what is often referred to as a regressive phase. Acid extractable P is a commonly used measure of plant available P. Across the 370 yr to 3000 yr old dunes the soils show progressive depletion of acid extractable P, where it declines to 0 mg/100 g at about 20 cm depth in the 3000 yr old soil. The 6000 yr old soil is apparently out of place in the sequence according to this and other measures of soil development. Bioturbation – mixing of the soil profile probably by tree overturn – in the soils' history may

Dune	Hor.	Fe (%)	Ca (%)	K (%)	P (%)	Si (%)	Al (%)	Mg (%)	Na (%)	V (ppm)	Cr (ppm)	Ni (ppm)	Cu (ppm)
370 yr	Cu1	2.32	0.84	0.73	0.03	38.2	4.1	0.4	1.42	52.5	18.3	9.9	3.1
370 yr	Cu1	2.98	0.94	0.86	0.03	37	4.3	0.46	1.53	68.4	20.5	22.2	4
370 yr	Cu2	2.13	0.75	1.06	0.04	38	4.6	0.54	1.58	53.6	17.1	11.3	7
1000 yr	BC(g)	2.22	0.91	0.9	0.03	37.5	4.3	0.36	1.73	52.3	21.6	9.9	4.9
1000 yr	Cu	2.55	1.05	1.1	0.03	36.6	4.9	0.47	1.54	61.9	26.6	13.6	6.6
3000 yr	Cg	1.78	0.64	0.66	0.02	39.4	3.8	0.35	1.11	41.4	17.7	8.7	2.2
3000 yr	Cg	1.72	0.72	0.7	0.03	39.1	4	0.41	1.25	45.9	20.5	8.6	<1.9
3000 yr	Cg	1.85	0.72	0.75	0.1	39	4	0.4	1.8	46.7	17.9	10	2.4
6000 yr	BC1	3.35	1.17	0.8	<0.01	35.4	5	0.45	1.39	72.7	29.7	14	5.9
6000 yr	BC2	3.45	1.42	0.98	0.03	35.8	5.2	0.59	1.62	76.4	34.8	16.3	4.1
6000 yr	Cu	2.79	1.32	1.11	0.04	36	5.2	0.52	1.65	69.1	30.9	13.5	5.8

Dune	Zn (ppm)	Sr (ppm)	La (ppm)	Pb (ppm)	Zr (ppm)	Nb (ppm)
370 yr	29.8	179	27.3	10.4	168	9.7
370 yr	34.9	184	22.7	9.7	262	12.9
370 yr	40.8	185	18.8	9.5	144	6.9
1000 yr	32.5	205	29.8	7.9	193	13.9
1000 yr	38.8	233	33.6	7.1	266	18.6
3000 yr	26.9	160	28.7	<4.1	162	10.6
3000 yr	28.3	166	22.7	6.2	143	10.8
3000 yr	29.5	169	24.7	<4.1	152	10.7
6000 yr	38.1	262	72.2	8.6	426	24.3
6000 yr	41.9	275	58.7	7	416	26.4
6000 yr	43.4	273	40.3	7.5	258	19.8

Table 3. Total element data for C horizons of soils on the Haast dune sequence.

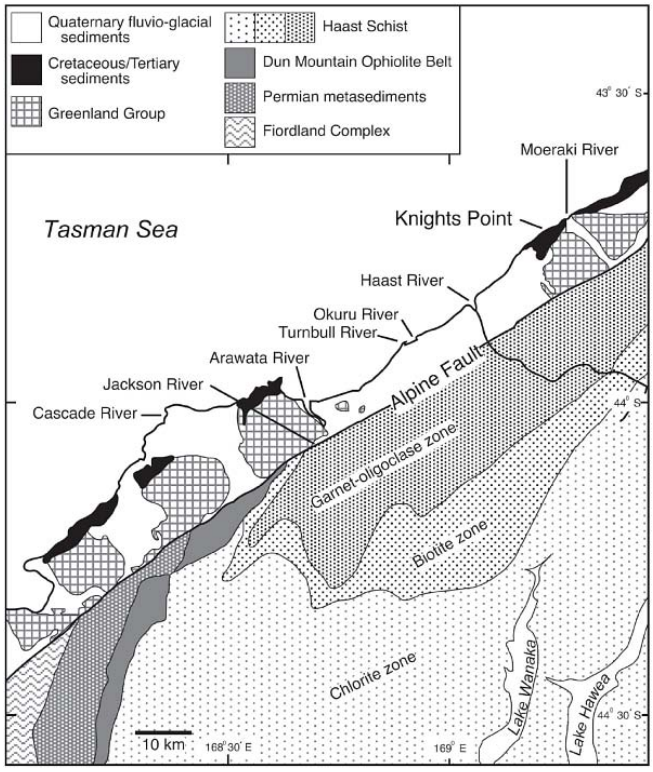

Fig 24. Knights Point location and simplified regional geology (from Cooper and Kostro, 2006).

have had the effect of rejuvenating it, or there may be some parent material effect that is unaccounted for (Table 3).

[1] Soil Survey Staff, 1999. Soil taxonomy : a basic system of soil classification for making and interpreting soil surveys, 2nd Edition. U.S. Dept. of Agriculture Natural Resources Conservation Service, Washington, DC, 869 pp.
[2] IUSS Working Group WRB. 2006. World Soil Resources Reports No. 103. FAO, Rome

Stop 3-2. Knights Point Marine Terraces

Just north of the Waita River S.H. 6 leaves the coastal plain and winds its way through steep hilly terrain formed into Cenozoic sedimentary rocks. Near-vertical coastal cliffs can be seen plunging to the Tasman Sea, where waves driven by the persistent westerlies break around stacks and against the bouldery coastline.

In the vicinity of Knights Point a flight of marine terraces cut into the Cenozoic sediments near the coast, and into hard Paleozoic greywackes of Greenland Group is preserved (Fig. 24). As part of a wider analysis of uplift rates adjacent to the Alpine Fault in Westland, Bull and Cooper (1986) used the altitudinal spacings of terraces at Knights Point and compared them to the spacings of the well dated Papua New Guinea marine terraces (Chappell and Shackleton 1986) to determine an uplift rate on the west side of the Alpine Fault in this southern part of South Westland of 0.87 $mmyr^{-1}$. Their estimate of uplift rates on the east side of the fault were an order of magnitude greater but the validity of these estimates has been drawn into question (Ward 1988) owing to uncertainty as to whether or not the bench-like features they recognised were indeed of marine origin. Bull and Cooper (1986) did not explicitly describe the terrace heights and distributions they used in their analysis, but it seems as if the 115 m AMSL terrace at Knights Point was assigned an age of 120 ka.

More recently, Cooper and Kostro (2006) carried out a detailed study of the sedimentology, stratigraphy and provenance of the terrace coverbeds, and produced an OSL age from beach sands (Figs. 25 & 26). They concluded that the beach environment at the time of cutting of the marine strath was a high energy environment similar to today, and, on the basis of heavy mineral assemblages, that although most of the sediment was Haast River-derived, longshore transport was capable of moving sediment from the Dun Mountain ophiolite belt, ca 70 km to the south. Two OSL samples were taken from the upper unit (Facies 7 Fig. 26) at 1.0 m and 4.0 m depth, which is an upward fining, coarse to medium sand interpreted as accumulating at the culmination of sea-level rise. The age from the lower sample was discounted on account of radioactive disequilibrium in the samples taken for dose rate estimation. The upper sample produced an age of 123 ± 7 ka (1 σ), on the basis of which the terrace was correlated to MIS 5e. The uplift rate at Knights Point based on this correlation is 0.86 $mmyr^{-1}$.

From Knights Point S.H.6 passes the glacial lakes Moeraki and Paringa, then traverses the floodplains of large rivers flowing from the Southern Alps. The piedmont reaches of

Fig. 25. The Knights Point terrace coverbeds (from Cooper and Kostro, 2006, *reproduced with permission of RSNZ—Publishing*)

these river valleys are bounded by lateral moraines or glacially modified, Palaeozoic sedimentary or crystalline rocks. In this part of South Westland the piedmont is narrow, and we are never far from the Alpine Fault or the Tasman Sea.

The Paringa River has produced a key radiocarbon date for the timing of the deglaciation following the LGM in Westland. About 1 km upstream of the Alpine Fault, shells dated at 14,200 ^{14}C yr BP (ca 16,500 cal. yr BP) (Suggate and Almond 2005), have been uplifted. Valleys like the Paringa in South Westland soon became fiords after deglaciation, which were then rapidly infilled with alluvium.

The Franz Josef Glacier and the Waiho Loop late glacial moraine

Stop 3-3. Canavans Knob

The Franz Josef Glacier along with Fox Glacier are two of the most accessible glaciers in the Southern Alps, flowing to as low as 300 m AMSL. These glaciers are fed from very high snowfall rates (> 10 m rainfall equivalent, Henderson and Thompson 1999) in the highest mountains of the Southern Alps (>3000 m). Franz Josef glacier is 35 km^2 in area and descends ca 11 km from about 3000 m altitude to just less than 300 m AMSL, where the mean annual temperature is 11 °C (Anderson and Mackintosh 2006). West of the Alpine Fault the Waiho River flows across a broad alluvial fan bounded by 400 m high lateral moraines dating from the LGM. Lake Mapourika was formed after the post-LGM collapse of a lobe of the Franz Josef (Waiho Glacier). The terminal moraine of the Waiho Glacier was some 5 km off the present shoreline (Fig. 27, A and B).

The late glacial Waiho Loop moraine has been the focus of much attention (e.g. Mercer, 1988; Denton and Hendy, 1994; Anderson and Mackintosh, 2006). Denton and Hendy (1994) produced 37 radiocarbon dates from wood within a diamicton, presumed to be related to the Waiho Loop at Canavans Knob (our Stop), in order to test hypotheses of forcing of Southern Hemisphere glaciation. On the basis of their error-weighted average age of 11,050 ± 14 ^{14}C years BP they concluded there was Southern Hemisphere cooling coeval with the Younger Dryas, which they then argued supported a hypothesis of near-simultaneous atmospheric transmission of Northern Hemisphere cooling, rather than cooling via ocean transmission via thermohaline circulation. These claims were immediately disputed (e.g. Mabin, 1995). David Barrell's reanalysis of the ages from Canavans Knob (in Alloway et al. 2007) and comparison with ice cores from Greenland and Antarctica suggests the Waiho Loop advance was underway before the Younger Dryas chron, and in fact overlaps the Antarctic Cold Reversal (ACR) and the Younger Dryas (Fig. 28).

Alternative hypotheses stressing a greater importance of more local origins for Southern Hemisphere glaciation have since been advanced. From a detailed and long pollen record from Okarito Bog (Fig. H) Vandergoes et al. (2005) proposed Southern Hemisphere glaciation corresponded with orbitally controlled insolation minima, and Sutherland et al. (2007) reached a similar conclusion on the basis of exposure ages from moraines in the Cascade Plateau south of Haast. In contrast, Shulmeister et al. (2004) have argued

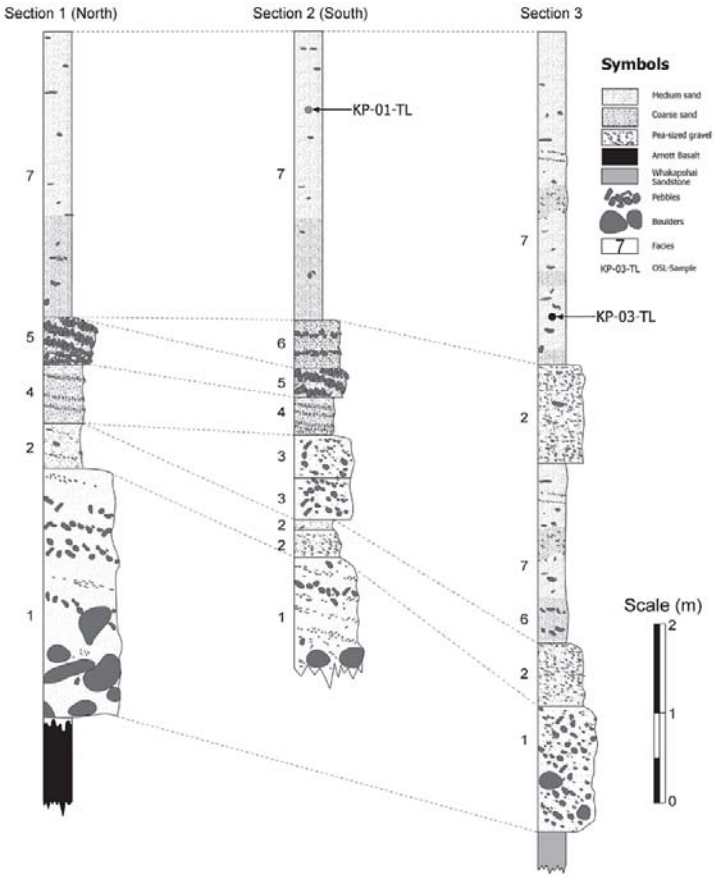

Fig 26. Stratigraphy of the Knights Point section (from Cooper and Kostro, 2006, *reproduced with permission of RSNZ—Publishing*).

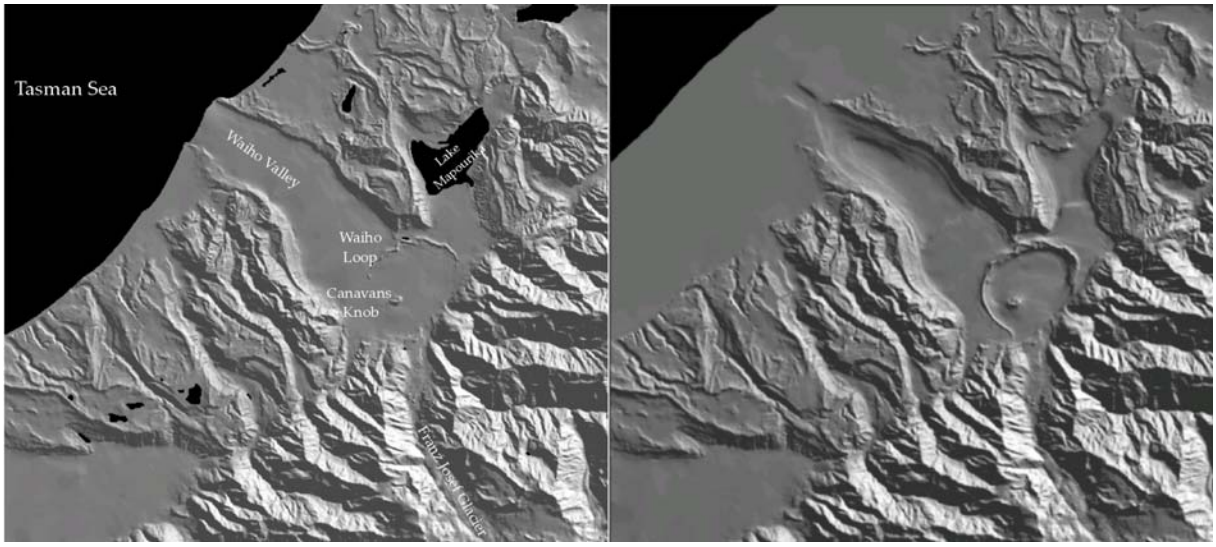

Fig 27. The Franz Josef glacier. A. Locations and features of relevance in the Waiho Valley. B. Waiho Glacier reconstruction for ca 11 ka.

that glaciation in the Southern Alps could be the result of increased precipitation arising from strengthened westerly winds during precessional minima. This hypothesis was based partly on historical responses of the Franz Josef glacier to El Niño-related increases in prevalence of south westerly winds. Using a process-based numerical model paramaterised for the Franz Josef Glacier at the time of the Waiho Loop advance, Anderson and Mackintosh (2006) challenged the latter hypothesis by showing that a precipitation increase of 350 to 450% above present was needed to drive the Franz Josef Glacier to the approximate position of the Waiho Loop moraine, whereas the same could be achieved with a 4.1-4.7°C cooling. Milder cooling of 1 to 2 °C would require a precipitation increase of over 100% above the present world maximum precipitation (Fig. 29). While not discounting increases in precipitation as a contributing factor, the authors favoured the cooling scenario because of the apparent synchronicity of the Waiho Loop advance with the ACR, at which time Antarctica cooled by 4°C and other areas of New Zealand appeared to have responded likewise (Newnham and Lowe 2000; Turney et al. 2003; Vandergoes et al. 2005). On these grounds they favoured a thermohaline circulation mode of inter-hemispheric teleconnection.

Rother and Shulmeister (2006) working on general glacial forcing in the Southern Alps, rather than the specific case of the Franz Josef, argued that the precipitation required to trigger glacial advances is already present as rain (there is a roughly 50:50 rain-snow split at the snow line on the western side of the Southern Alps) – and that minor temperature changes at the snowline can trigger significant advances. Furthermore, several authors have highlighted the singular nature of the Waiho Loop. It is the only major late-glacial re-advance moraine west of the divide, while several are observed on the eastern side (e.g. the Birch Hill Moraine from Day 2). Shulmeister et al., (2005) have consequently argued that only glaciers with very high elevation catchments re-advanced during the late-glacial and they consequently favour a precipitation forcing mechanism .

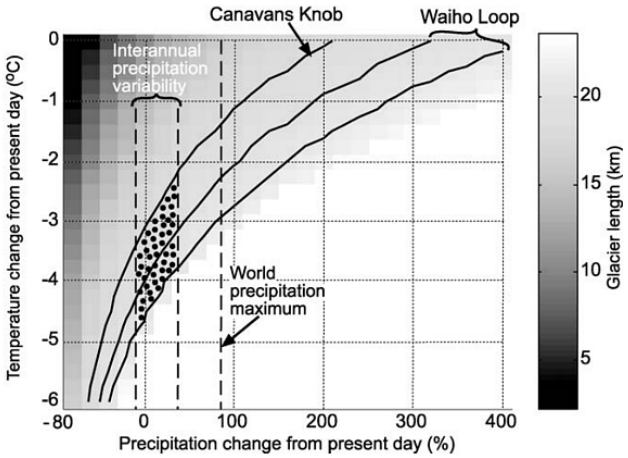

Fig 29. Sensitivity of the Franz Josef glacier to temperature and precipitation changes relative to present day (from Anderson and Mackintosh, 2006).

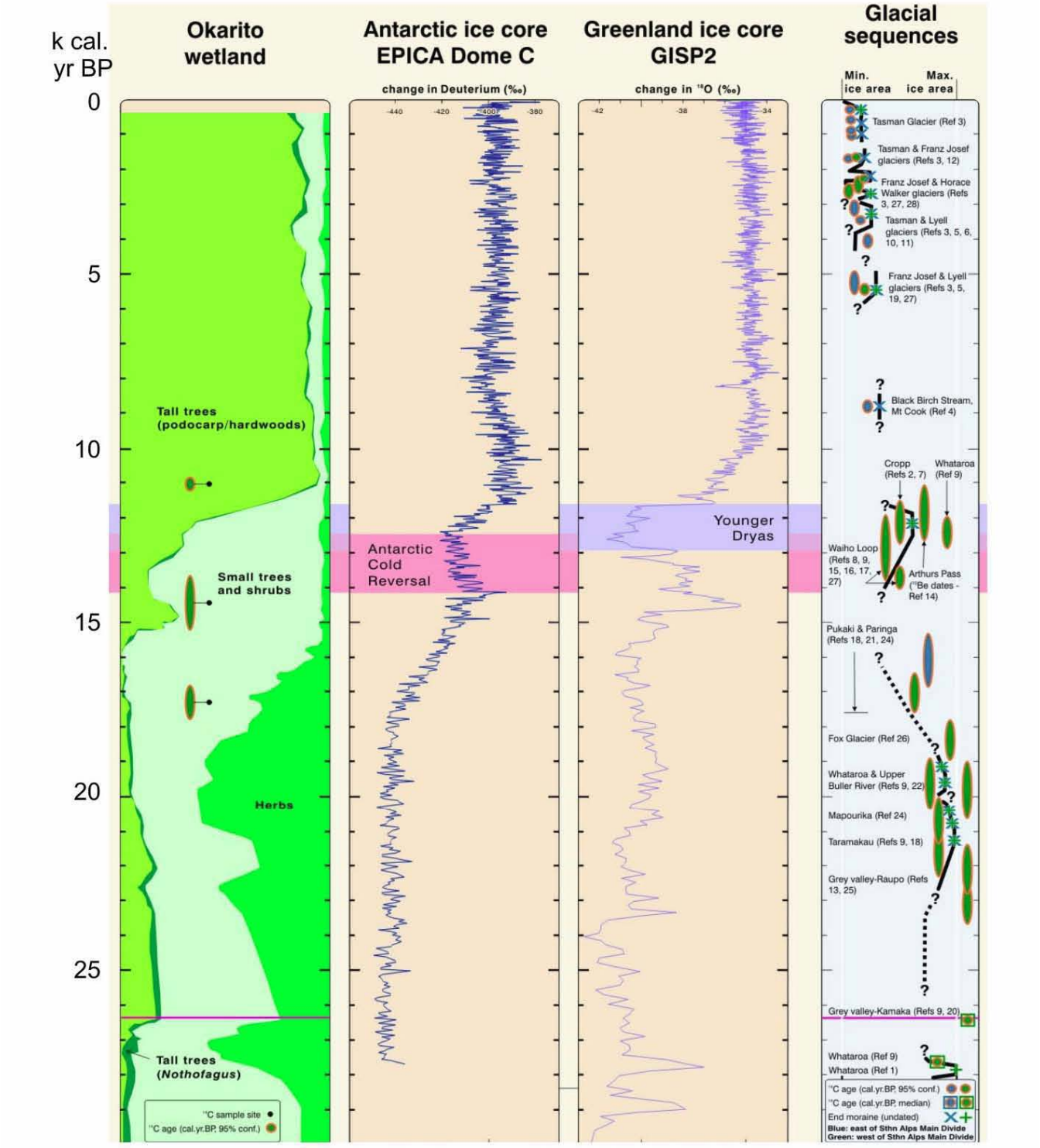

Fig 28. Okarito pollen record, Antarctic EPICA Dome C and Greenland GISP2 d^{18}O records, and glacial advances of the Southern Alps (adapted from Barrell et al., 2005)

Day 4. Franz Josef to Hokitika (Almond and Vandergoes)

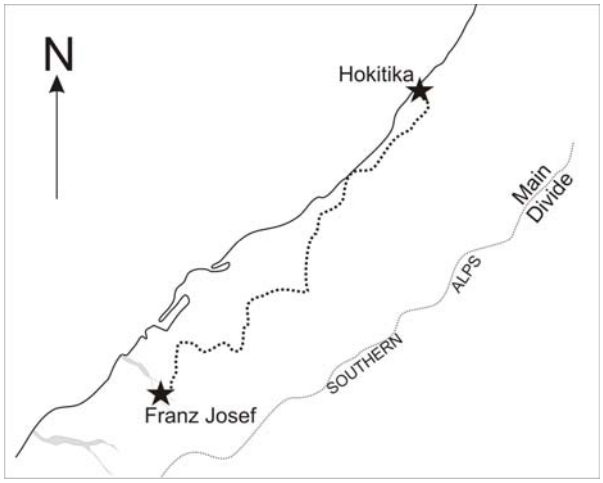

Post-glacial behaviour of Franz Josef Glacier

From Canavans Knob our route takes S.H.6 to the bridge over the Waiho River and then follows the glacier access road on the true left of the river to Franz Josef Glacier. We will view the glacier from Sentinel Rock, and take a walk to near the terminal face, or across the young moraines down valley, depending on time and the weather conditions.

Stop 4-1. Sentinel Rock

After the Waiho Loop advance, the next advance of the Franz Josef Glacier, sometime before 4730 ± 75 ^{14}C yr BP, remained within the alpine valley, but nearly reached the range front (Fig. 30). The next set of advances, corresponding with the Little Ice Age, built moraines at ca. AD 1500, AD 1750, AD 1830, each advance being smaller than the previous. By AD 1880 an advance left till at Sentinel Rock, and minor advances occurred at AD 1909 and AD 1934. The 1930s marks the beginning of a sustained period of rapid glacier retreat, punctuated by minor re-advances in the late 1940s and 1960s, culminating in a minimum glacier length in the early 1980s. From the mid 1980s the glacier began advancing and presently has re-advanced to about the 1960 position (Figs. 30, 31). Hooker and Fitzharris (1999) carried out a correlation analysis of glacier behaviour and various climate data, including precipitation, temperature, and indices of atmospheric circulation between 1955 and 1994. They concluded that much of the behaviour through this time could be explained by variation of atmospheric circulation (Table 4).

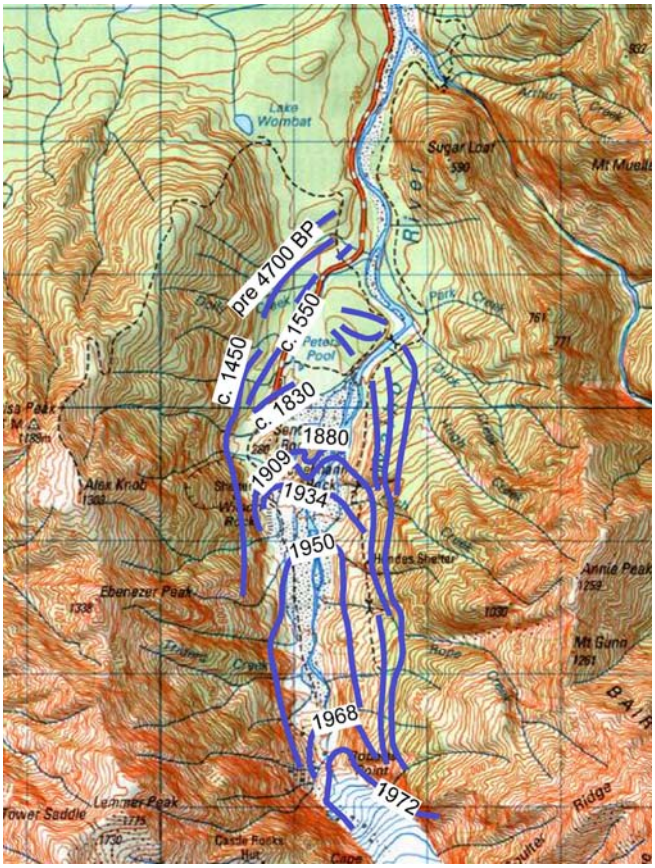

Fig 30. Postglacial advances of the Franz Josef glacier (adapted from Wardle, 1973).

Anderson et al. (2006) came to a different conclusion, showing glacier mass balance changes were most strongly correlated with summer temperature. Anderson et al. (2006) developed a degree-day glacier mass balance model that calculates ablation from air temperature, accumulation from

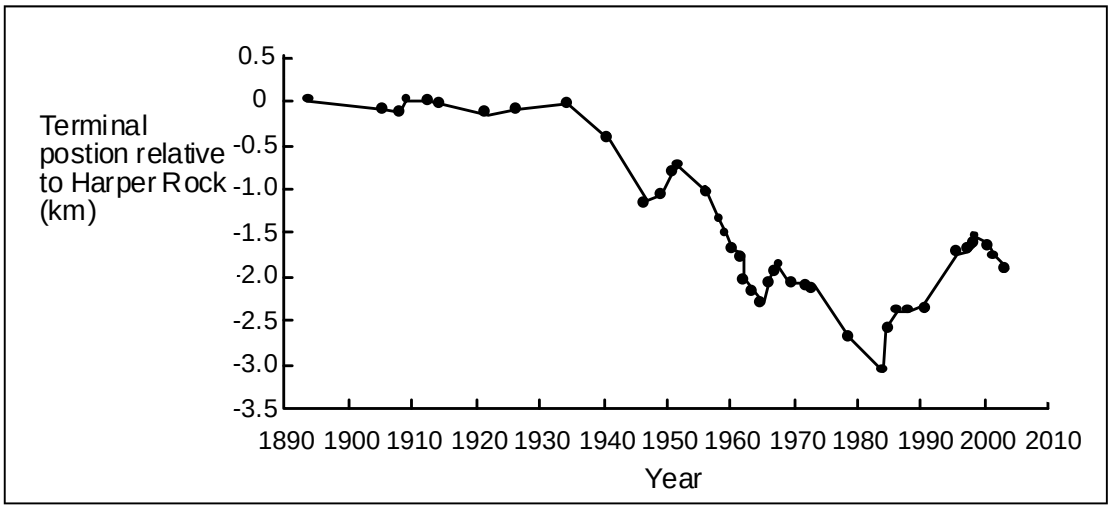

Fig 31. Terminal position of Franz Josef glacier relative to Harper Rock (just up valley of Sentinel Rock) for the period 1890 to 2005 (Anderson et al., 2006).

Retreat phase	Advance phase
Drier	Wetter
Warmer in ablation season	Cooler in ablation season
Weaker westerlies in accumulation season	Stronger westerlies in accumulation season
Westerlies further south	Westerlies further north
Subtropical high pressure zone further south in ablation season	Subtropical high pressure zone further north in ablation season
Anomalous northeast flow in accumulation season	Anomalous southwest flow in accumulation season
Positive pressure anomaly over New Zealand in ablation season	Negative pressure anomaly over New Zealand in ablation season
Positive SOI	Negative SOI (El Niño)

Table 4. Summary of climate parameters with significant differences between the retreat and advance phases of Franz Josef Glacier (from Hooker and Fitzharris, 1999)

precipitation, and the balance as mass accumulation/loss. The model calculates daily mass balance from daily climate data transformed by empirical functions, derived from detailed climate data, to account for sub-daily variation. It assumes elevation is the only source of spatial variation. Elevational trends in precipitation and temperature were based on local instrumental records, and the model was driven by a long (1890 to present), high quality meteorological record from Hokitika, 100 km to the north. Comparison of the Hokitika record with a short Franz Josef record allowed appropriate data transformations to be defined. They showed that periods of positive and negative mass balance corresponded with periods of glacier advance and retreat, respectively, but that the magnitudes of the mass balance excursions and the magnitudes of shifts of terminal position were not well correlated. They attributed this to the vagaries of ice flow dynamics. They argued that because of the strong non-linear response of the glacier to mass balance changes, correlation analysis between glacier length and climate variables (c.f. Hooker and Fitzharris 1999) may not be appropriate. The best correlation coefficients they got (r values) were 0.88 for summer temperature and 0.41 for annual precipitation.

The Franz Josef chronosequence

The array of moraines of different age covered by unmodified vegetation has been the basis for important studies of vegetation succession and soil evolution (Table 5). Walker and Syers (1976) seminal study of the temporal variations in the forms and amounts of phosphorus in soils, and the implications for ecosystem function, was based heavily on the chronosequence study carried out by Stevens (1963; 1968).

STOP 4-2 Okarito Bog Vegetation and Paleoclimate Record

Okarito Pakihi (Bog)[1] is situated close to the present coastline of south Westland (43^o 14’ 30”S, 170^o 13’E, 70 m above sea level), on the formerly glaciated western foreland of the Southern Alps. During the Pleistocene, repeated expansion of alpine glaciers from these ranges extended at times to beyond the present coastline in the west. As a result, surface deposits in Westland provide a complex record of late Quaternary glaciation (Suggate and Almond, 2005), which has been linked to global climate change (Denton and Hendy, 1994; Lowell et al., 1995; Vandergoes et al., 2005, Newnham et al., 2007).

Okarito Bog is a moraine impounded peat bog situated outside the limits of ice advance during the Last Glacial Maximum (LGM). As suggested below, the bounding moraines are likely to have formed during a period of extensive glaciation that preceded the Last Interglacial. Atypically in many glacial environments, the subsequent depositional situation at Okarito Bog remained intact during successive phases of regional glaciation, largely because of ongoing north-eastwards lateral displacement of the Westland foreland across the Alpine Fault (Wellman and Wilson, 1964; Norris and Cooper, 2001). As a consequence, valleys and glacial deposits to the northwest of the fault become dislocated from their source areas to the southeast and thus protected from erosive ice or meltwater discharge during subsequent advance and retreat phases. A displacement rate of 2677 mm/yr across the Alpine Fault has been estimated at sites from South Westland, resulting in the offset of LGM moraines by 4407m (Sutherland and Norris, 1995). Lowland podocarp/hardwood forest dominated by *Dacrydium cupressinum* surrounds the site, montane and subalpine low forest and shrubland occurs regionally between 400 and 1,200 m AMSL and alpine grassland above 1,200 m AMSL. (Wardle, 1979).

Vandergoes et al. (2005) recovered multiple cores from Okarito Bog using a 5-cm-diameter square-rod piston corer and Russian D-section corer which provide the basis for detailed palynological investigations. They developed an independent chronology by AMS radiocarbon dating organic sediments in the upper part of the sequence, OSL dating inorganic silts in the lower part, and utilising a unique tie point provided by the ca 26.5 cal ka Kawakawa Tephra (Fig. 32). The extensive dating was carried out in an attempt to circumvent the reliance on orbital tuning as a primary means of establishing age control. In this study they utilised the distinct altitudinal zonation in the modern vegetation, which is mainly controlled by temperature (Wardle, 1979), as a means for linking major change in the pollen assemblages at the study site to climate change and in particular temperature variation over time.

The pollen profile extends from near present back to Marine Isotope Stage (MIS) 6 and provides a continuous record of vegetation and climate change for the past two glacial cycles (Fig. 33). The pollen record indicates that

Estimated age of surface (yr)	5	10	50		150	500	1,000 2,000	5,000	13,000
Vegetation phase	pioneer →	early transitional scrub	→	early transitional forest low forest	→	transitional rata forest →	transitional to mature kamahi-mixed podocarp forest →	mature rimu-kamahi forest	
Prominent plant species	bare rock debris with *Epilobrium* spp., h *Raoulia* spp., h *Poa Novaezelandiae*, hg *Racomitrium crispulum*, hm *Stereocaulon* sp., l	*Carmichaelia grandiflora*, s* *Olearia avicenniaefolia*, s *Coprosma rugosa*, s *Coriaria arborea*, s*	*Olearia*, s *Coriaria*, s* *Schlefflera digitata*, t *Melicytus ramiflorus*, t *Pseudopanax colensoi*, s		*Aristotelia serrata*, t *Fuscia excorticata*, t *Griselinia littoralis*, t *Hoheria glabrata*, t	*Metrosideros umbellata*, t *Weinmannia racemosa*, t *Carpodetus serratus*, t	*Weinmannia*, t *Prumnopitys ferruginea*, tp *Podocarpus hallii*, tp *Dacrydium cupressinum*, tp other angiosperm trees, *Cyathea* sp. tf	*Dacrydium cupressinum*, tp *Weinmannia*, t *Quintinia acutifolia*, t other podocarps and angiosperms trees	
Rate of change	very rapid	rapid	rapid but slowing			slow	slow	very slow	
Soil profile form	L C	L,F,H weak A C	L,F,H A C				L,F,H Ah Bg Bw Cr	L,F,H Ah Br Bw Cg	O Er Bs 2Bg 2C
Soil class	Raw Soil	Typic Orthic Recent Soil	Typic Orthic Recent Soil		Acidic Orthic Recent Soil	Acidic Weathered Recent Soil	Acidic Orthic brown Soils	Mottled Acid Brown Soil	Typic Perch-gley Podzol
Key									
h herb (g = grass, m = moss) l lichen s shrub (*with nitrogen fixing symbiont)					t tree	tf treefern	tp podocarp (gymnosperm)		

Table 5. Soil and vegetation development along the Franz Josef chronosequence (adapted from Stevens, 1963; Stevens, 1968a; Wardle, 1980)

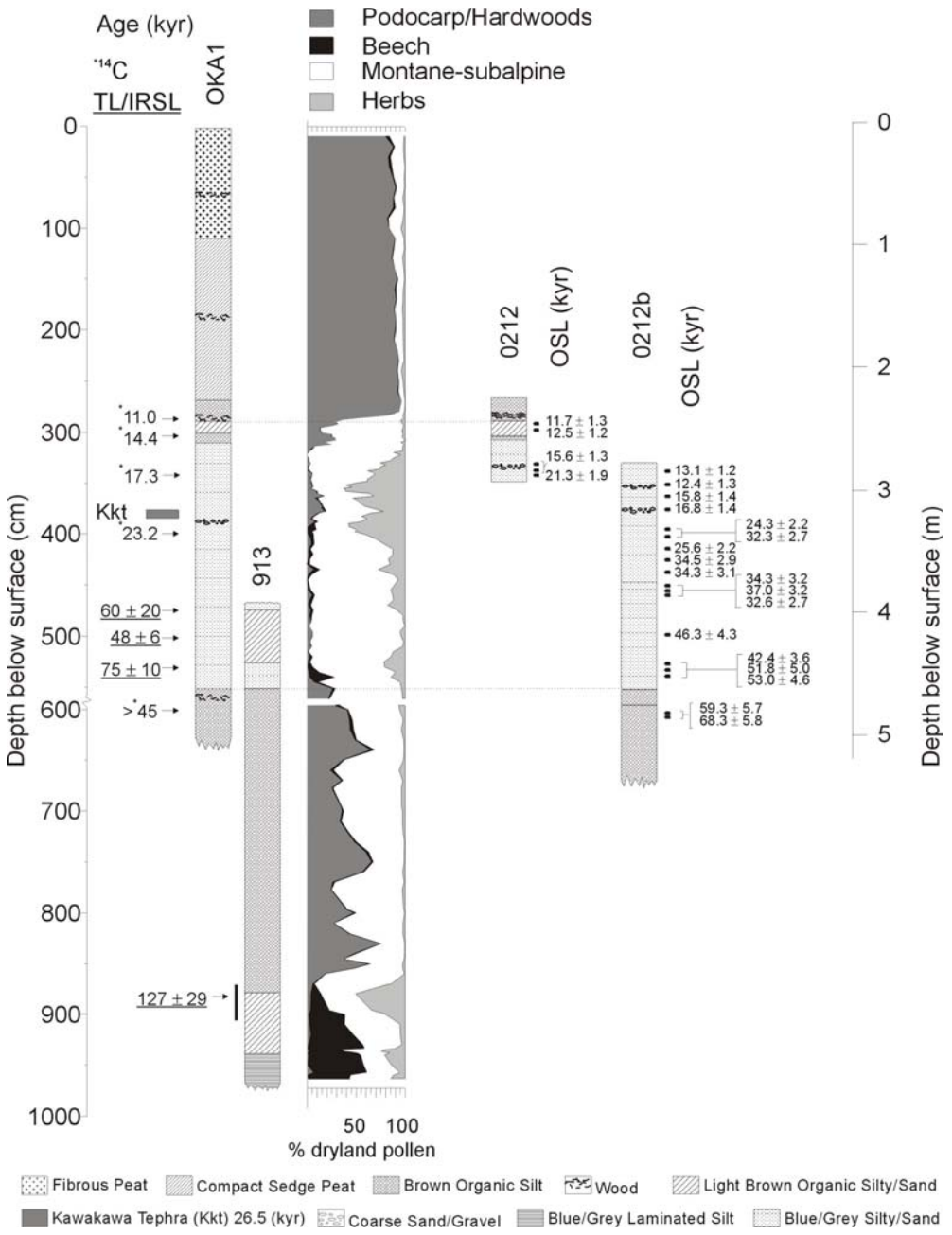

Fig 32. Lithostratigraphy, chronology and summary palynology of critical cores from Okarito Pakihi Bog. From left to right: Radiocarbon (cal ka) and OSL ages from OKA1 and 913, summary pollen diagram from OKA1 and 913; OSL ages from 0212 and 0211b (From Vandergoes et al., 2005)

both organic units in the core stratigraphy are dominated by pollen of tall podocarp forest, with *Dacrydium cupressinum* the predominant taxon, although subalpine podocarp taxa *Phyllocladus* and *Halocarpus* are a strong but variable component of the lower organic silts. In contrast, the two inorganic (micaceous) units are dominated by pollen from grasses, other dryland herbs, subalpine forest and shrubs in varying proportions (Fig. 33).

Vandergoes et al. (2005) and Newnham et al. (2007) indicate that there is good correspondence between inferred periods of substantial treeline depression represented by increased abundance of grass pollen in the pollen profile and the record for ice advance in this region (Table 6). More grass-inferred cooling events are evident in the pollen record than recognised moraines, however, presumably due to the fragmentary nature of glacial geomorphology. The pollen record also shows broad consistency with the MIS record and hence with the Milankovitch orbital forcing model. These features include the 5-fold subdivision of MIS 5 and the periods of cooling indicated during MIS 4 and 2 (Fig. 34). However, Vandergoes et al. (2005) and Newnham et al. 2007 suggest that there are some departures from this pattern, including an early onset to the LGM and several sub-Milankovitch scale events, such as a mid-LGM warming and Lateglacial reversals during both the last and the penultimate deglaciation. Based on the consistency of these patterns in other mid-southern latitude records, they propose that departures such as the early onset of the LGM may be driven by a regional insolation minima reached at 35–30 kyr ago and propagated across the Southern Ocean by geophysical phenomena related to the Antarctic ice sheets, in particular, meridional displacement of sea ice, the circumpolar current system and related westerly winds. They argue that at times, regional insolation variation may

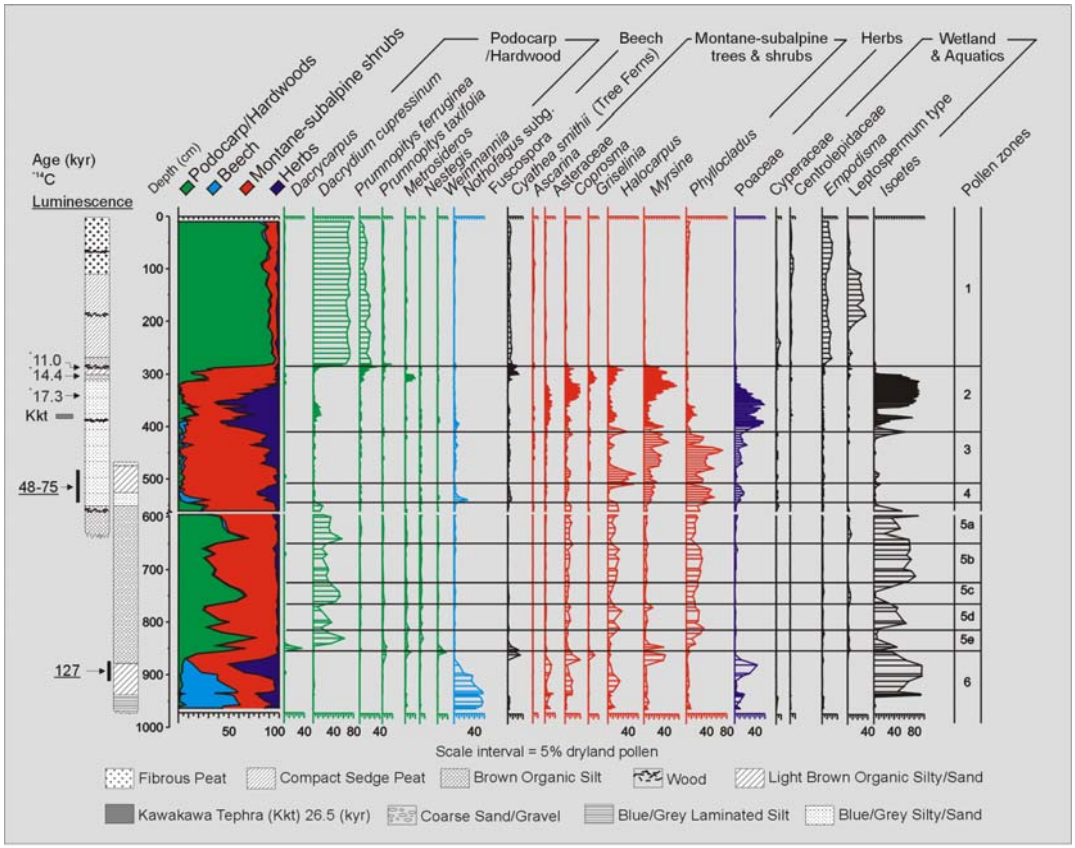

Fig 33. Condensed pollen diagram from Okarito Pakihi. Luminescence ages (underlined) and radiocarbon ages (asterisked) represent the most reliable ages for the stratigraphy (From Vandergoes et al., 2005)

MIS	New Zealand					South America	Australia
	Okarito cooling intervals[a]	Sth Westland Moraine/ Outwash terrace sequence[b]	Sth Westland Loess sequence[c]	Nth Westland glacial formation[b]	Fiordland glacial sequence[d]	Straights of Magellan glacial stages[e]	Snowy Mts, glacial maxima[f]
	W, 14–11 ka[g]				Aurora 1, 14–11 ka	Stage E, 15.5–11.7 ka	
2	S, 21–18 ka	M6/T6, 20.5–19 ka	L1a, 24–16 ka	Moana, 20.5–19 ka	Aurora 2/3, 15–20 ka	Stage D, > 17.5 ka, Stage C, 21.7–20.3 ka	16.8 ± 1.4 ka
	S, 25–23 ka	M5/T5, 24.5–21.5 ka	L1a, 24–16 ka	Larrikins 2, 24.5–21.5 ka		Stage B, 25.2–23.1 ka	19.1 ± 1.6 ka
	S, 30–27 ka	M4b/T4b, 34–28 ka	L1b, 36–24 ka	Larrikins I, 34–28 ka			32.0 ± 2.5 ka
3	M				Aurora 4, 41–40 ka		
	M		L2, 50–45 ka		Aurora 5, 48–46 ka		
4	M	M2/T2 M3/T3	L3/L4	Loopline	Aurora 6		59.3 ± 5.4 ka
5b	W			?Loopline[h]			
5d	W			?Loopline[h]			
6	S	M1/T1	L5		Aurora 7	?Stage A, > 90 ka	

Correlation with marine isotope stratigraphy (MIS) for MIS 4–6 is based on presumed correspondence with major northern hemisphere glaciations. Note that each of the inferred cooling intervals at Okarito has at least one correlative in the New Zealand glacial or loess records but none of these other records individually show all the cooling episodes inferred at Okarito. Records of glaciation from Australia and South America show similar complexity but do not conflict with inferred cooling intervals at Okarito.

[a]This study. S—strong cooling showed by major grass peak; M— moderate cooling showed by minor grass peak; W—weak cooling shown by partial replacement of forest by shrubland elements.

[b]From Suggate and Almond (2005).

[c]From Almond et al. (2001).

[d]From Williams (1996).

[e]From McCullough et al. (2005).

[f]From Barrows et al. (2001).

[g]This cooling interval is broadly coeval with glacial advance reported from South Westland (Denton and Hendy, 1994) and mid-Canterbury (Ivy-Ochs et al., 1999).

[h]Suggested MIS 5 glaciation is from Preusser et al. (2005).

Table 6. Comparison of inferred Okarito cool episodes with New Zealand glacial and loess sequences and records of glacial advance from southern South America and Australia (From Newnham et al., 2007).

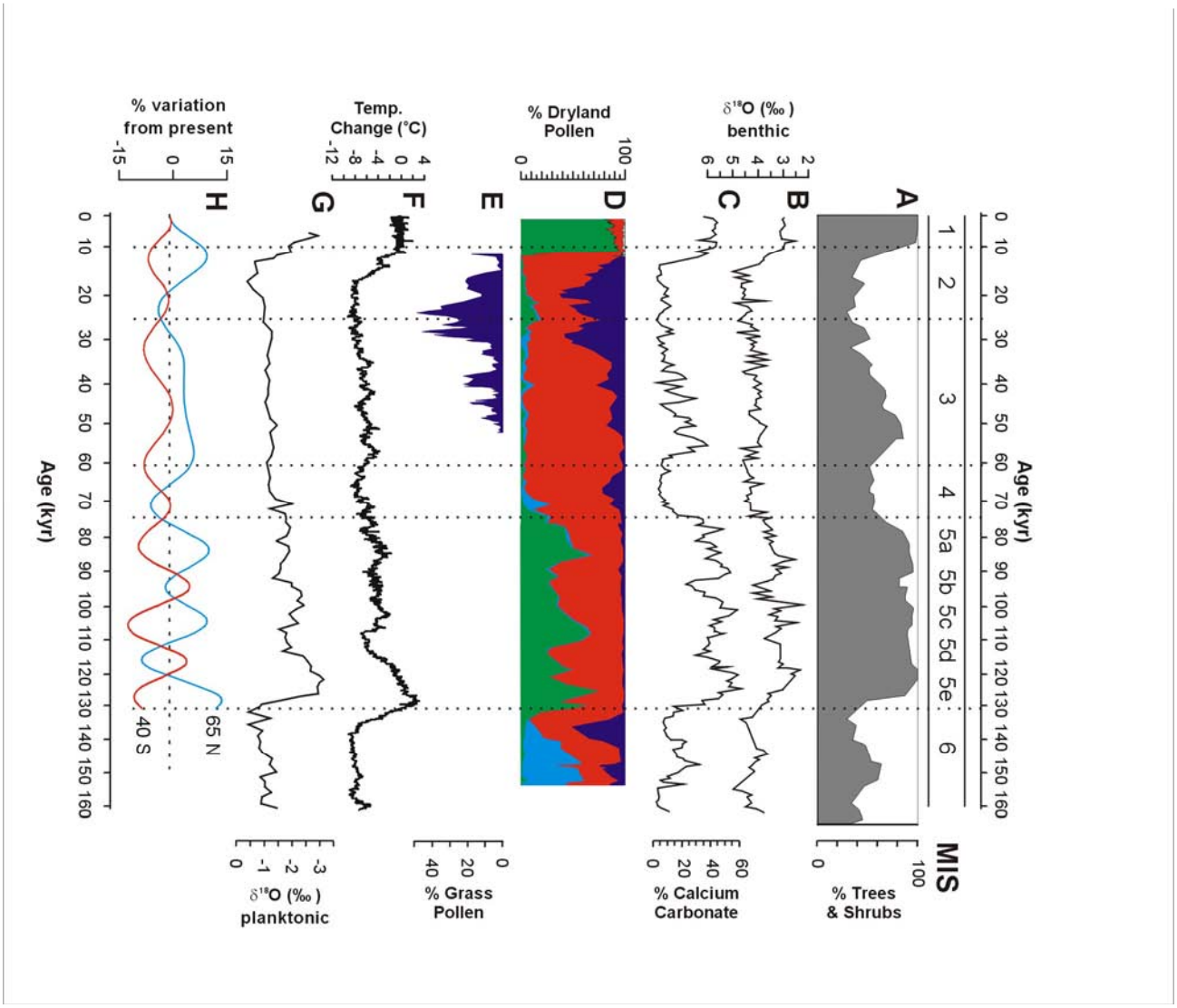

Fig 34. Comparison of Okarito pollen and other records of climate change with summer insolation variation curves for the past 160,000 yr. a–c, DSDP 594 pollen, benthic d18O and calcium carbonate records; d, Okarito Pakihi pollen stratigraphy:e, Taiquemo´ (HE94-2B) grass pollen curve for the past 50 kyr; , Vostok temperature reconstruction; g, MD 90-0963 planktonic d18O record; h, Plot of summer insolation for 408 S and 658N (data is archived at theWorld Data Center for Paleoclimatology, Boulder, Colorado, USA. http://www.ncdc.noaa.gov/paleo/forcing.html). The climate trends at Okarito show broad similarities with records that invoke a northern driver including maximum glaciation before 130 kyr and from 25–10 kyr with less pronounced cooling from 60–75 kyr; a fivefold subdivision between 75 and 130 kyr; subdued warming from 26–60 kyr relative to the Holocene and much of the period between 75–130 kyr; and broadly synchronous warming at around 12–11 kyr. An early onset of LGM cooling at approximately 28.5–30.5 kyr, however, precedes the northern insolation minimum at about 24 kyr but occurs soon after the southern insolation minimum at 32 kyr. (From Vandergoes et al., 2005)

have played a greater role in climate change in the mid-southern latitudes than the previously considered Milankovitch orbital forcing hypothesis that invokes a Northern Hemisphere climate driver.

[1]The Maori term ‘‘Pakihi’’ is generally applied to wetlands under mainly rush-fernland in forest openings on lowlands in Westland (Mew, 1983; Williams et al., 1990).

Stop 4-3. Poerua Valley

At this stop sited near the head of the fan of the Poerua River we discuss the moraines formed during the “Extended LGM” in New Zealand, and the morphology and behaviour of post glacial fans occupying the formerly glaciated valleys of the major rivers.

The Poerua River is relatively small by West Coast standards. In the LGM the Poerua glacier did not extend beyond the present coastline as did the glaciers of the neighbouring Wanganui catchment to the north and Whataroa catchment to the south. LGM moraines form the valley walls visible from our stop, and LGM terminal moraine forms a short gorge about 12 km downstream from the range front (Fig 35). Saltwater Forest, bounded to the south and north by the Whataroa and Poerua Rivers, respectively, is constructed of glacial moraines and outwash fans of the last (Otira) and the penultimate (Waimea) glaciation. The morphostratigraphy of the glacial landforms and the soil stratigraphy of the loess coverbeds on them have been studied in detail (Almond 1996; Almond et al. 2001). Importantly, within Saltwater Forest, geomorphic and soil stratigraphic evidence exists that complements the

climate proxies from the Okarito Bog for an early onset to the LGM in New Zealand, and for the presence of a mid-LGM interstadial.

A triplet of LGM lateral moraines forms the boundaries of the forest on the true right and true left of the Whataroa and Poerua Rivers, respectively. Within the forest itself, three belts of related terminal moraine occur. The youngest belt (M6) includes low lateral moraines on the inner margins of the Poerua and Whataroa Valleys, and terminal moraines forming the SE margin of Saltwater Forest above Lake Rotokino. The next older advance ($M5_2$) produced lateral moraines outboard of the M6 laterals, and a broad swath of hummocky terminal moraine seaward (northward) of the M6 terminal moraines. The $M5_1$ advance produced the lateral moraines that are outboard of the $M5_2$ laterals, and although no morphological expression of the associated terminal moraine survives, its existence is confirmed stratigraphically. The stratigraphic relationships between the $M5_1$, $M5_2$ and Kawakawa Tephra are significant and are demonstrated at Joan Rd (Figs, 35, 36), which, unfortunately because of access problems for the coach, we cannot visit. At this site, fluvio-glacial and lacustrine sediments of the $M5_2$ advance bury a Brown Soil formed in a coarse boulder gravel sitting on till. Kawakawa Tephra is concentrated in the A horizon of the buried soil. The site demonstrates:

- The $M5_2$ advance postdated Kawakawa Tephra (ca. 26.5 k cal. yr BP), $M5_1$, which predated Kawakawa Tephra, was an advance of similar magnitude,
- The duration of the interstadial between the two advances is estimated to be in the order of a few thousand years on the basis of the degree of development of the buried soil formed in the $M5_1$ till.

About 100 m north of the Joan Road site beyond the limit of the $M5_2$ ice limit, $M5_1$ till is mantled with a 40 cm-thick loess sheet (L1a) with concentrations of Kawakawa Tephra at the base. The loess sheet, derived in part from the outwash fans of the $M5_2$ advance, is chronstratigraphically equivalent to the glacio-fluvial and lacustrine sediments at Joan Rd. Its presence, along with the occurrence of Kawakawa Tephra in its base, has been used as a criterion for discriminating and mapping moraines and outwash terraces of LGM age.

The M6 advance was demonstrably smaller than the M5 advances, although still much larger than the late glacial (Waiho Loop) advance, which is absent in the Poerua

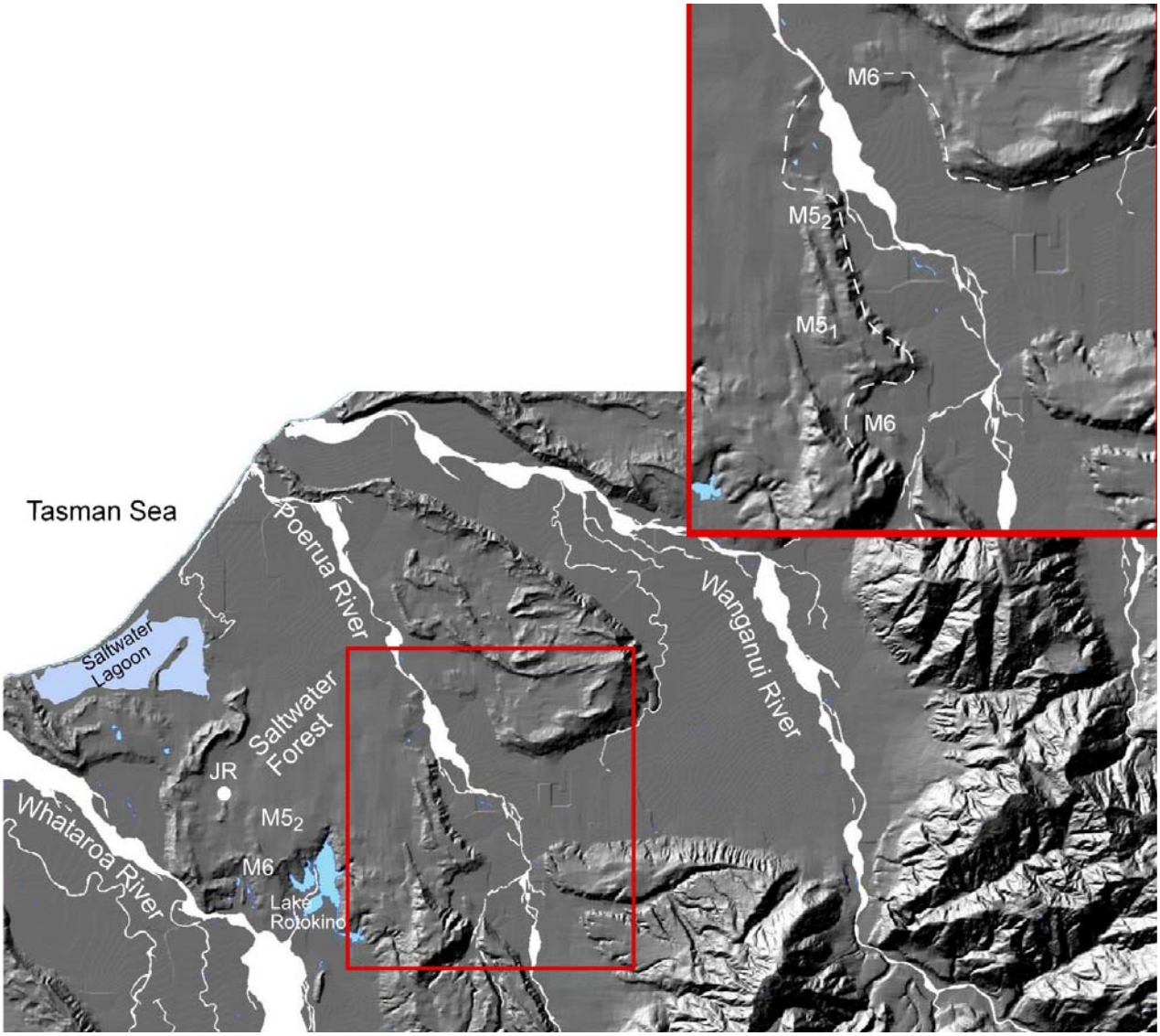

Fig 35. Shaded relief model showing the Poerua Valley and Saltwater Forest. JR refers to the Joan Road site discussed in the text.

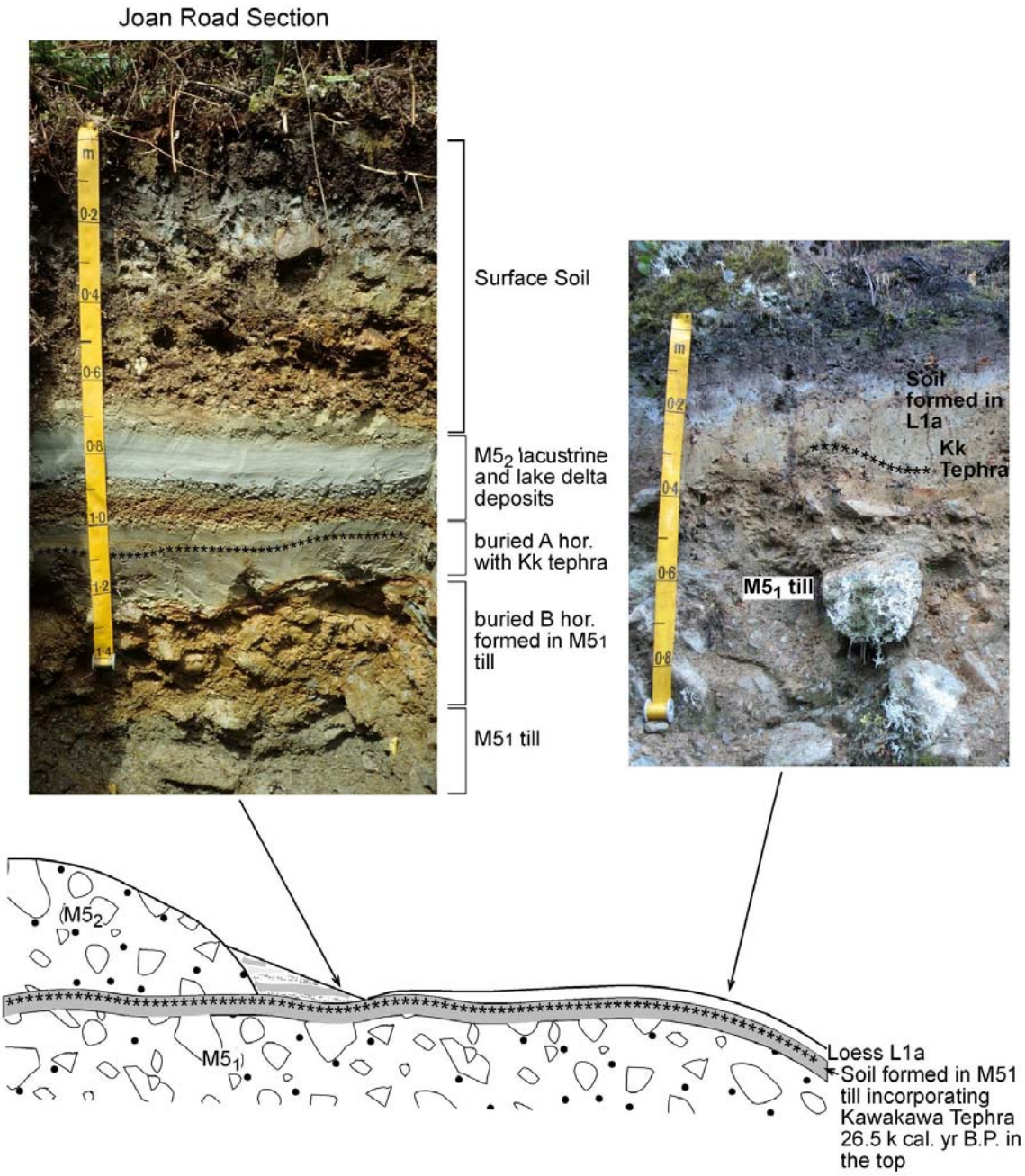

Fig. 36. Stratigraphy and context of the Joan Road section in Saltwater Forest. $M5_2$ and $M5_1$ advances stratigraphically overlie and underlie the 26.5 k cal. yr B.P. Kawakawa Tephra from Central North Island. The period of time between the two advances is represented by the degree of development of the buried soil at Joan Road.

Valley, and only tentatively identified in the alpine reach of the Whataroa Valley. On the basis of the Saltwater Forest evidence and a wider regional analysis of stratigraphy, pollen data, radiocarbon ages and tephrastratigraphy, Suggate and Almond (2005) included $M5_1$, $M5_2$, and M6 (and their North Westland equivalents la_1, la_2, and mo) within an extended New Zealand LGM. They placed the culminations of the advances at 28,000, 21,500 and 19,000 cal. yr BP, and argued for a NZ LGM starting more than 5000 yr before the global LGM.

Post Glacial Fans

In the night of October 6 1999, a large rock avalanche fell from near the summit of Mt Adam to create a 120 m-high landslide dam that blocked the river. The landslide involved approximately 10-15 million m^3 of biotite schist and colluvium (Hancox et al. 2005) that fell as a broad, relatively thin slab up to 1800 m to the valley floor, down a slope averaging 37°. At its maximum, the temporary lake that formed extended for about 1200 m upstream and held 5-7 million m^3 of water (Figs. 37 and 38). The landslide was first reported by local residents who heard loud rumblings at about 3 am on the morning of 6 October that lasted another two hours. Later analysis of seismic records showed the landslide occurred at 2.35 am that morning as a single major event followed by minor rockfalls. No direct trigger is known for the

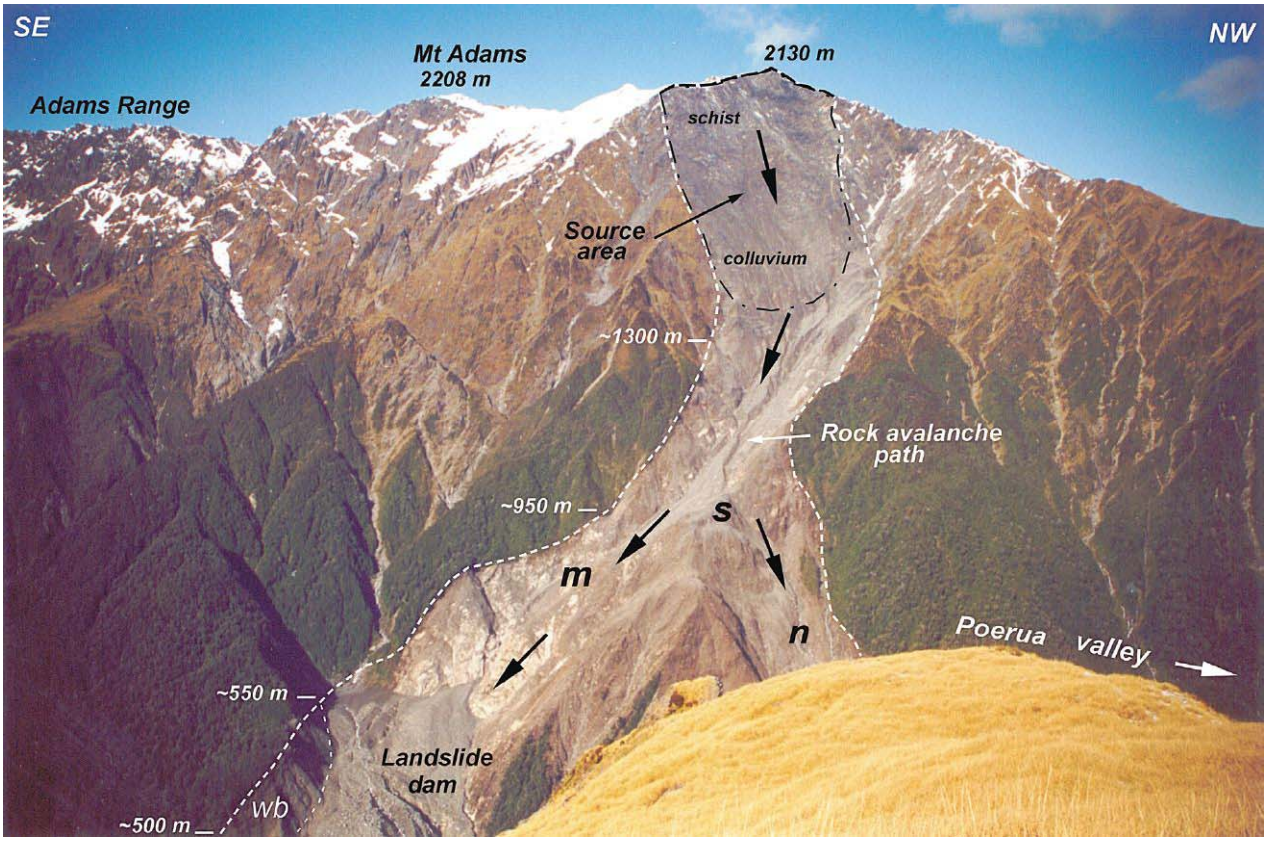

Fig 37. The north peak of Mt Adam after the landslide of 6 October 1999. Part of the landslide dam that formed is visible in the left foreground. The slide involved a slab of schist in the upper part of the failure and colluvium below. Most of the debris was channelled by a steep side stream. Wind blast damage (wb) can be seen (from Hancox et al., 2005, *reproduced with permission of RSNZ—Publishing*).

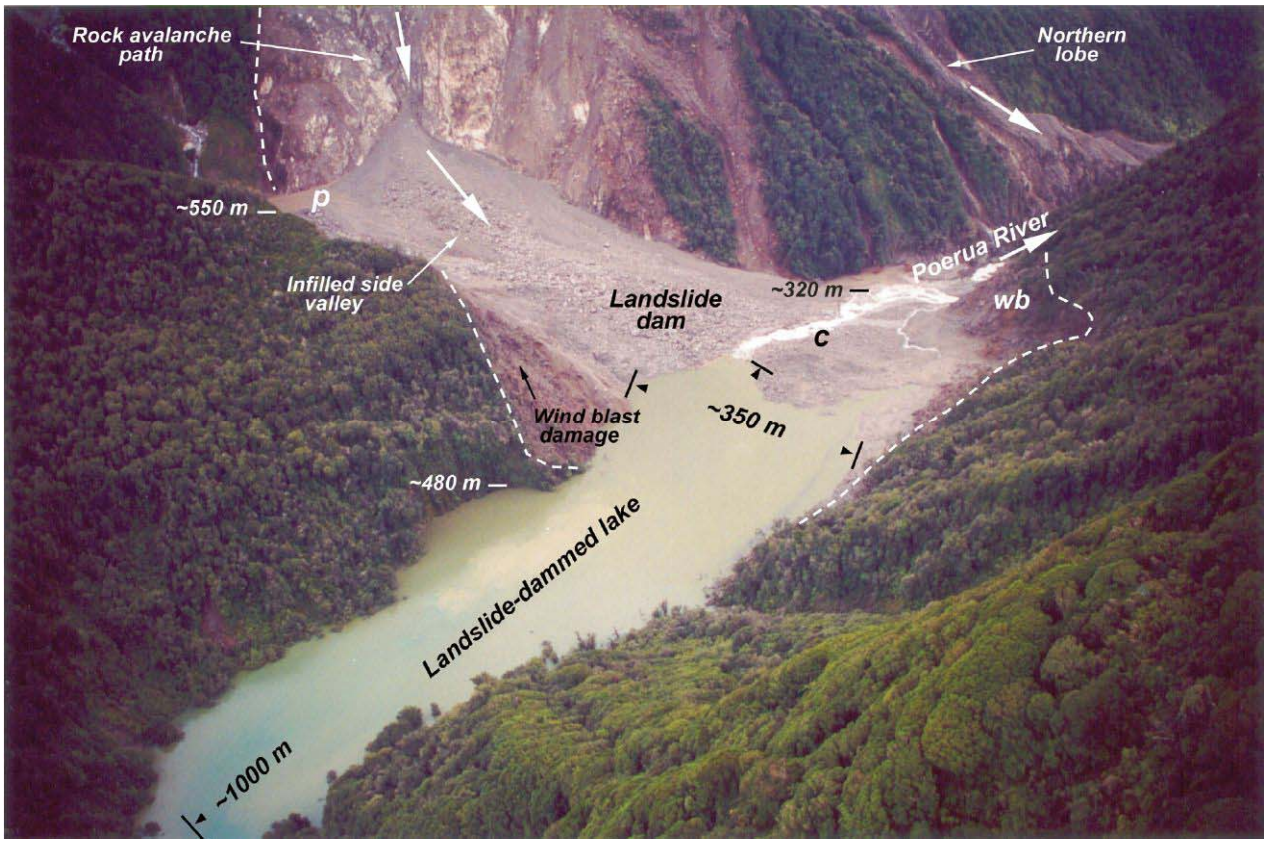

Fig 38. The landslide dam on 8 October. The overflow channel is established but the dam is not breached (from Hancox et al., 2005, *reproduced with permission of RSNZ—Publishing*).

rockfall, although a M4 earthquake centred ca 10 km ENE of Mt Adam 10 days earlier may have primed the slope for failure.

On the morning of 7 October residents reported reduced flow in the Poerua River. After aerial inspection of the landslide site showed the lake was filling rapidly, residents in the upper Poerua Valley were asked to evacuate their homes in preparation for a possible dam-break flood. By 8.00 pm that evening a flow of dirty water in the river indicated the dam had overtopped. An assessment of the dam and overflow channel suggested it was stable under low flow conditions, and the following day residents were allowed to return to their homes. The long term survival of the dam under high flow conditions was considered unlikely and the decision was made to evacuate residents whenever heavy rain occurred. Heavy rain starting on 11 October caused the landslide dam to breach shortly before 8 am on 12 October, sending a flood wave down the Poerua Valley that inundated the river flats. Residents of the valley were again evacuated and the flood peaked at about 2 m above normal flow at the S.H.6 bridge. Evacuation was predicated on an expectation, based on empirical modelling, of a dam-burst flood in the order of 2000-3000 m^3s^{-1}. As it happened, the flood peak was estimated at only 800-1000 m^3s^{-1} (about that of the annual flood); the reduction being due to attenuation of the peak on the alluvial fan. By 1.10 pm the flood peak had passed and residents were allowed to return to their homes.

The flood wave was confined largely to the active channel of the river (true left channel Fig. 39) and relatively little damage was caused to farmland and no damage to property. In contrast, the chronic, post-landslide effects have been much more destructive and costly. A succession of floods since 1999 has brought much of the landslide debris down onto the alluvial fan causing sedimentation, erosion and flooding. By February 2002 it was estimated that 1.7 million m^3 had been deposited. Aggradation on the fan immediately below the gorge on McKenzie's dairy farm has been severe; at Rata Creek the bed is now 25 m above its 1992 level. In 2001 an avulsion sent the main channel 800 m to the east (Fig. 39), eroding and depositing gravel on farm land and undermining paddocks and infrastructure sited on the fan of Dry Creek. The farm is now inoperable.

Our understanding of alluvial fan behaviour under conditions of episodic, massive sediment impulses has been greatly illuminated by the post-landslide response of the Poerua River and changes in morphology of the fan. Davies and Korup (2007) classify the piedmont reaches of the major rivers in South Westland as confined alluvial fans: lateral confinement is provided by moraine valley walls, while confinement at the fan toe is established by the Tasman Sea. Unlike unconfined fans, which grow and prograde indefinitely with ongoing sediment supply, they argue the West Coast alluvial fans can reach a state of dynamic equilibrium when the sediment flux rate delivered to the fan from the mountains is equalled by the output offshore, the balance being achieved by adjustment of fan profile so that river gradient allows sufficient sediment throughput. In support of their contention they cite the fact that, (1) fan gradients increase in parallel with increasing denudation rates along the range front, (2) sediment input to the Waiho River fan since stabilisation of postglacial sea level is in the order of four times the amount stored in the fan, (3) the Waiho fan is aggrading at the same rate as long

Fig 39. The upper Poerua Fan in August 2001, showing the major avulsion channel that destroyed much of McKenzie's dairy farm (from Hancox et al., 2005, *reproduced with permission of RSNZ—Publishing*).

term sea level rise (2 $mmyr^{-1}$), and importantly, (4) active truncation of moraines by wave erosion shows the fan toes are not prograding. This steady state is thought to establish over time scales of 10^3 years. The fan heads, however, behave in a very different manner. Using evidence from scaled physical models, and soil stratigraphy of fan heads such as the Poerua, Davies and Korup (2007) conclude that these components are undergoing long-term cumulative aggradation at times of massive sediment pulses. For the most time the fan head is entrenched and inactive. They estimate a period in the order of 10^4 years necessary for the fan head to reach a steady state, i.e. longer than the duration of the Holocene. They caution against over-interpreting climatic or tectonic signals on the basis of fan head trenching.

Day 5. Hokitika to Punakaiki (Almond)

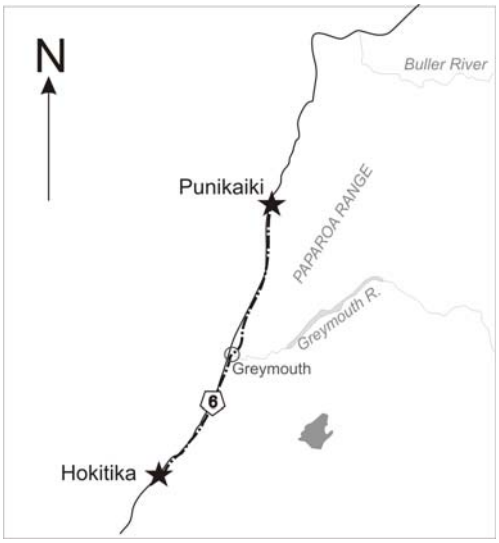

The day involves visiting key sites of the Kumara-Hokitika region exemplifying the stratigraphic and geomorphic evidence on which much of New Zealand's glacial chronostratigraphy is based. We start around Hokitika, and then head to Kumara, about half way between Hokitika and Greymouth, for lunch. We have one site to see near Kumara after lunch. The final part of the day is spent travelling through Greymouth to Punakaiki along the coastal road.

Introduction

The region between the Hokitika and Taramakau Rivers (Fig. 40) features large in the chronostratigraphy of New Zealand glaciation; as does Pat Suggate, for whom this area has been a focus for fifty years. The iterations involved in the development of the glacial stratigraphy are revealed sequentially in Suggate (1965), Suggate (1990), Suggate and Waight (1999) and Suggate and Almond (2005). The features of this area that have combined to make it so important are:

- A narrow coastal piedmont onto which glaciers extended during glacials, and over which the sea transgressed during interglacials;
- Tectonic uplift, which on the one hand has helped to preserve glacial and interglacial deposits and landforms during successive glacial cycles, while on the other providing good exposure as a result of stream incision in response to base level lowering;
- High rainfall, which has helped to preserve pollen and other organic material by creating saturated, anaerobic environments;
- Gold mining, which has provided other valuable exposures.

Glaciers advancing onto the piedmont from the large Hokitika and Taramakau catchments constructed belts of lateral and terminal moraines, to which seaward sloping outwash surfaces are graded. Over the last three glacial cycles, glaciers have waned so that progressively younger moraine belts are nested within older ones. Outwash fans

Glacial	Interglacial	MIS	Formation	Interglacial formation	Glacial advance
	Aranui Post-glacial	1		Nine Mile Formation	
Otira glaci-ation		2	Moana		mn (=M6)
			Larrikins		la_2 (=$M5_2$) la_1 (=$M5_1$)
		3	*Important inter-val*		
		4	Loopline		lo
	Kaihinu Inter-glacial	5		Awatuna Rutherglen	
Waimea glaciation		6	Waimea		we
	Karoro	7	Scandinavia	Karoro Scandinavia	
Wai-maunga		8	Tansey		ta
		9		not known	

Table 7. Westland glacial stratigraphy following Suggate (1990) and Suggate and Almond (2005).

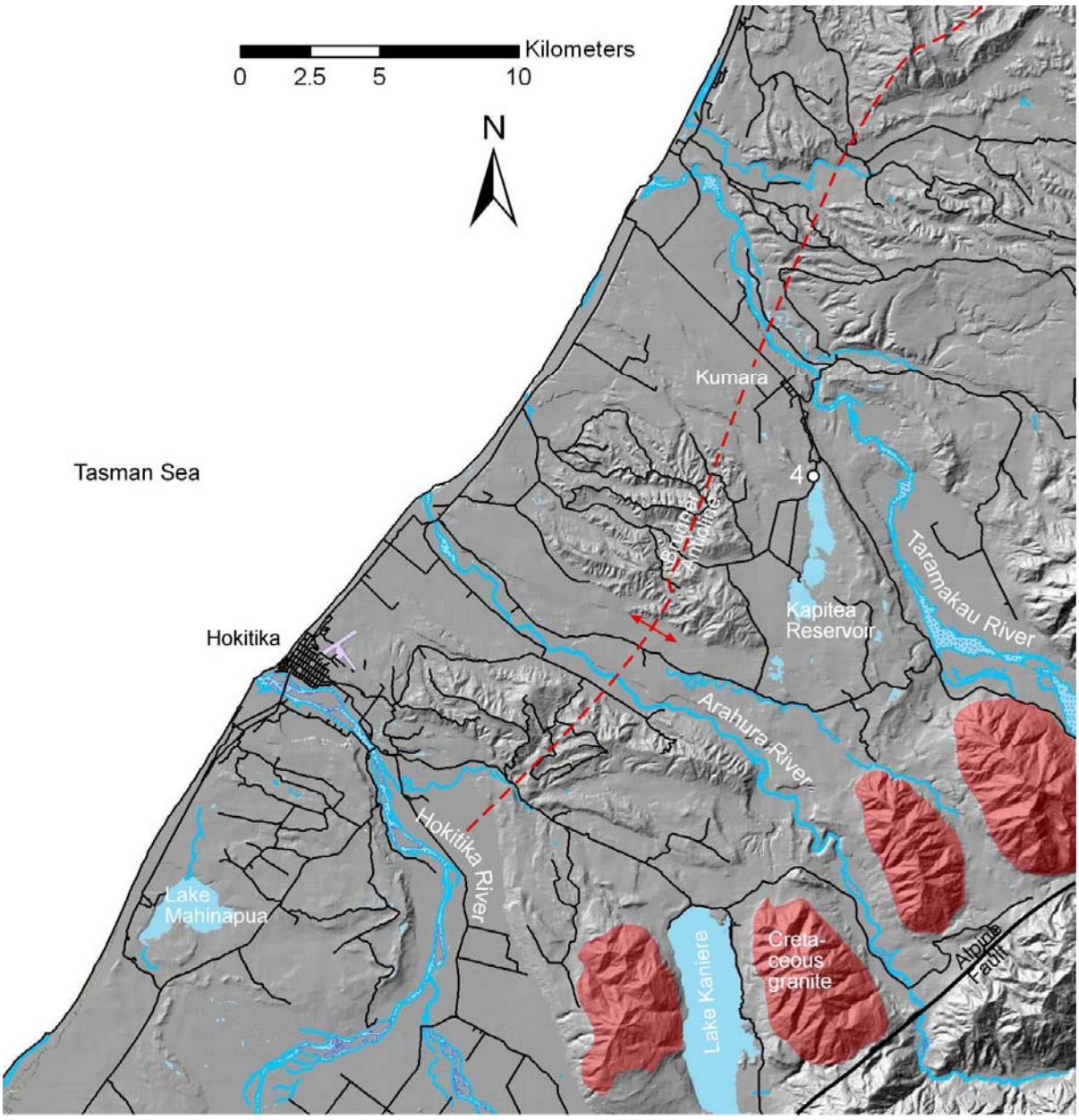

Fig 40. Shaded relief model of the Hokitika-Kumara area, Westland.

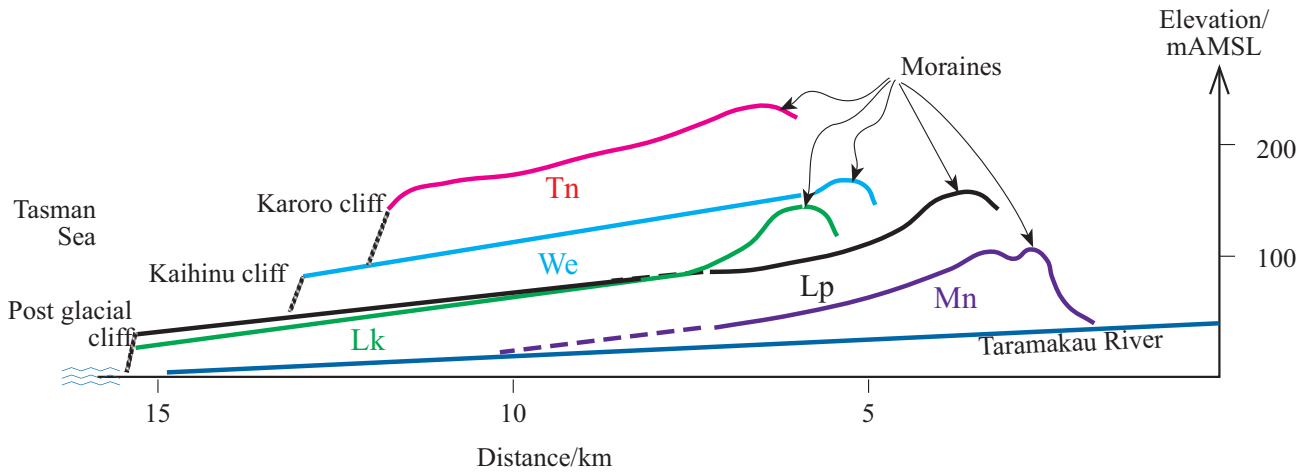

Fig 41. Cartoon of the relationships among glacial and interglacial deposits and landforms for the Hokitika-Kumara district in Westland (adapted from Suggate, 1965).

graded to successively older moraines appear higher in the landscape owing to uplift on the Brunner Anticline and associated minor folds (Suggate, 1987). The anticline's axis is about 10 km inland, aligned roughly parallel with the present coastline, and it plunges to the southwest. It is mapped no further south than the Hokitika River. Further north, uplift is much greater and the axis of the anticline corresponds with the crest of the Paparoa Range. Towards the coast, outwash surfaces are truncated by coastal cliffs. Last (Otira) glaciation outwash terraces are truncated by the post glacial sea cliff. Strandlines from prior interglacials truncate outwash terraces from the penultimate (Waimea) and older glaciations. As a result of tectonic uplift, older strandlines are further inland and higher in elevation. Some strandlines occur at the landward limit of identifiable uplifted shore platforms, although many are recognised only as uplifted coastal plain, beach or shoreface deposits at the foot of a degraded sea cliff, and buried by outwash gravels of subsequent glacials. These deposits were favoured targets of early gold miners, because, like on today's beaches, heavy minerals were concentrated by energetic seas of previous interglacials. These gold bearing deposits (called leads) were mined by systems of shafts and drives, and their locations were very helpful in early geological mapping. The outwash terraces, which form flights adjacent to the major rivers, are mantled with loess, the thickness and stratigraphic complexity of which increases with age.

Using the kinds of stratigraphic relations outlined above, and in close collaboration with Neville Moar, a palynologist, the sequence and relative status (e.g.

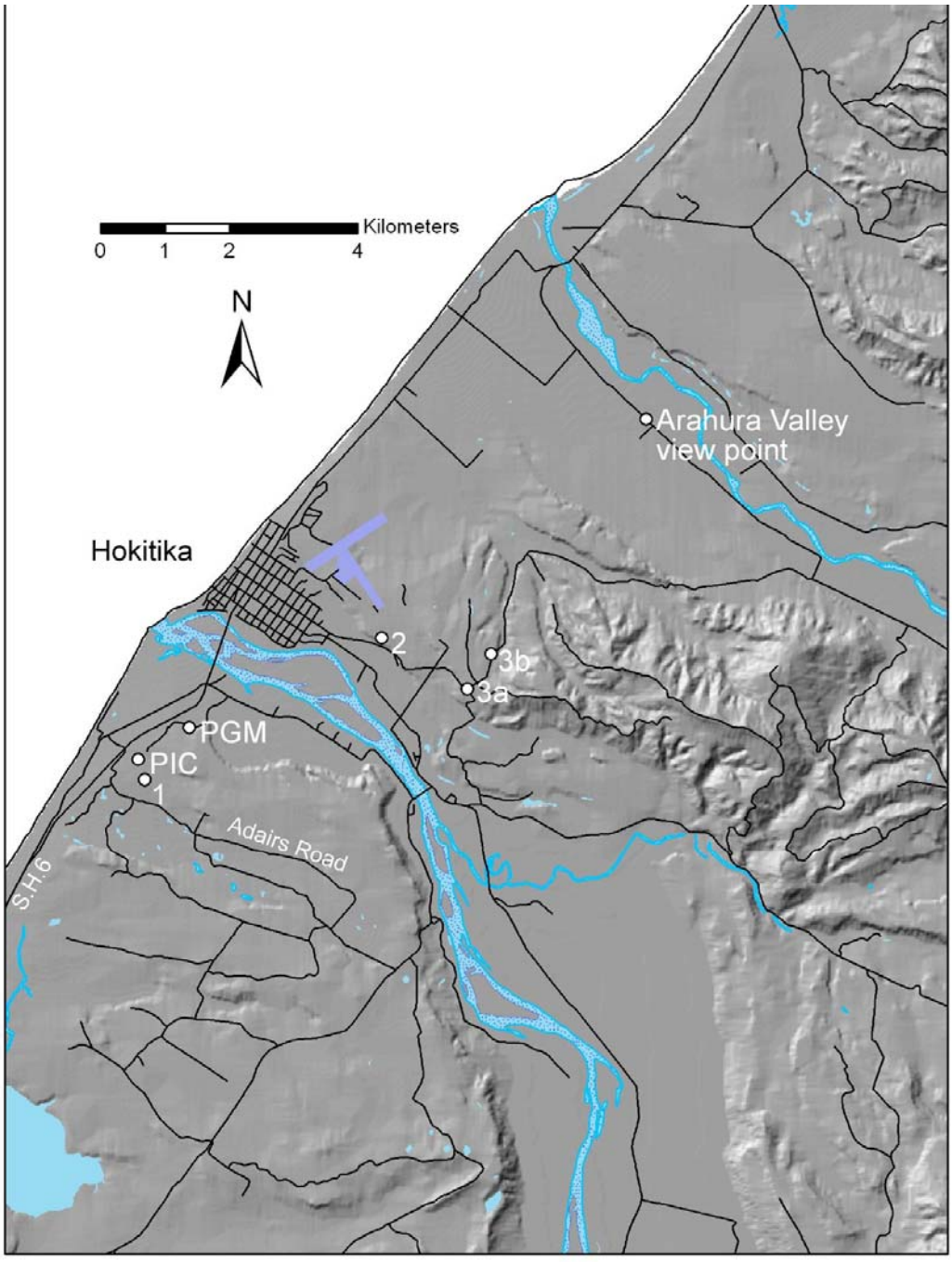

Fig 42. Shaded relief model of the lower Hokitika River showing stops (numerals) and other relevant sites for the morning of Day 5. PIC = Pine Creek Quarry, PGM = Phelp's Goldmine.

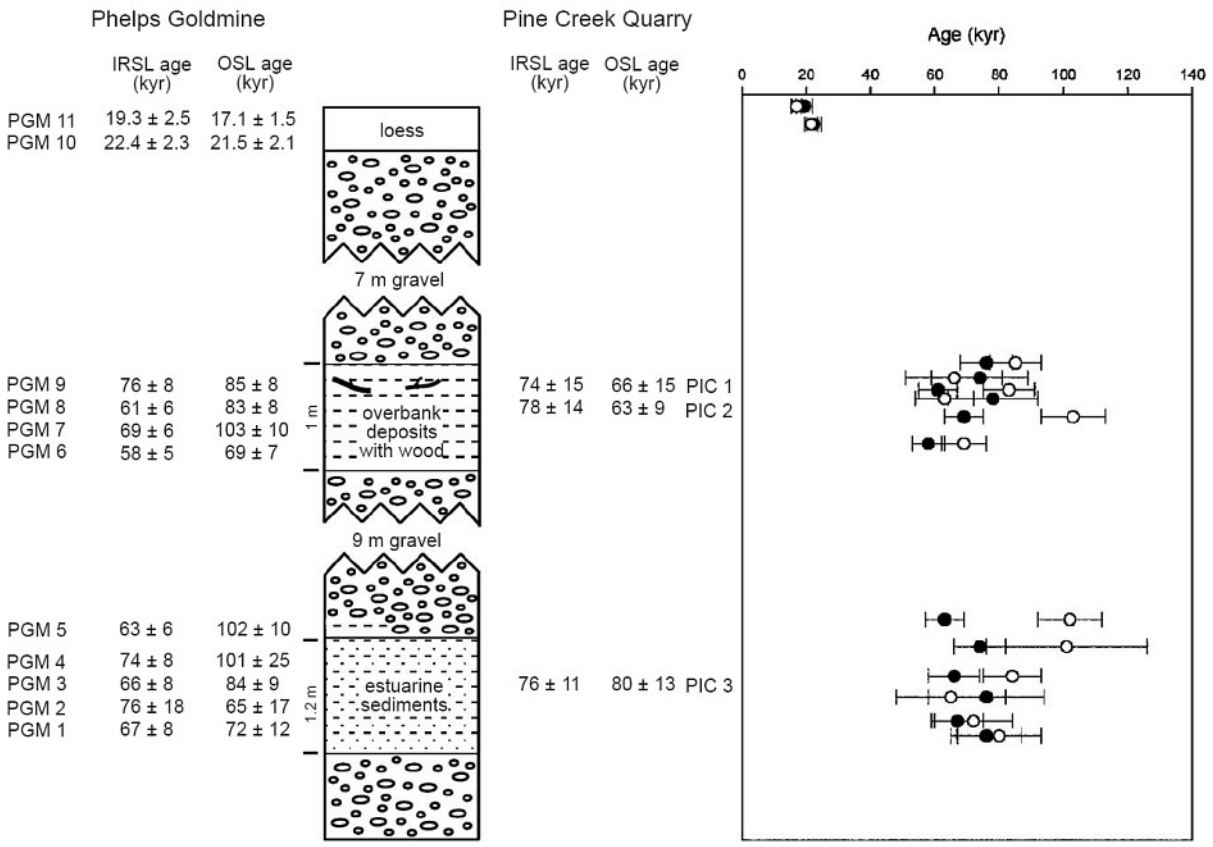

Fig 43. Stratigraphy and luminescence ages from Phelps Goldmine and Pine Creek Quarry (from Preusser et al., 2005). *Reproduced with permission of Elsevier.*

stadial:interstadials, glacial interglacial) of events were deciphered and published in 1965 as part of a DSIR Geological Survey Bulletin (Suggate, 1965) covering the Pleistocene geology of the northern half of the South Island. At this time, five glacial advances were recognised; three within the last (Otira) glaciation, and two older advances each of full glacial status. The chronology at this time was supported only by a few radiocarbon dates, which helped to constrain the two most recent advances. Over time, more radiocarbon dates became available, but it soon became clear, given the relatively robust stratigraphy, that dates were not always reliable. In circumstances where there was potential for translocation of modern carbon, radiocarbon samples were often contaminated and dates were too young (Grant-Taylor and Rafter, 1971; Dickson, 1972). By 1990 (Suggate, 1990) formation names had been subtly revised, and glacials and interglacials had been correlated to the marine oxygen isotope stratigraphy. It is essentially this stratigraphy that is shown in Table 7 and Fig. 41, except for the splitting of the Larrikins advance into two phases, in recognition of the early (pre Kawakawa Tephra) advance (Suggate and Almond, 2005) discussed previously on the tour. It is only recently that numerical dating techniques that extend beyond the limit of radiocarbon have been used to test the chronology. Luminescence dating has been used to date loess, and fluvial and marine sands and silts, and exposure age dating of boulders on moraines is in progress.

Stop 5-1. Birchfield's Mine (J33: 419272) – Last Interglacial beach deposits (Awatuna Formation)

Head south from Hokitika across the Hokitika River along S.H. 6 on the post glacial coastal plain for about 3 km, and then turn left into Adairs Rd. The road rises up the post glacial sea cliff, which has been heavily modified by gold mining. Birchfield's mine entrance is about 800 m down Adairs Rd on the left (Fig. 42).

This mine is no longer active, but at the bottom of a ca 25 m deep pit, strongly cemented, dark reddish brown, coarse beach sands and gravels are visible beneath glacial outwash gravel. This the farthest south of the mined uplifted beach leads. The section we see has been heavily modified by gold mining, such that the upper ca 15 m is a sequence (from top) of 1 m of rehabilitated silty soil, 7.5 m of massive non-stratified boulder gravel, over 7.5 m of cross bedded coarse sands derived from "float" mining. Gravel is dug by a machine excavator then passed through screens on a floating pontoon. The sands are deposited first through a chute and gravels are passed by a conveyor on top of them. Beneath the cross bedded sands a 1 m-thick layer of massive silts and sands passes to the right of the section underneath undisturbed gravels with an olivey matrix. Beneath this layer another 10 m of similar gravels overlies the beach sands. Aside from the disturbance of part of the upper 15 m of the section, the stratigraphy is very similar to that described by Preusser et al. (2005) at the nearby Phelps Goldmine and Pine Creek Quarry (Fig. 43). In 2000 and

2002, Preusser et al. (2005) dated, by luminescence, estuarine deposits at a similar elevation to the beach sands at Birchfield's, and overbank silts about 9 m above (i.e. similar stratigraphic position to the silts we see). The dated sections are now destroyed or overgrown. On the basis of the ages (Fig. 43), they assigned a basal gravel beneath the estuarine deposits to MIS4-5, and the gravels between the estuarine deposits and the overbank silts to Loopline Formation (MIS 4). Dates of ca 20,000yr from loess at the top of the section established a minimum age for the upper gravel package, which Preusser et al. (2005) correlated with early Larrikins time (MIS2-3). The lack of substantial time represented by buried soils between the base of the loess and the overbank sediments at 7 m depth suggests, however, there are unrecognised unconformities. Because of the relatively large uncertainties and scatter of the luminescence ages in the overbank sediments and the estuarine deposits, the assignment of the intervening gravels to MIS 4 and Loopline Formation is fraught. These gravels may be related to sea level rise-initiated aggradation at the end of MIS 5, or by an earlier (and presumably MIS5) glaciation.

We return via the same route to Hokitika. Take Fitzherbert St as far as Hampden Rd and turn right. At this point we rise on to the Larrikins terrace. Continue on Hampden St, which drops down onto a Moana terrace where it becomes Hauhau Rd. A high terrace riser up to the Loopline terrace appears on our left hand side. The next stop is accessed via a small road that climbs the terrace riser.

Stop 5-2. Hokitika Gravel Pit (J33: 456294), Loopline outwash gravel

Hokitika Gravel Pit exposes coarse gravel of the Loopline Formation, which forms the outwash terrace Hokitika Airport is sited on (Fig. 44). The gravel is overlain by blue-grey loess. IRSL ages from sand layers 1.2 m from the top of the gravel (Preusser et al., 2005) were 82,000 ± 8000 yr, 85,000 ± 6000 yr, 88,000 ± 8000 yr. Two samples from the base of the loess produced ages of 21,900 ± 2100 yr (IRSL-UV) and 27,200 ± 2800 yr (post-IR OSL), and 22,000 ± 2200 yr (IRSL-UV) and 25,100 ± 2800 yr (post-IR OSL). As at Phelps Goldmine and Pine Creek Quarry, the large break between the end of gravel aggradation and the beginning of loess accumulation, in the absence of evidence for a period of sustained soil formation, suggests some unrecognised unconformity exists in the section. The Loopline Formation has been correlated with MIS 4 on the grounds that the gravels accumulated during "full glacial conditions" (Suggate and Waight, 1999) and it stratigraphically overlies marine sediments of Awatuna Formation (MIS 5c) (Table 7). Given the luminescence ages at Hokitika Gravel Pit, Phelps Goldmine and Pine Creek Quarry, and the recent recognition of ca 80 ka moraines from Cascade Plateau south of Haast, the possibility of MIS 5 glacial advances (and associated aggradation) needs to be seriously considered.

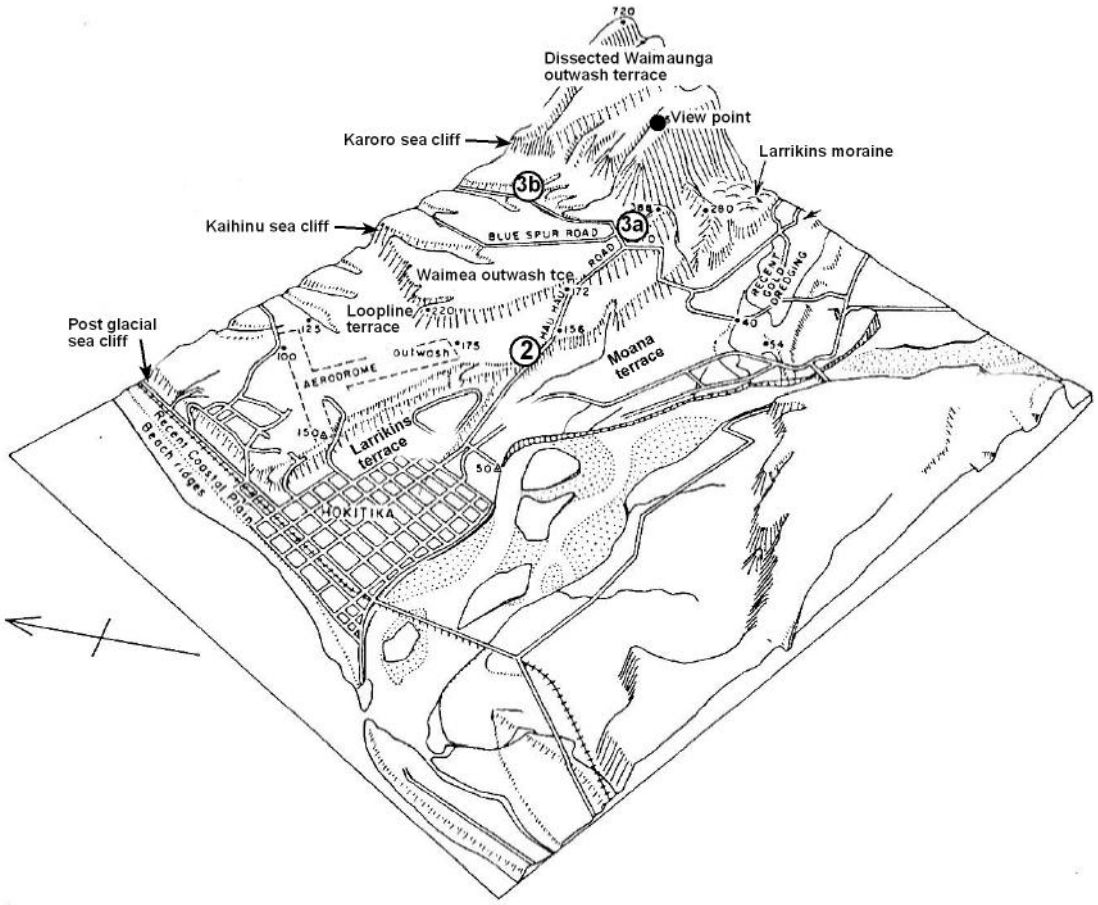

Fig 44. Block diagram of the glacial morphostratigraphy and landmarks of the lower Hokitika Valley. Numerals mark stops (adapted from Soons and Selby, 1982).

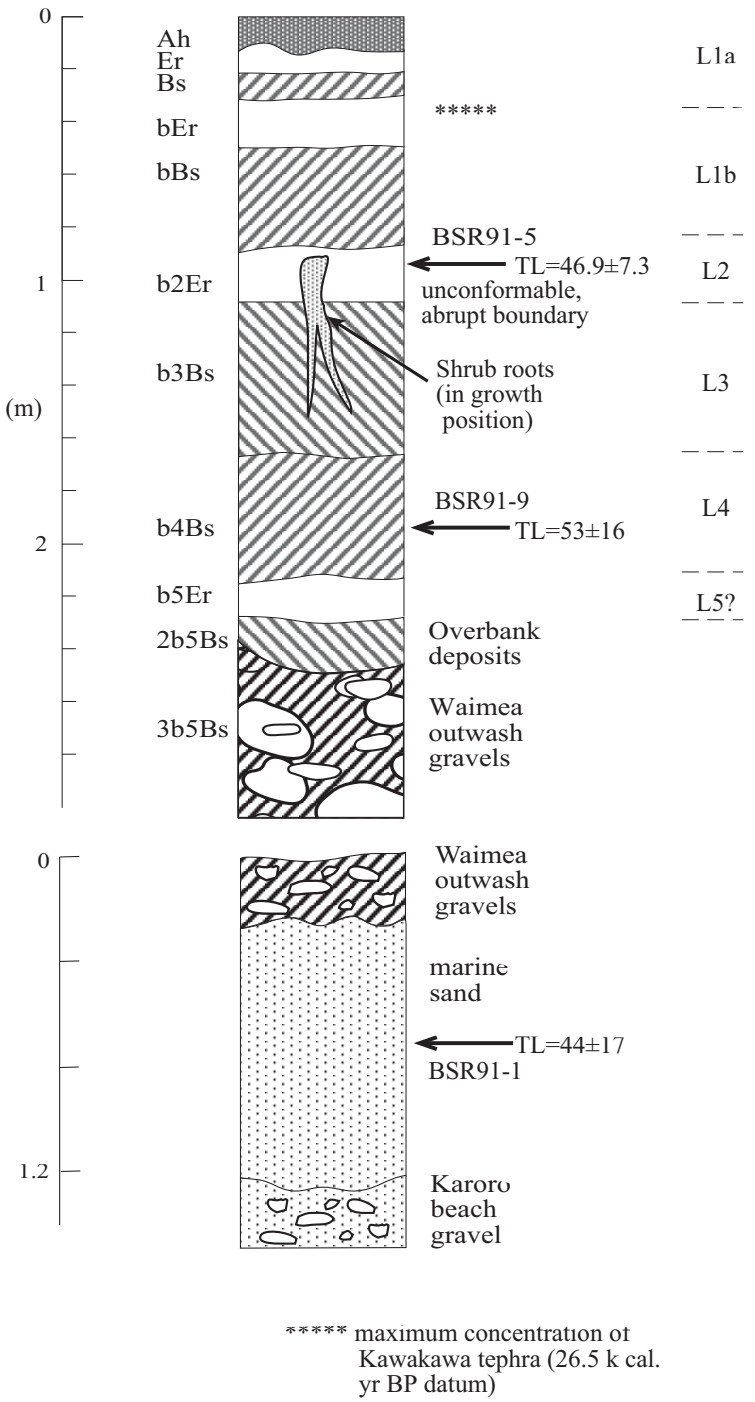

Fig 45. Composite stratigraphic diagram of the Blue Spur loess section and underlying Karoro marine deposits (from Berger et al., 2001).

Stop 5-3. Blue Spur loess section

Our stop is divided into two parts: Site 3a (J33: 469287) involves a discussion of the soil stratigraphy and luminescence chronology of the loess at the terrace surface, and the second, Site 3b (J33: 473292), shows marine sediments and peat beneath Waimea outwash gravel.

Berger et al. (2001a) described the soil stratigraphy of the loess at Blue Spur at our stop, and dated two horizons by thermoluminescence (Fig 45). Another age datum was provided by concentrations of Kawakawa Tephra (26.5 k cal. yr B.P.) at 35 cm depth. Moar and Suggate (1973) described a section, now destroyed, about 5 m to the east, which exposed an infilled channel with a basal woody peat overlain by about 75 cm of grey to grey-brown silty clay. Pollen and radiocarbon analyses from the basal peat showed a succession from podocarp forest to *Nothofagus* forest about 30,000 yr B.P. The dates were later rejected, on the grounds of likely contamination (Moar and Suggate, 1996), in favour of a Last Interglacial (Kaihinu) age for the peat. The terrace is cliffed to the north at the Awatuna and Rutherglen shorelines, though most of the marine deposits are buried by the Loopline gravel seen at Stop 2. To the south a prominent cliff assigned to the Karoro interglacial (MIS 7) truncates a higher, older (Waimaunga) outwash terrace. If time allows we will climb up on to the terrace for a view of the landscape (Fig 44).

The loess stratigraphy is broadly consistent with sites further south thought to be a similar age (Almond et al., 2001; Berger et al., 2001a). The TL ages are stratigraphically acceptable, although the lower sample in the loess is a little younger than expected. The dating at Blue Spur was part of a wider luminescence dating campaign led by Glenn Berger in the early 1990s. Initially, samples were only dated by TL, but anomalous results obvious in the samples from Saltwater Forest (Fig. 46) prompted Berger to apply the IRSL technique to the same samples. Many, but not all, of the stratigraphic inconsistencies disappeared. IRSL ages younger than their TL counterparts were considered to be more accurate, the discrepancy being attributed to the more sensitive bleaching of the IRSL signal in comparison to the TL signal. An IRSL age significantly older than the corresponding TL age (HRI91-12, Fig. 46) was thought to be a result from the broad bandpass filter used in the TL protocol sampling malign luminescence from zircon that compromised the age determination (Berger et al., 2001a). Detailed mineralogical analysis of the samples from Saltwater Forest also raised potentially serious problems for the IRSL measurements, however: The 410 nm filter used for IRSL targeted the deep-blue emission of K-feldspar, and yet mineralogical analysis showed the samples to be completely devoid of this mineral. Berger et al. (2001a) concluded that it was probably part of the IR emission spectrum of albite that was being sampled with this filter. At the time, little was known of the IR luminescence behaviour of albite, although Berger et al. (2001) argued on the basis of thermal activation energies that the luminescence was probably well behaved. Interestingly, one of the moraines (M3) correlated by Almond et al. (2001) to MIS 4 has a minimum age (HRI91-1, Fig. 44) of 89,000 ± 15,000 yr. With the Saltwater Forest experience in mind, we must view the TL ages from Blue Spur with some caution. The results of Preusser et al. (2005) from central Westland suggest incomplete bleaching of the TL signal to be the most significant problem. They attribute the general high level of reproducibility of their results in comparison to Berger et al. (2001a) to different

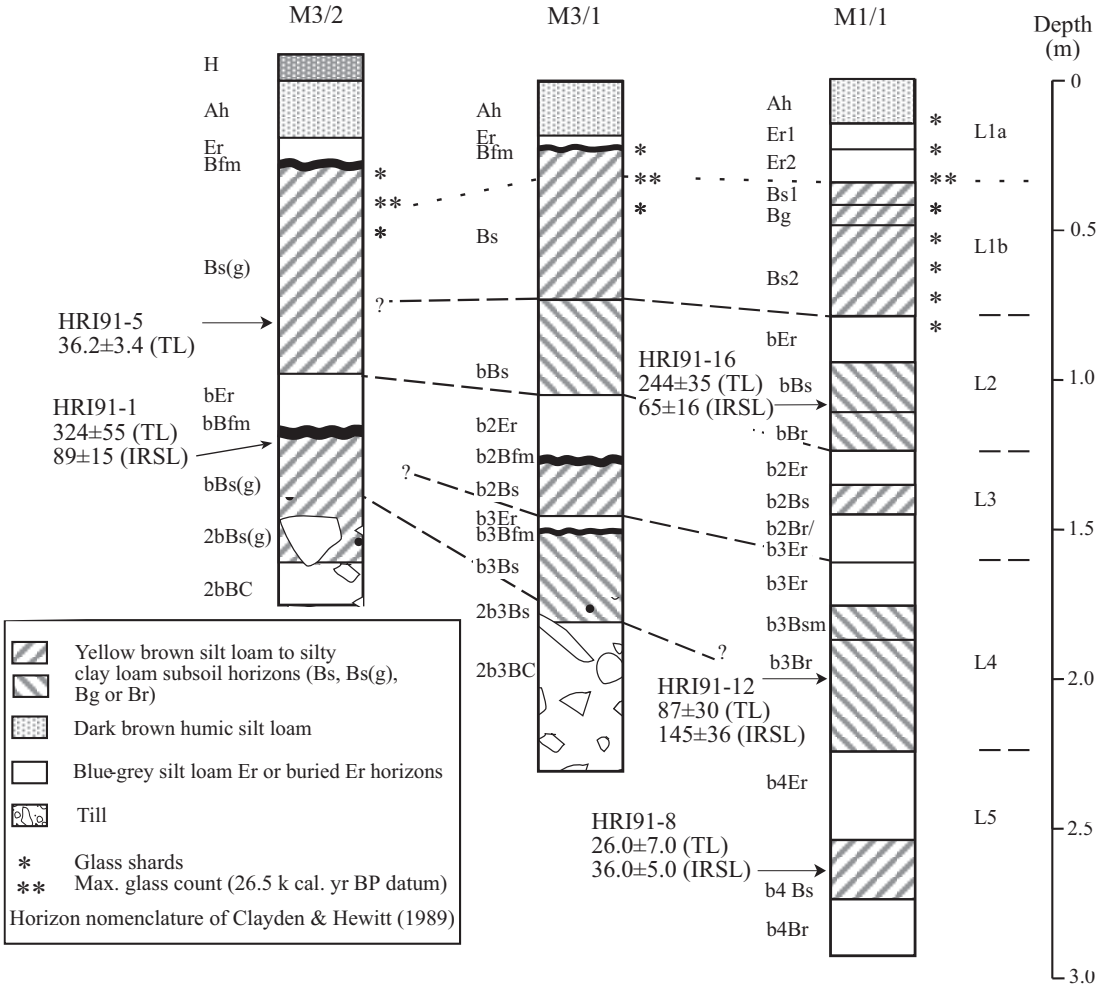

Fig 46. Loess stratigraphy and luminescence ages from Saltwater Forest (from Berger et al., 2001).

luminescence protocols (bandpass filters, ED techniques), and possibly to the provenance of the sediments dated. The catchments of the Hokitika and Taramakau Rivers include Cretaceous granites (Fig. 40) that are rich in K-feldspars, unlike the K-feldspar-devoid schists of south Westland.

About 1 km to the east in the walls of a gully cut into the Waimea terrace, marine sands and gravel of the Karoro Formation are exposed. On the road side, an older miner's drive into beach deposits marks the site of the luminescence sample shown in Fig. F. This age is clearly wrong. Berger et al. (2001a) suggested the dated polymineral 4-11 μm fraction of beach sands at this site may have been contaminated by silts translocated from above to give this anomalously young age. The TL signal of the sample was saturated.

Immediately to the east of the dated section, spectacular new exposures of the Karoro beach sediments and an overlying peat, incorporating logs and plant fossils, can be found. The peat is overlain by gravel of the Waimea Formation that forms a terrace remnant at the same elevation as Blue Spur.

From Stop 3 we continue along Blue Spur Road to the junction with Arahura Valley Road, where we turn left. Just past the junction with Two Mile Line we can look to the south west to see the Rutherglen and Awatuna marine terraces of the Kaihinu Interglacial (MIS5e, 5d, respectively). We then continue to S.H.6, where we turn right and traverse along the coastal plain at the foot of the postglacial sea cliff. About 13 km past the Arahura Bridge we turn a sharp right up onto the Larrikins Terrace. We stay on the same terrace to Kumara and our lunch stop.

After lunch we continue east on S.H.73 for about 2.5 km, then turn right onto Stafford Loop Road at Dillmanstown. We drive for 1 km to Stop 4a. Stop 4b is another 500 m along the road.

Stop 5-4. Dillmanstown: moraines of the Taramakau system and Kawakawa Tephra

At stop 4a on the west of Kapitea Reservoir, we can see the high lateral moraines of the LGM Larrikins (la_2) advance. Where we stop, the tills on either side of the road are mapped as Loopline Formation (MIS4). A section on the western side of the road, however, shows two packages of till with an organic rich soil sandwiched between (Fig. 47). Kawakawa Tephra is concentrated in the base of this organic soil. Radiocarbon dates of plant macrofossils found in organic-rich sediments on the eastern side of the road, presumably equivalent to the soil we see, returned an error weighted mean age of 17,890 ± 170 ^{14}C yr B.P. These two till units are now thought of as representing la_1 (basal) and la_2 (upper) advances, although no clear topographic expression of the moraines remains. Site 4b is included because it is one of the few sites, and the westernmost to date, where Kawakawa Tephra can be found

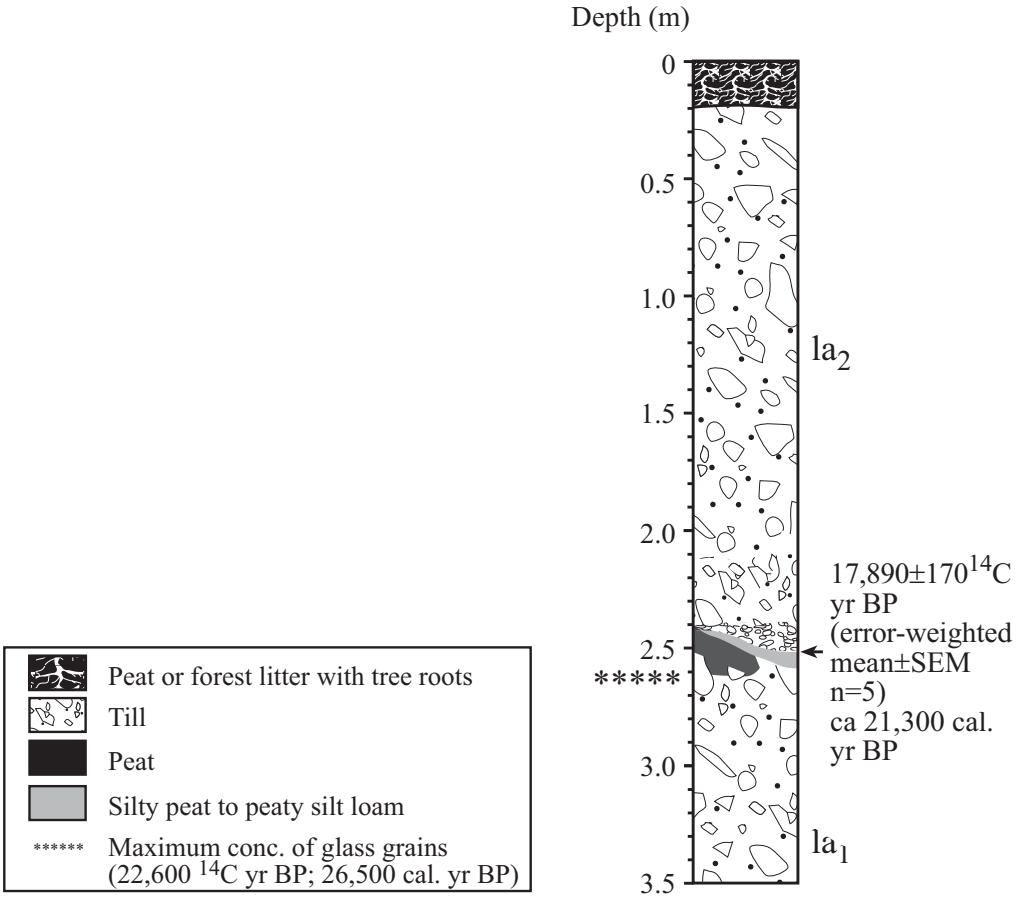

Fig 47. La2 till overlying la1 till at Kapitea Reservoir, Dillmanstown. The buried peaty soil incorporates the 26.5 k cal. yr BP Kawakawa Tephra (adapted from (Suggate and Almond, 2005)

macroscopically outside of lacustrine environments. The stratigraphy is equivocal but of interest is the fact that the small yellow puffballs of tephra appear in a slightly organic stained horizon thought to be a buried soil A horizon. The grey silty material burying this horizon may be purely alluvium, or perhaps loess overlain by alluvium.

From Stop 4b we retrace our route as far as Kumara Junction, and then turn right on to S.H. 6 heading to Greymouth. Beyond the Taramakau River, the highway once again traverses the post glacial coastal plain. In Greymouth we cross the Grey River, then travel for 8 km on S.H. 6 up a valley carved in soft Paleogene sedimentary rocks, through Runanga, and emerge at the coast at Rapahoe. From Rapahoe, the road hugs the flank of the Paparoa Range, which becomes notably steeper after about 8 km where the Neogene sedimentary rocks and late Cretaceous coal measures give way to hard Paleozoic greywacke of the Greenland Group. Shore platforms are carved into the Paparoas, but because of the hardness of the rock, they appear only as narrow benches. About 13 km beyond Rapahoe we descend onto the Barrytown coastal plain at Seventeen Mile Bluff. This 17 km-long, 1.5 km-wide coastal lowland backed by a sea cliff is formed from a progradational sequence of gravel beaches, swamps, beach faces and dune ridges. Suggate (1989) mapped two sets of shorelines on the lowland, a younger and an older set. The older set has four shorelines varying in elevation from 3.5 to 8.5 m ASL reflecting regional uplift. The younger set shows no significant altitude difference from present sea level. A step change in the altitude of the older shorelines occurs across the trace of the south-west striking Canoe Fault, which crosses the coastal plain in the southern half. On the south east (upthrown) side of the fault, each one of the four terraces is about 3 m higher than its counterpart on the other side of the fault, indicating a single uplift event occurred after formation of the youngest shoreline. In the north, inland of the post glacial cliff, broad Pleistocene shore platforms are formed across soft Neogene sediments. We rise on to one of these broad shore platforms just before Punakaiki, our stop for the night.

DAY 6. Punakaiki to Christchurch

(Rother and Shulmeister)

From Punakaiki we now proceed back towards Christchurch. The first stretch continues along the coast northward, past Fox River and Charleston. As we approach Westport the coastal terraces broaden and we divert towards Cape Foulwind along Wilsons Lead Road.

Warning: There is a surprising amount of traffic along this road and the site is somewhat blind to the traffic. Care is needed at this stop.

Stop 6-1. The Hill, Wilsons Lead Road – North-Westland

This site (approximately K29:850350), is an in-filled hollow within a dune field about 9km south west of Westport (Fig. 48). The site was first examined by Neville Moar in the late 1970ties. He (Moar and Suggate,1979) reconstructed a pollen record that extends from well before the last glacial maximum (c. 35,000 years) to the postglacial transition (c. 14,000 years ago). The value of this long pollen record has been enhanced by the recognition of the marker Kawakawa Tephra (c. 22,600 ^{14}C yr BP) in the deposit (Suggate and Almond, 2005). The pollen record suggests a transition from an open shrubland to a grassland at about 30,000 calendar years ago. The glacial age grassland is remarkable because this site would have been only about 150 m above low-stand sea-level and very close to the Tasman Sea. It implies extreme cooling during the LGM in an area widely regarded as a likely plant refugium during glacial times. Consequently, it has been argued that special factors including high windiness and killing frosts, rather than low mean temperatures limited woody vegetation at this site.

The current outcrop is not identical to the exposure used for pollen analyses by Moar and Suggate (1979) but Suggate and Almond (2005) who re-evaluated the outcrop a few years ago concluded that the stratigraphy was so similar

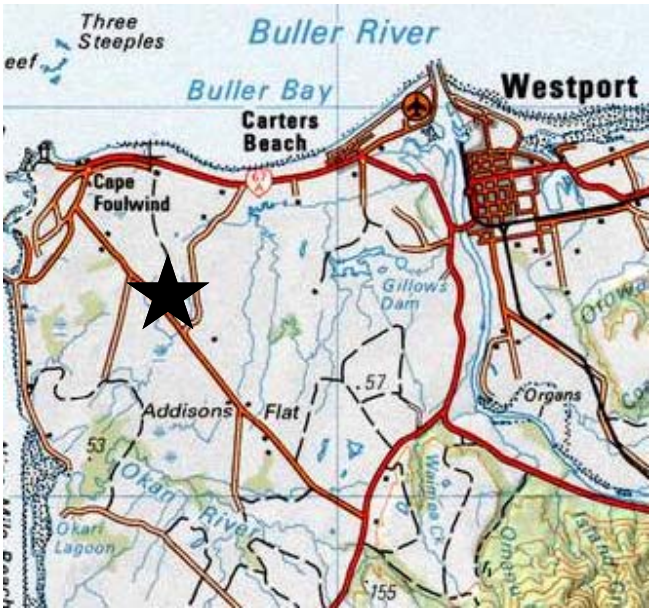

Fig 48. Approximate location of the Hill (marked by the star).

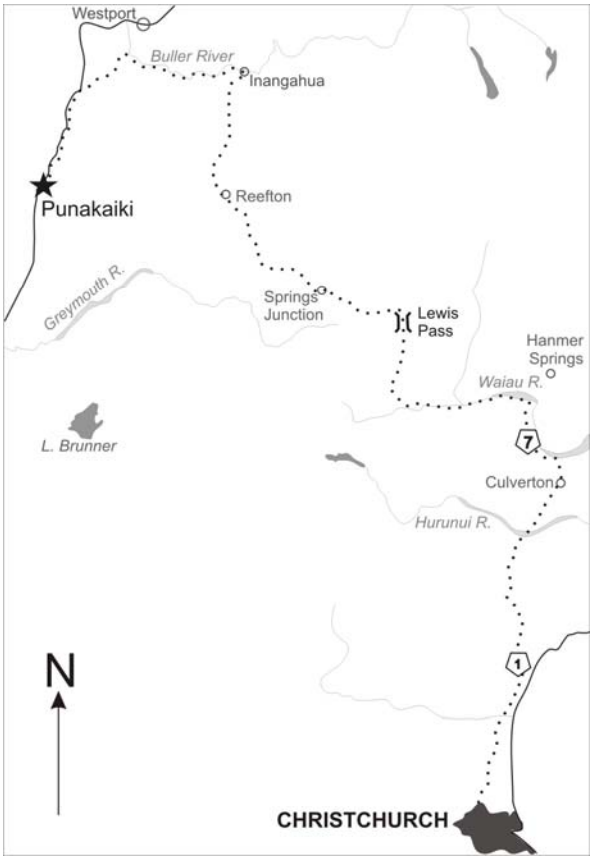

that a direct comparison could be made. The new outcrop was sampled for beetles by Phil Burge. He (Burge and Shulmeister, 2007) recovered 18 separate fossil beetle assemblages from a 90 cm organic layer that extends from c. 35,000 to c. 20,000 calendar years ago (Figs. 49 and 50). The beetle assemblages are hard to reconcile with the pollen given that 80-90% of the faunas are associated with woody vegetation, even during the period where the pollen suggests only grassland. It is highly unlikely that either data set is incorrect. The zone changes in the pollen record coincide with those in the beetle records and in both cases the attribution of forested or open environments is clear-cut. Rather Burge and Shulmeister inferred that the likely vegetation was some sort of a forest-grassland mosaic with pollen production from woody taxa limited by factors other than absence of trees.

The road passes along the Buller Gorge and inland to Reefton before proceeding to Springs Junction. Just beyond Springs Junction there is a reserve beside the Maruia River where there is a low wall that crosses a trace of the Alpine Fault. This was built at the behest of a famous NZ geophysicist, Frank Evison, to determine whether there was continual slip on the Alpine fault. The wall is over 40 years old and shows no deformation… but whether this is diagnostic is questionable. We will make a lunch stop at the wall (weather permitting). From here we follow up the Lewis Pass. Once we cross over the Lewis Pass we will enter the last area where we will examine glacial records – the Lewis/Hope system.

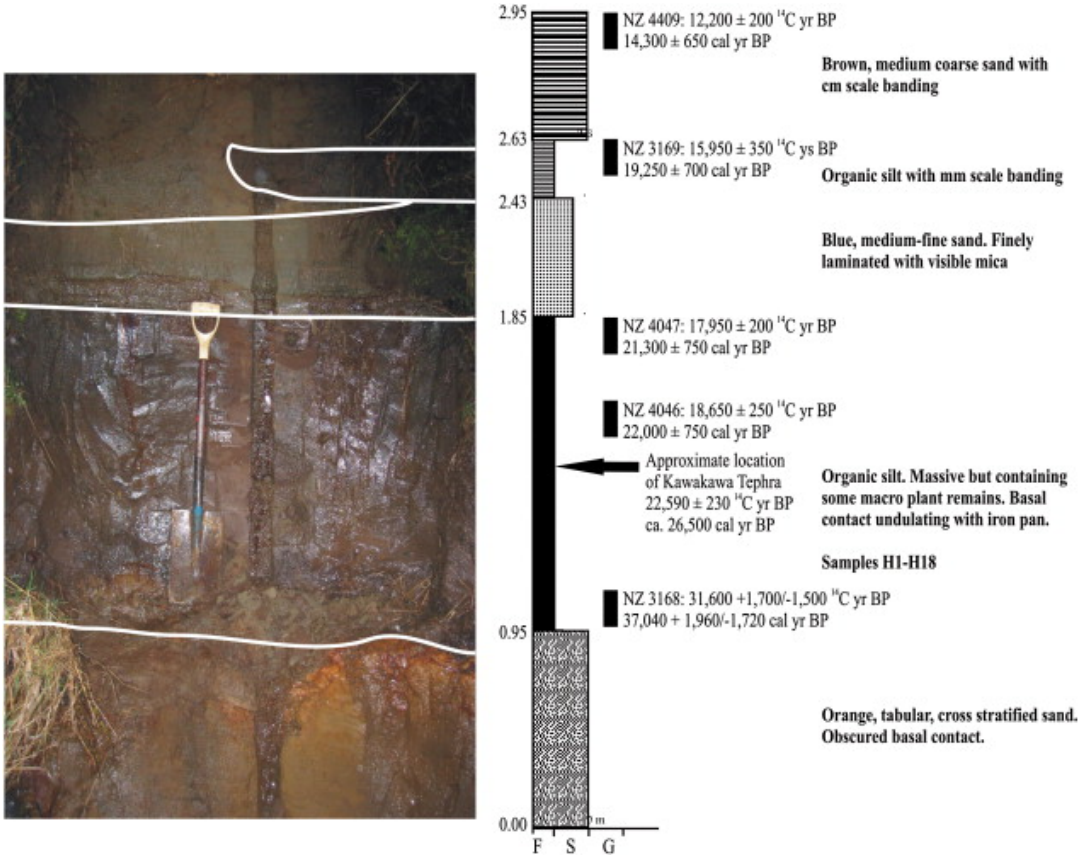

Fig 49. The outcrop at the Hill – with inferred chronology attached.

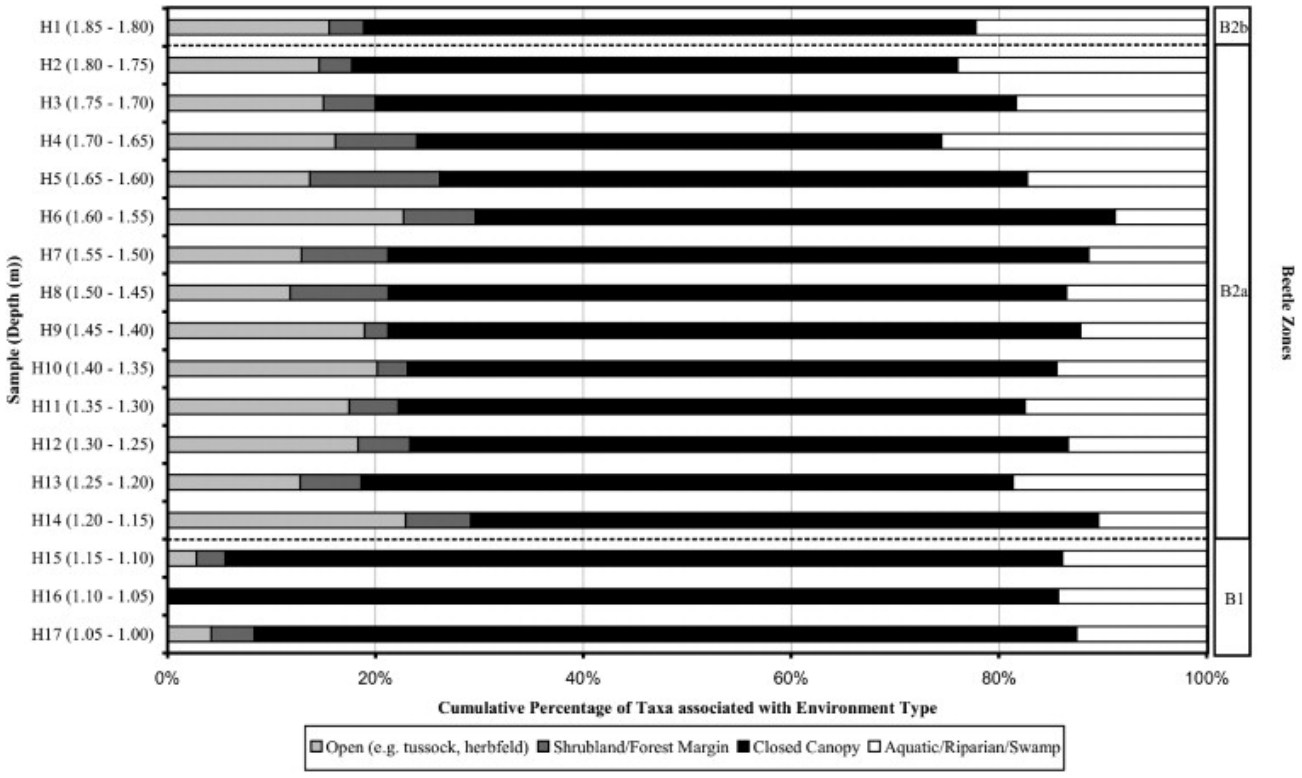

Fig 50. Summary beetle-environment attribution for 18 samples from the organic silt covering the LGM and late OIS3.

Fig 51: Geographic overview of the Waiau-Hope Valleys and locations discussed in the text.

Glacial Geology of the Waiau – Hope Valleys

Introduction

The alpine portion of the Waiau-Hope Valleys extends over roughly 2000 km^2 of mountainous terrain (up to 2300 m a.s.l.), located between the Spenser Range in the north, the Hope Valley in the south and the alpine divide in the west (Fig. 51). Regional bedrock is dominated by Triassic greywacke (Torlesse Supergroup) and comprises minor units of volcanics, conglomerates and limestone (Gregg, 1964). The catchment is part of the tectonically highly active Marlborough Fault Zone, and several NE-SW trending strike-slip faults traverse the catchment. Evidence for geologically recent faulting is highlighted by the dextral offset of the Boyle and Waiau Valleys along the Clarence Fault (Fig. 51), and the displacement of glacial moraines at Glynn Wye Station in the lower Hope Valley. The last major seismic event in the area occurred in 1888 during an estimated 7.3 magnitude earthquake along the Hope Fault (Cowan, 1991).

Climatically, the Waiau-Hope valleys are under temperate influence with mean monthly temperatures (at Boyle Lodge, 600 m a.s.l.) ranging from 15.5º (January) to 3.8ºC (July). Present annual precipitation peaks at about 5000 mm near the alpine divide but rapidly falls to below 1200 mm in the lower Hope Valley. Observed end-of-summer snowlines lie between 1950 - 2050 m a.s.l. and only the highest parts of the Spenser Range are permanently above ELA and carry small cirque glaciers. Large U-shaped valleys, moraines, ice overrun surfaces, and erratics indicate extensive late Pleistocene glaciations. Fresh glacial landforms are usually preserved in the upper valleys, while most middle and lower valley reaches are deeply incised displaying thick aggradational fills and spectacular flights of fluvial terraces.

The glacial sequence in the Waiau - Hope Valleys was first systematically investigated by Clayton (1968) who differentiated six Late Pleistocene episodes, which were subsequently correlated with major ice advances during OIS 8, OIS 6 and OIS 2 (Clayton, 1968, Suggate, 1990). The differentiation of glaciations in the valley was primarily based on the discrimination of glacial landform associations (i.e. moraine - outwash systems) which were found to be associated with distinct elevation levels in the valley. The model assumes that successively older glacial sequences are preserved at successively higher elevations in the valley due to rapid tectonic uplift throughout the Pleistocene. The process resulted in the vertical "stacking" of glacial sequences, an example of which will be inspected in the lower Hope Valley.

Lower Hope Valley

The valley reach constitutes a 4 km wide segment, which represents a medium sized tectonic depression along a releasing bend of the Hope Fault (Cowan, 1991). The area is critical for glaciation in the catchment as four of the six ice advances recognized have their 'type location' here (Fig. 52). Glacial surfaces are found over a wide range of elevations above the present river. LGM moraines and outwash are situated 160 m (610 m a.s.l.) above the present river, while the highest (and presumably oldest) glacial surface is located on Kakapo Hill 430 m (840 m a.s.l.) above the Hope River (Kakapo advance). Between these two advances an intermediate level of outwash is preserved at about 300 m (700 m a.s.l.) above river level (Horseshoe advance). As part of a more extensive study into the regional glacial geology, Rother (2006) investigated valley fill associated with the main aggradational terrace in the lower Hope Valley. In the following, two sites at Glynn Wye Station and Poplars Gully will be discussed in detail.

Stop 6-2. Glynn Wye

Depositional fill on the southern side of the Hope Valley is exposed in a spectacular outcrop at Glynn Wye station. The local fill sequence is 120 m thick and is directly overlain by a terminal moraine (Glynn Wye moraine, Fig. 53). Variation in clast lithology, colour and bedding orientation separates two well defined gravel units, which are visually distinct (Fig. 53C). A 55 m thick basal unit (G1) comprises 45 m of steeply dipping beds (~33º) with interbedded lacustrine silt, and an overlying 10-m unit of horizontally bedded gravels (Fig. 53D). Both gravel units are dark grey in colour and consist of mainly subangular argillite clasts (Ø 40-120 mm). The sequence is interpreted as a delta deposits comprising foreset and topset beds. Based on the thickness of the foreset deposit, the reconstructed Hope paleolake had a minimum water depth of 45 m.

A compositionally different gravel package (G2 gravels) consisting of ~65 m of well rounded coarse gravel overlies the delta deposit. Most of the clasts range between 150-250 mm in diameter. The lighter sediment colour (compared to underlying delta units) is due a high proportion of greywacke clasts. Several subunits of upwards coarsening gravels and some beds of sand and silt can be distinguished. G 2 gravels are interpreted as a fluvial sediment deposited by the aggrading Hope River. No evidence for significant erosional scouring at the contact between lacustrine (G1)

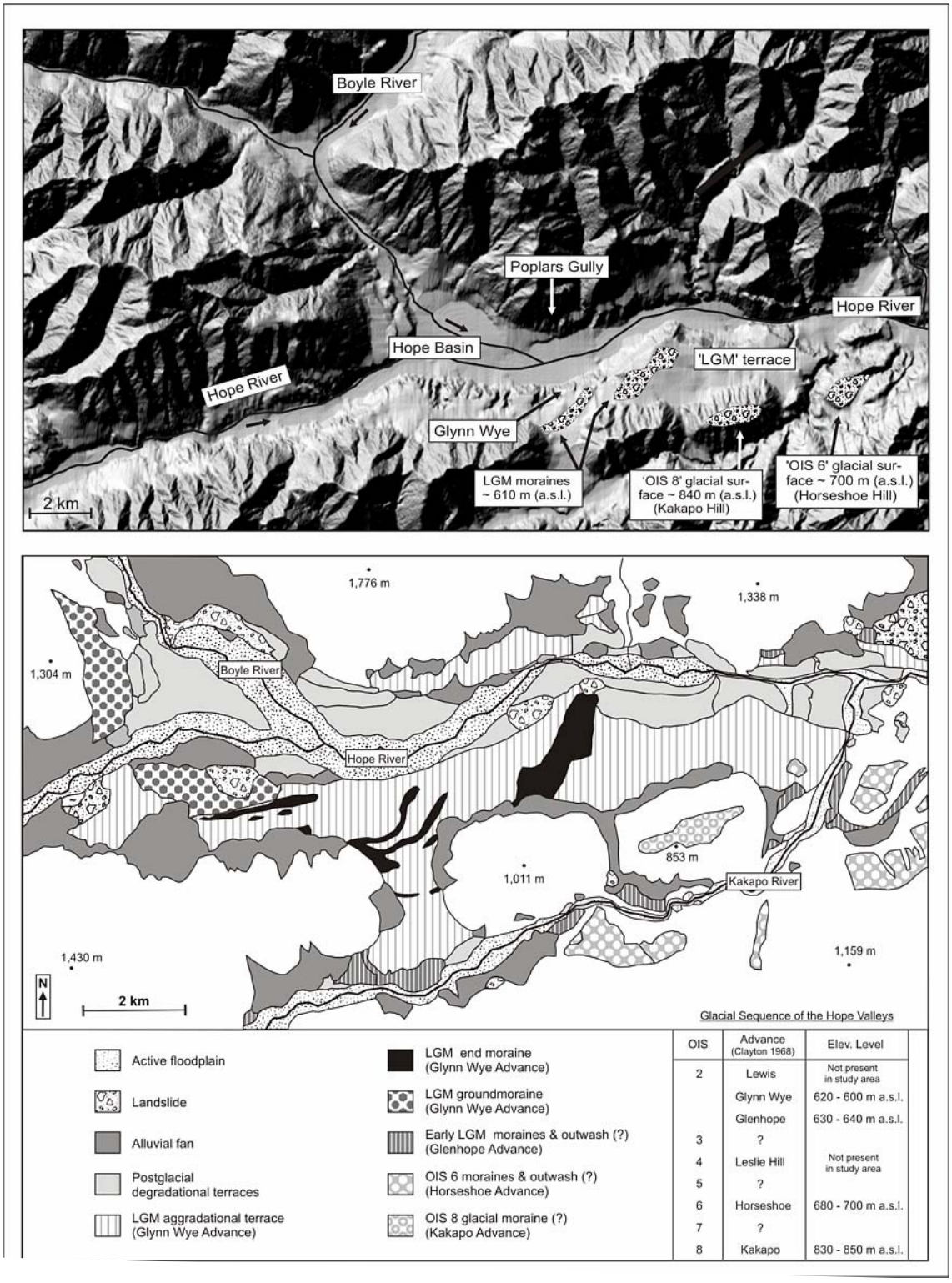

Fig. 52. DEM of the lower Hope Valley and Quaternary geology map (based on Clayton, 1968).

and fluvial (G2) units was found and we suggest that the contact is depositional in nature. This is supported by the completeness of the underlying delta sequence, which includes the fully preserved topset beds.

The lithological difference between the deltaic and fluvial gravels (dominance of argillite vs greywacke lithologies) indicates separate source areas for both gravel sequences. In addition, variations in clast angularity suggests that the deltaic gravels (G1) were transported over a shorter distance than the well rounded overlying G2 gravels. Furthermore, the depositional orientation of the foreset beds (330 - 030˚) is inconsistent with the W-E drainage of the Hope River, which therefore cannot have deposited the delta. The most probable explanation is deposition from the south through Dismal Valley by the Kakapo River (Fig. 53A). This would also account for the subangularity of clasts in the delta beds as fluvial transport out of the Kakapo catchment into the Hope paleolake would not have exceeded 10 km.

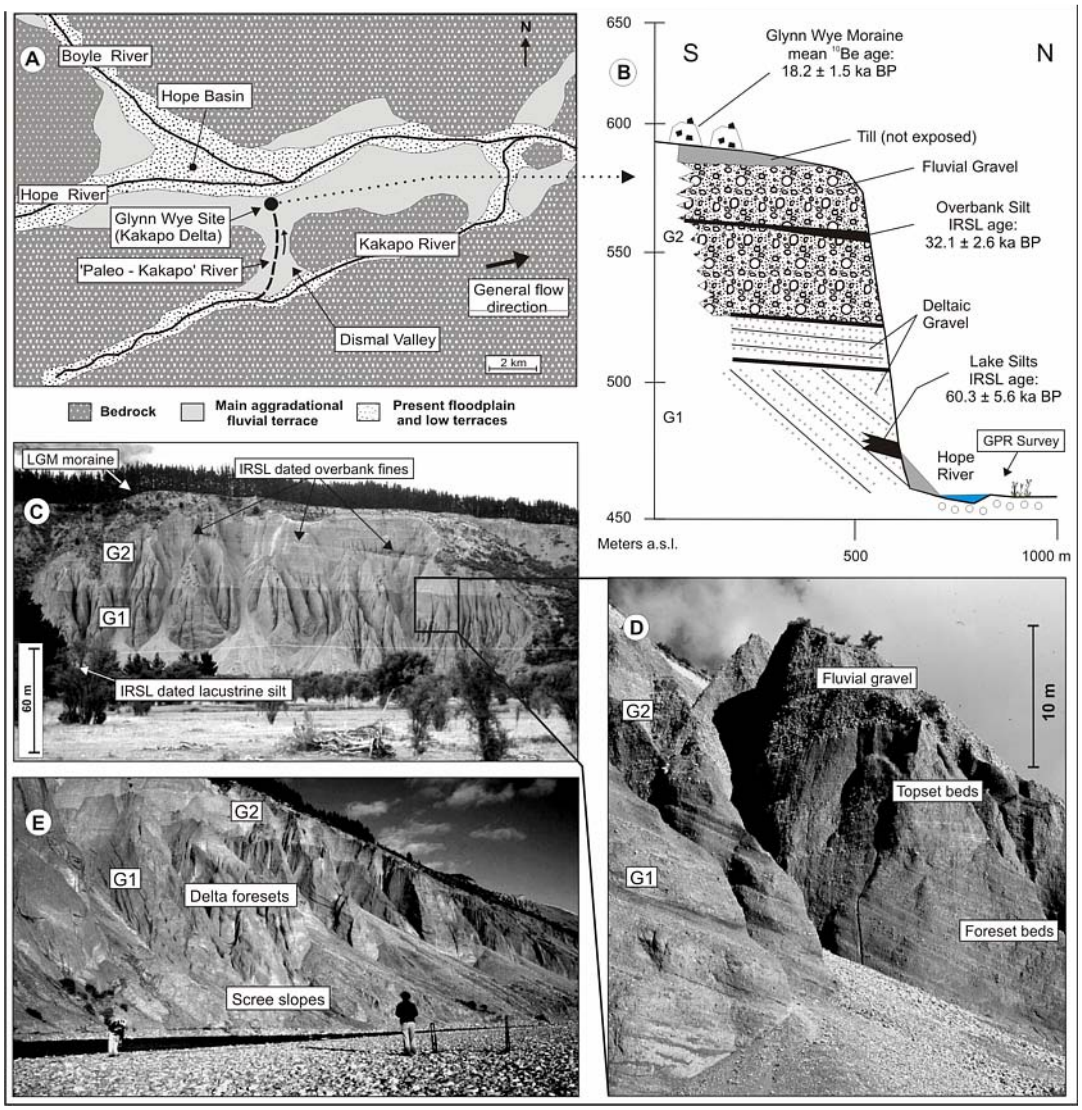

Fig 53: Location, context and stratigraphy of aggradational deposits at Glynn Wye Station

Age control for depositional events recorded in the Glynn Wye sequence is provided by two luminescence ages as well as four ^{10}Be exposure ages from the overlying moraine (Fig. 53B). Lacustrine silts interbedded with deltaic gravels at the base of the sequence yielded an age of 60.3 ± 5.6 ka BP, while a bed of overbank fines within the G2 fluvial gravels was dated to 32.1 ± 2.6 ka. Preliminary ^{10}Be exposure ages for the overlying moraine gave a mean age of 18.2 ± 1.5 ka. The results suggest that the Hope paleolake formed at the end of OIS 4. The lake terminated probably due to complete infilling and was buried under 65 m of fluvial gravels during OIS 3 before the progression of an LGM ice advance over the site. The outcrop is described and discussed in detail in Rother et al. (2007).

Stop 6-3. Poplars Gully

Poplars Gully is located directly opposite of Glynn Wye Station (see above) and exposes a portion of the same paired terrace on the northern side of the valley. The outcrop was produced by a landslide in October 1994, which left a gully complex that is c. 130 m wide, 120 m deep and about 200 m long. Because sediments at Poplars Gully are stratigraphically in the same position as deposits at Glynn Wye, a similar sedimentary sequence was expected. However, major differences were found and the complex stratigraphy of the section is summarized below.

Lithofacies descriptions and interpretations

Basal deposits (lithofacies A) at Poplars Gully comprise just under 6 m of laminated silt and sand overlain by 10 m of sand and gravel (lithofacies B; Fig. 54). The bedding in the fines is contorted with local mobilization of silt (flame structures). Interbedded with the silts are dropstones and a thin cobbly diamicton with impact structures in the surrounding fines. Small scale normal faults are pervasive throughout the fines, but are entirely contained within the unit. We interpret the laminated fines of facies A as a proglacial kettlehole deposit. This is based on the presence of dropstones, indicating the input of ice rafted debris, and the occurrence of normal faulting, which suggests the removal of volume in underlying deposits, probably through the melting of buried dead ice. All units of facies A and B dip uniformly (~18º to SSW), which is inconsistent with the original depositional angles. The likely explanation is postdepositional block rotation.

Facies C is a 7 m thick package of diamictons and gravel, which truncate and unconformably overlie facies A & B. In total six units of stratified and massive diamictons can be distinguished. We interpret the diamictons to represent a series of ice proximal mass flows and subglacial tills. Mass flows were identified based on their crude stratification, the incorporation of sediment lenses that show ductile deformation and a high orientational macro-fabric variability. Two stratified diamictons are interpreted as basal melt-out tills because of the draping of sediment bands over lodged clasts and the presence of intradiamict lenses of fluvial sand. Only one diamicton appears to have been deposited by actively moving ice. This massive unit was found near the base of facies C where it is associated with shear planes in the underlying sediment. The fabric signal suggests ice flow from SW. In summary, facies C provides evidence for an ice advance into the lower Hope Valley.

The diamictons are overlain by 23 m of clast and matrix supported gravels and cross stratified sands (facies D). Individual units comprise moderately to well sorted and conformably bedded gravel and sand sheets. Intense extensional deformation that resulted in the disruption of bedding and rotation of blocks is noted in the basal part of facies D. The overall assemblage is interpreted as glacio-fluvial outwash and represents the stratigraphic transition from till and mass flows (facies C) to collapsed ice proximal glacio fluvial gravels (basal facies D) to less deformed proglacial fluvial units of the middle and upper facies D. This is overlain by facies E, which comprises two units of stratified diamictons, laminated fines and clast supported gravel. The basal diamicton directly overlies a spectacular ~4 m high glacio-tectonic fold which incorporated strata of facies D and C. Orientational data obtained from the excavated fold limb as well as from nearby thrust planes suggest compression from W or WSW, respectively. This is broadly consistent with the measured fabric in the overlying diamicton indicating deposition from SW. The facies indicates an ice re-advance over the site

Above facies E are 44 m of alternating units of laminated and massive mud, which are interbedded with ripple cross-stratified sand (facies F). Dispersed stones with impact structures in underlying beds are present throughout the mud units. Facies F comprises mainly lacustrine sediments, which accumulated in a proglacial lake as is indicated by input of ice rafted debris. In the context of the ice re-advance indicated by the underlying facies E it is probable that the lake formed in front of the retreating ice margin and was dammed either by moraines or thick proglacial fan heads.

Deposits at Poplars Gully are capped by 14 m of alluvial and coarse fluvial gravels (facies G). The mature sorting and roundness of the boulders in the fluvial gravel suggest medium to long distance transport. This represents a depositional environment markedly different from all other sediments at Poplars Gully, which indicate mainly ice proximal and proglacial deposition. In addition, the fan and fluvial deposits of facies G are directly related to the terrace surface morphology. Lithologically very similar fan/fluvial gravels at equal elevation and identical stratigraphic position are found below the terrace surface on the southern side of the valley (Glynn Wye). Here a luminescence age of 32.1 ± 2.6 ka BP was obtained and a similar age for gravels of facies G is likely.

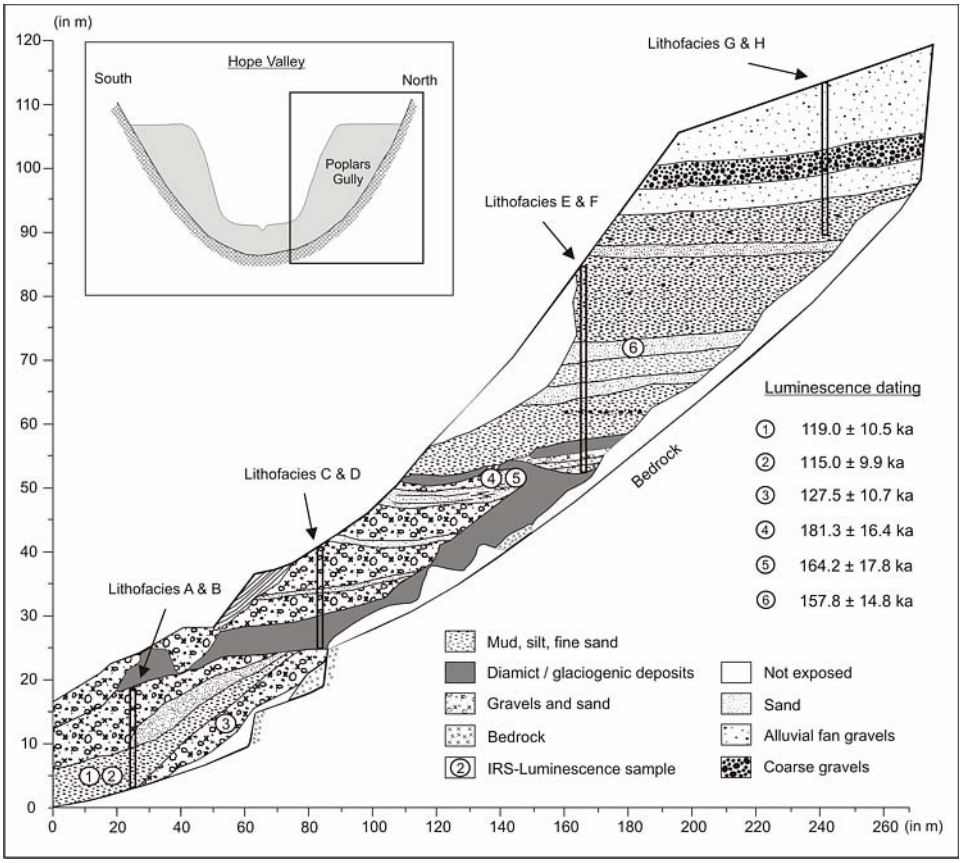

Fig 54.: Overview of deposits at Poplars Gully.

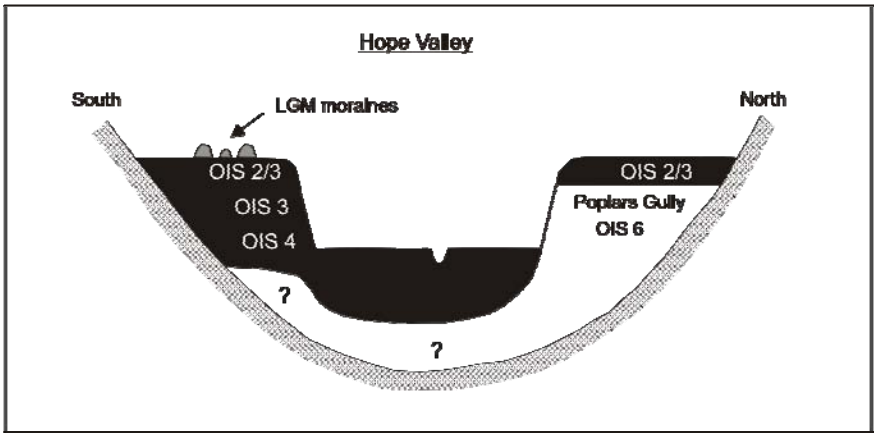

Fig 55. Schematic cross-section through fill deposits in the lower Hope Valley.

Luminescence dating results

Infrared stimulated luminescence (IRSL) samples from Poplars Gully were obtained from lacustrine and fluvial sands (sample positions in Fig. 53). The samples targeted three (A, D, F) stratigraphically widely spaced facies assemblages (65 m vertical distance between samples 1 and 6). Samples 2, 3, 4, and 6 were dated by a multiple aliquot additive-dose (MAAD) technique which uses feldspar crystals, whereas samples 1 and 5 where dated through a Single Aliquot Regenerative (SAR) technique which dates quartz crystals. The MAAD and SAR ages agree within error. Dating yielded six ages of 119.8 ± 10.5 ka (1), 115.0 ± 9.9 ka (2), 127.5 ± 10.7 ka (3), 181.3 ± 16.4 ka (4), 164.2 ± 17.4 ka (5), and 157.8 ± 14.8 ka (6). We note partial stratigraphic age reversals with the younger ages of samples 1, 2 and 3 below the older ages of samples 4, 5 and 6. All samples returned ages greater than 115 ka indicating that sediments at Poplars Gully were deposited during the OIS 6 glaciation.

Study results from valley fill in the lower Hope Valley show that deposits of the paired aggradational terrace from the southern (Glynn Wye) and northern (Poplars Gully) valley sides are stratigraphically and chronologically incompatible. We suggest that the fill succession in this part of the valley represents a composite structure of at least two valley fill generations (Fig. 55). We also note that pre-LGM and OIS 6 sediments constitute the dominant portion of the fill stratigraphy, which was unexpected in so far as that sizable LGM ice advances are documented to have reached and overrun the lower Hope Valley, yet the depositional volume associated with these advances is comparably small. This could be explained if local LGM advances were to have been largely erosive, but this can be ruled out based on the documented survival of thick older fill sequences, often stratigraphically below LGM deposits. Similarly, OIS 6 glaciers excavated a larger and deeper valley trough than is observed for advances during OIS 4 or the LGM, respectively. We suggest that local glacial advances during OIS 6 were considerably larger than those of the last glacial cycle.

From this last stop we will follow the Hope down valley to the Hanmer Basin near Hanmer Springs and then head through to Culverden. From here we head back through Weka Pass to the Waipara wine region and then follow the main highway back to Christchurch.

Acknowledgements

We are grateful to Shane Wilson for design of the INQUA 2007 NZ Glacial Field Tour logo; Amanda Clifford for help co-ordinating logistical aspects of the field tour; Bruce Smith of Hokitika for organising access to the Hokitika Airport Company quarry; and Andrew Birchfield of Ross for access to Birchfield's mine.

Appendix

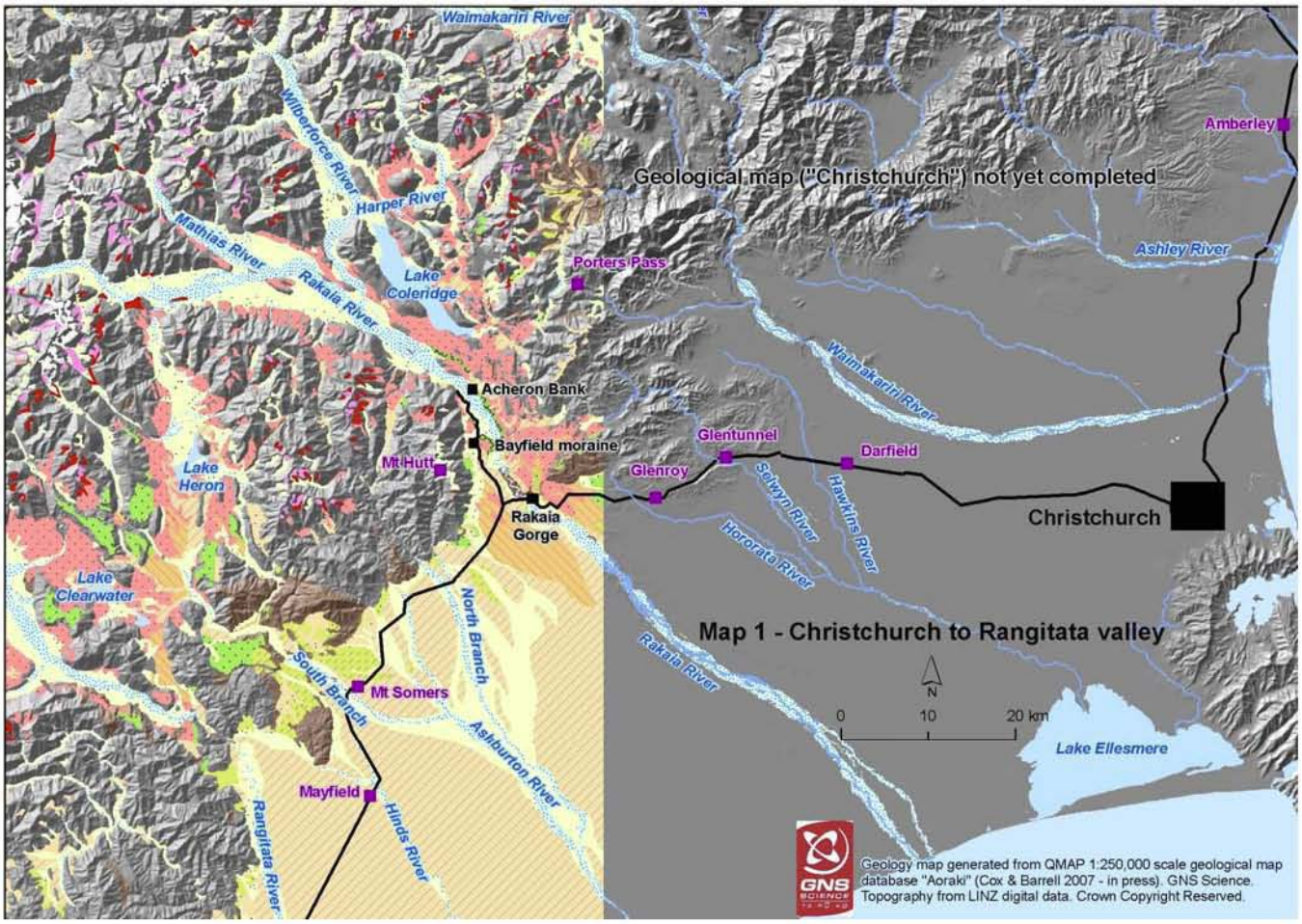

Key for maps

- Scheduled stop
- Feature of interest
- Trip route
- active floodplain
- ice
- water
- anthropogenic
- landslide
- Holocene alluvial fan or scree
- Holocene alluvium & beach deposits
- Holocene moraine
- Late-Glacial moraine
- LGM alluvial fan, scree or felsenmeer
- LGM alluvial deposits (late LGM outwash if differentiated)
- Early-mid LGM outwash (if differentiated)
- LGM moraine
- Pre-LGM lake or beach deposits
- Pre-LGM alluvial fan
- Pre-LGM alluvial deposits
- Pre-LGM moraine
- Cretaceous-Tertiary sedimentary & minor volcanic rocks
- Paleozoic - Mesozoic greywacke, schist, gneiss or granitoids

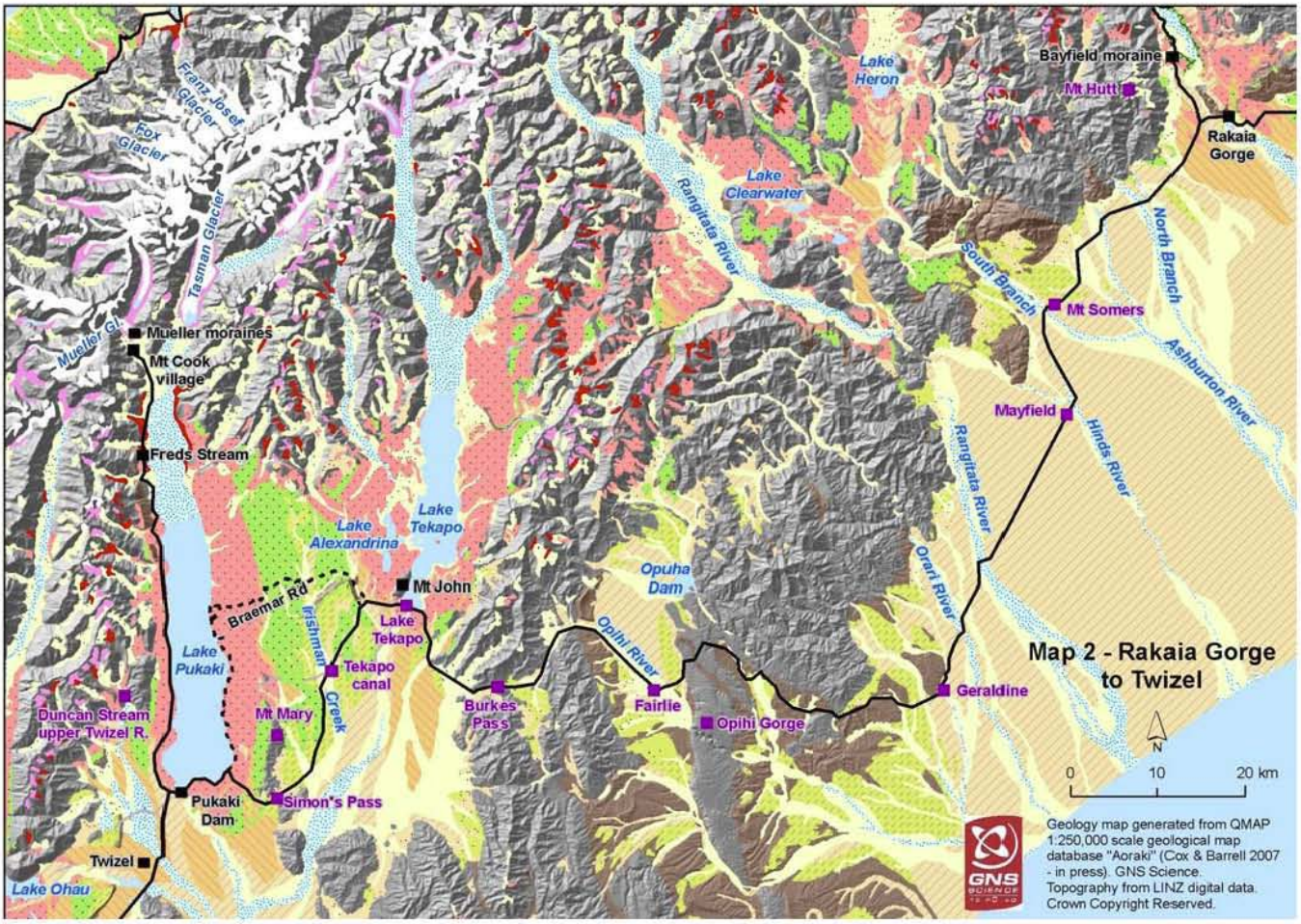
Map 2 - Rakaia Gorge to Twizel
Bayfield moraine
Mt Hutt
Rakaia Gorge
Lake Heron
Lake Clearwater
Rangitata River
South Branch
North Branch
Mt Somers
Ashburton River
Mayfield
Hinds River
Rangitata River
Orari River
Franz Josef Glacier
Fox Glacier
Tasman Glacier
Mueller Gl.
Mueller moraines
Mt Cook village
Freds Stream
Lake Alexandrina
Lake Tekapo
Opuha Dam
Mt John
Braemar Rd
Kirkman Creek
Lake Tekapo
Tekapo canal
Lake Pukaki
Opihi River
Duncan Stream upper Twizel R.
Mt Mary
Burkes Pass
Fairlie
Opihi Gorge
Geraldine
Pukaki Dam
Simon's Pass
Twizel
Lake Ohau
0
10
20 km
Geology map generated from QMAP 1:250,000 scale geological map database "Aoraki" (Cox & Barrell 2007 - in press). GNS Science. Topography from LINZ digital data. Crown Copyright Reserved.

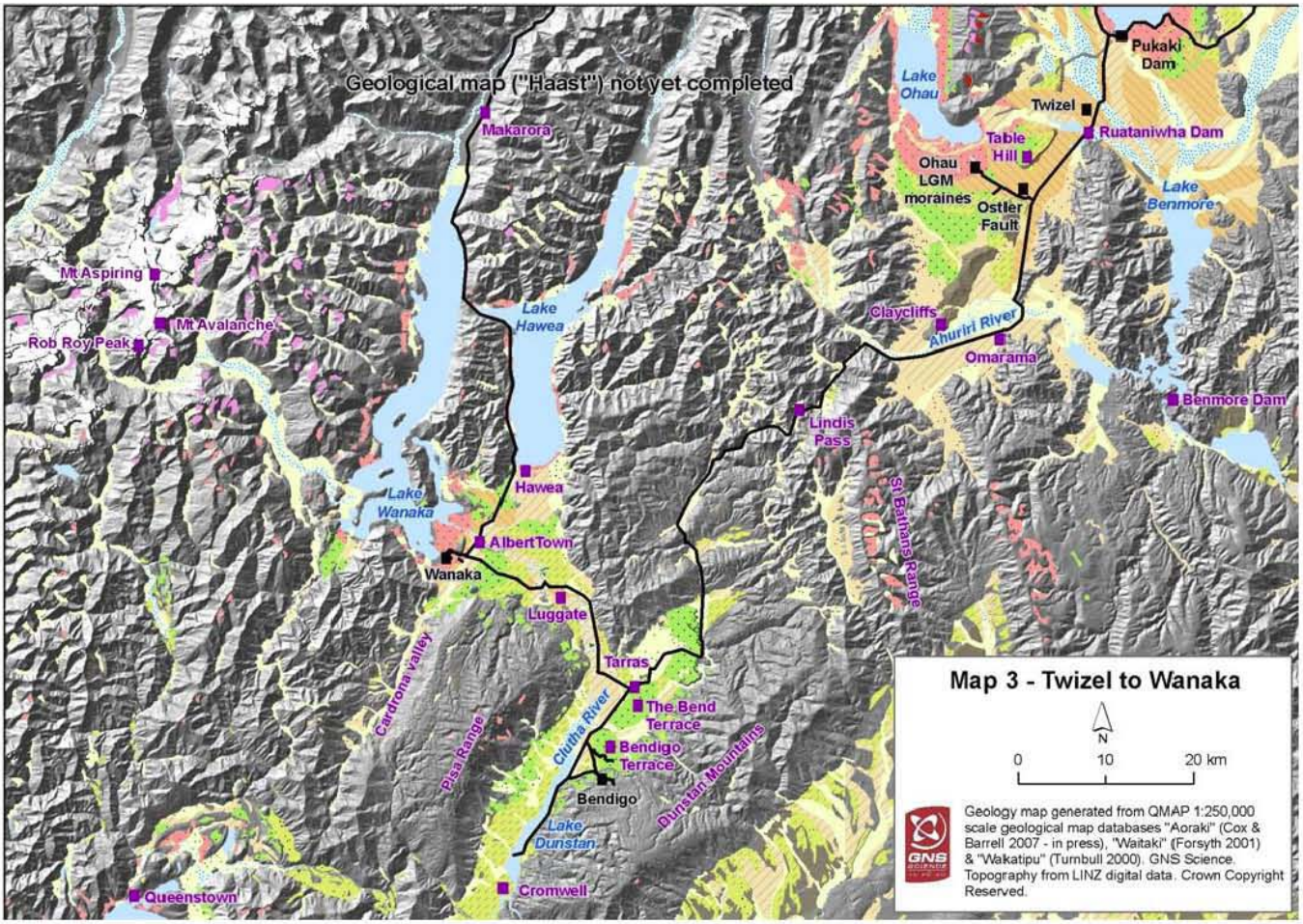
Geological map ("Haast") not yet completed
Map 3 - Twizel to Wanaka
Pukaki Dam
Lake Ohau
Twizel
Ruataniwha Dam
Table Hill
Ohau LGM moraines
Ostler Fault
Lake Benmore
Benmore Dam
Makarora
Mt Aspiring
Mt Avalanche
Rob Roy Peak
Lake Hawea
Clayclifts
Ahuriri River
Omarama
Lindis Pass
Hawea
Lake Wanaka
St Bathans Range
Albert Town
Wanaka
Luggate
Tarras
Cardrona valley
The Bend Terrace
Clutha River
Pisa Range
Bendigo Terrace
Bendigo
Dunstan Mountains
Lake Dunstan
Queenstown
Cromwell
0
10
20 km
Geology map generated from QMAP 1:250,000 scale geological map databases "Aoraki" (Cox & Barrell 2007 - in press), "Waitaki" (Forsyth 2001) & "Wakatipu" (Turnbull 2000). GNS Science. Topography from LINZ digital data. Crown Copyright Reserved.

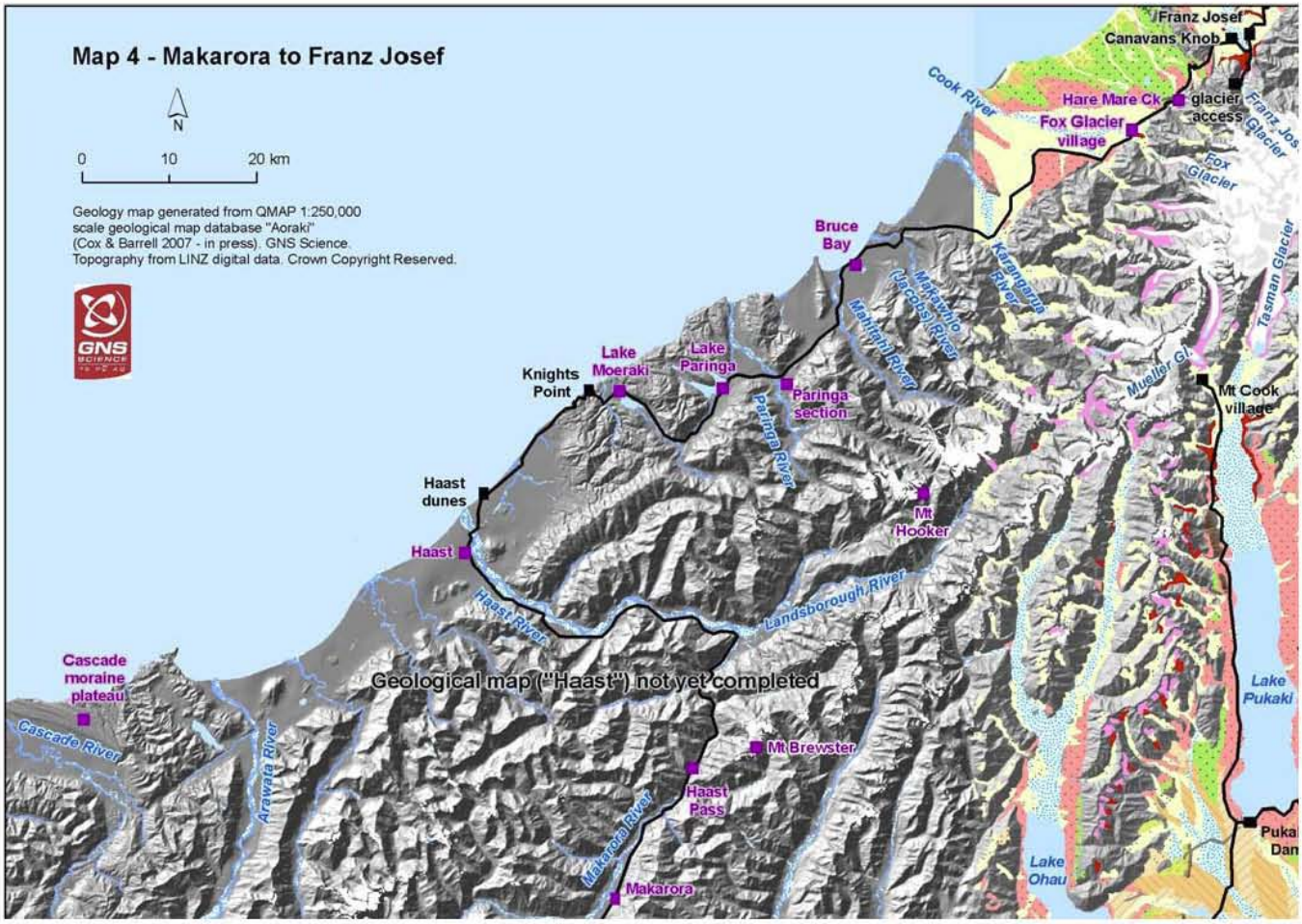
Map 4 - Makarora to Franz Josef
N
0
10
20 km
Geology map generated from QMAP 1:250,000
scale geological map database "Aoraki"
(Cox & Barrell 2007 - in press). GNS Science.
Topography from LINZ digital data. Crown Copyright Reserved.
GNS SCIENCE
Franz Josef
Canavans Knob
Cook River
Hare Mare Ck
glacier access
Fox Glacier village
Franz Josef Glacier
Fox Glacier
Bruce Bay
Karangarua River
Makawhio (Jacobs) River
Mahitahi River
Tasman Glacier
Lake Moeraki
Knights Point
Lake Paringa
Paringa section
Paringa River
Mueller Gl.
Mt Cook village
Haast dunes
Haast
Mt Hooker
Haast River
Landsborough River
Cascade moraine plateau
Cascade River
Arawata River
Geological map ("Haast") not yet completed
Lake Pukaki
Mt Brewster
Haast Pass
Makarora River
Makarora
Lake Ohau
Puka Dan

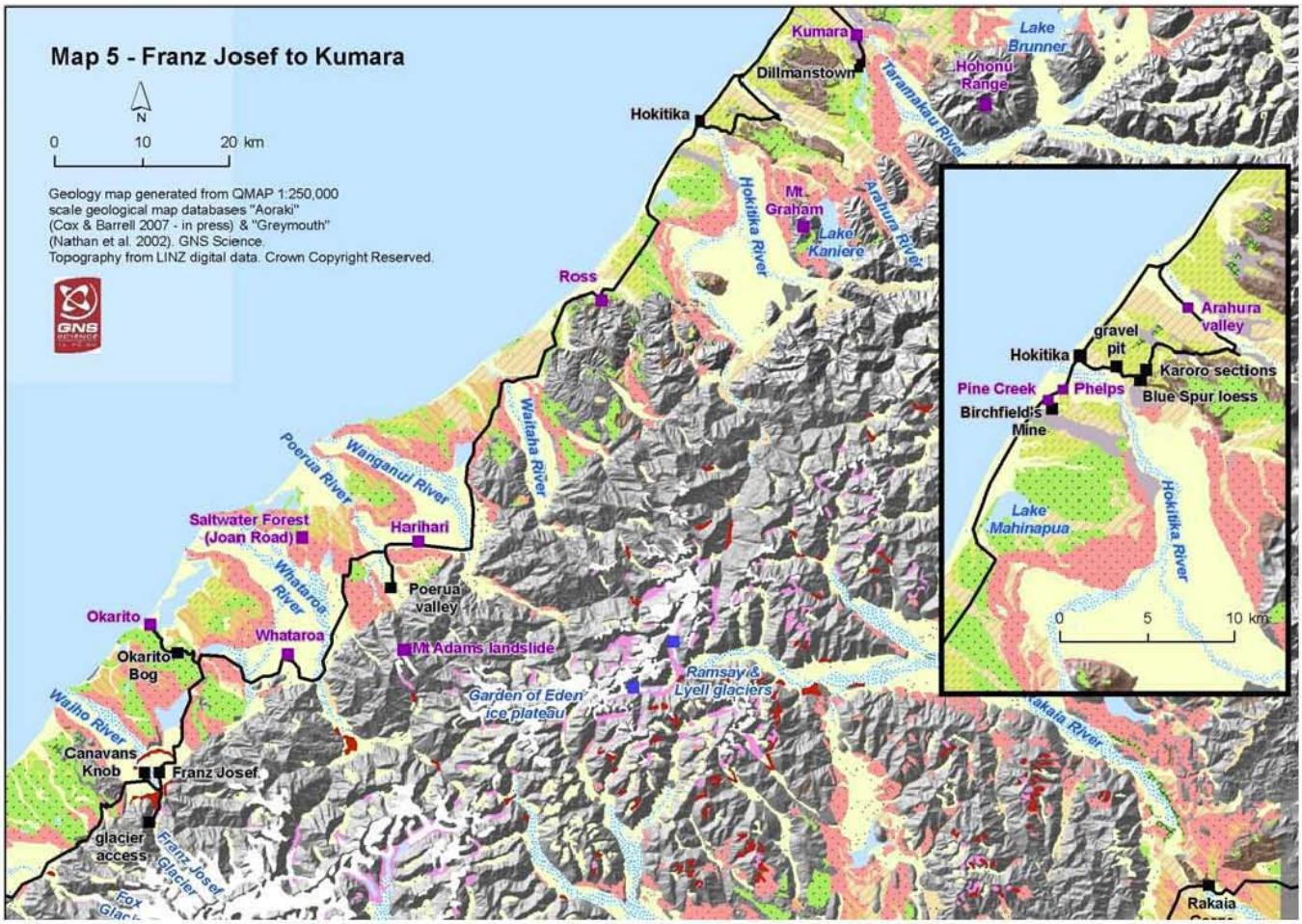
Map 5 - Franz Josef to Kumara
N
0
10
20 km
Geology map generated from QMAP 1:250,000
scale geological map databases "Aoraki"
(Cox & Barrell 2007 - in press) & "Greymouth"
(Nathan et al. 2002). GNS Science.
Topography from LINZ digital data. Crown Copyright Reserved.
GNS SCIENCE
Kumara
Lake Brunner
Dillmanstown
Hohonu Range
Taramakau River
Hokitika
Hokitika River
Mt Graham
Arahura River
Lake Kaniere
Ross
Arahura valley
gravel pit
Hokitika
Karoro sections
Pine Creek
Phelps
Blue Spur loess
Birchfields Mine
Lake Mahinapua
Hokitika River
0
5
10 km
Poerua River
Wanganui River
Waitaha River
Saltwater Forest (Joan Road)
Harihari
Whataroa River
Poerua valley
Okarito
Whataroa
Okarito Bog
Mt Adams landslide
Ramsay & Lyell glaciers
Garden of Eden ice plateau
Wahho River
Canavans Knob
Franz Josef
glacier access
Franz Josef Glacier
Fox Glacier
Rakaia River
Rakaia

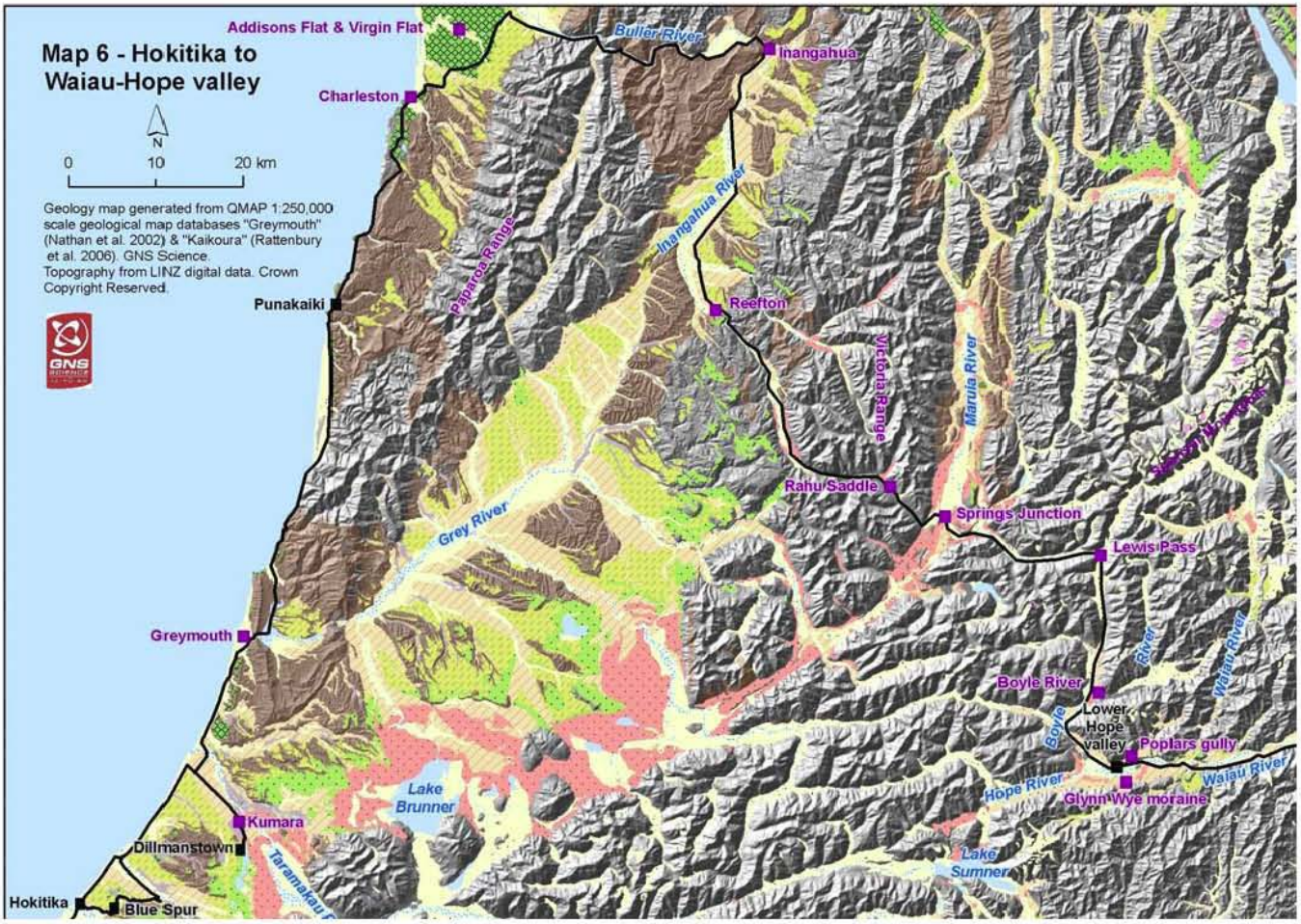
Map 6 - Hokitika to Waiau-Hope valley
N
0 10 20 km
Geology map generated from QMAP 1:250,000 scale geological map databases "Greymouth" (Nathan et al. 2002) & "Kaikoura" (Rattenbury et al. 2006). GNS Science. Topography from LINZ digital data. Crown Copyright Reserved.
Addisons Flat & Virgin Flat
Buller River
Inangahua
Charleston
Inangahua River
Paparoa Range
Punakaiki
Reefton
Victoria Range
Maruia River
Rahu Saddle
Springs Junction
Lewis Pass
Grey River
Greymouth
Boyle River
Lower Hope valley
Poplars gully
Waiau River
Hope River
Glynn Wye moraine
Lake Brunner
Kumara
Dillmanstown
Lake Sumner
Hokitika
Blue Spur

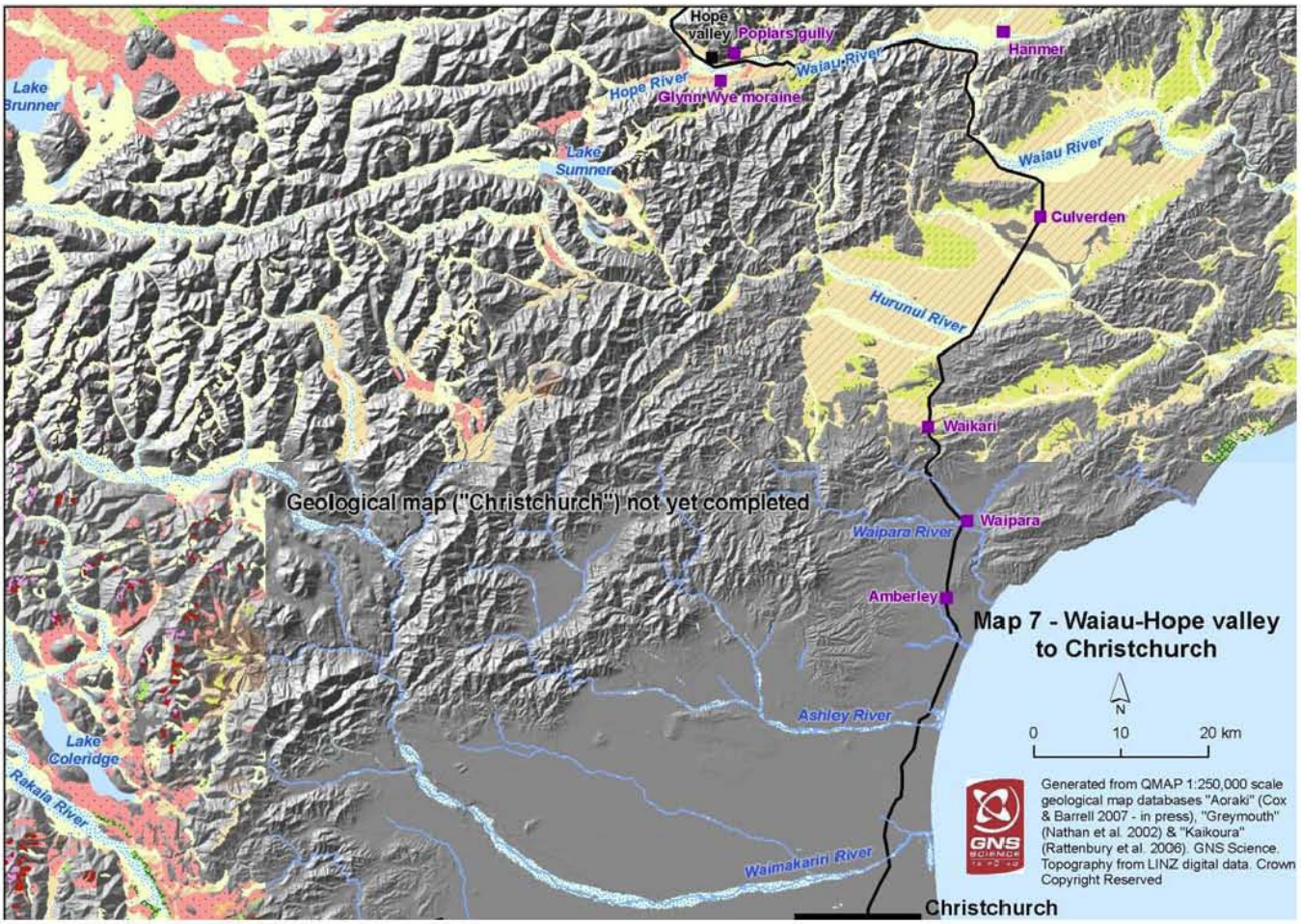
Hope valley
Poplars gully
Waiau River
Hanmer
Lake Brunner
Hope River
Glynn Wye moraine
Lake Sumner
Waiau River
Culverden
Hurunui River
Waikari
Geological map ("Christchurch") not yet completed
Waipara River
Waipara
Amberley
Map 7 - Waiau-Hope valley to Christchurch
N
0 10 20 km
Ashley River
Lake Coleridge
Rakaia River
Waimakariri River
Christchurch
Generated from QMAP 1:250,000 scale geological map databases "Aoraki" (Cox & Barrell 2007 - in press), "Greymouth" (Nathan et al. 2002) & "Kaikoura" (Rattenbury et al. 2006). GNS Science. Topography from LINZ digital data. Crown Copyright Reserved

References

Adams, J.A., 1980. Paleoseismicity of the Alpine Fault seismic gap, New Zealand. Geology, 8(2): 72-76

Alloway, B.V., Lowe, D.J., Barrell, D.J.A., Newnham, R.M., Almond, P.C., Augustinus, P.C., Bertler, N.A.N., Carter, L., Litchfield, N.J., McGlone, M.S., Shulmeister, J., Vandergoes, M.J., Williams, P.W. and members, N.Z.I., 2007. Towards a climate event stratigraphy for New Zealand over the past 30years (NZ-INTIMATE project). Journal of Quaternary Science, 22(1): 9-35.

Almond, P. C. (1996). "Loess, soil stratigraphy and Aokautere Ash on late Pleistocene surfaces in south Westland: interpretation and correlation with the glacial stratigraphy." Quaternary International 32/33: 163-176.

Almond, P.C., Moar, N.T. and Lian, O.B., 2001. Reinterpretation of the glacial chronology of South Westland, New Zealand. New Zealand Journal of Geology and Geophysics, 44: 1-15.

Anderson, B., Lawson, W., Owens, I. and Goodsell, B., 2006. Past and future mass balance of "Ka Roimata o Hine Hukatere" Franz Josef Glacier, New Zealand. Journal of Glaciology, 52(179): 597-607.

Anderson, B. and Mackintosh, A., 2006. Temperature change is the major driver of late-glacial and Holocene glacier fluctuations in New Zealand. Geology, 34(2): 121-124.

Barrell, D.J.A.; Forsyth, P.J.; McSaveney, M.J. 1996: Quaternary geology of the Rangitata fan, Canterbury Plains, New Zealand. Institute of Geological and Nuclear Sciences Science Report 96/23. 67 p.

Barrell D.J.A., Alloway B.V., Shulmeister J., Newnham R.M., (eds) 2005. Towards a climate event stratigraphy for New Zealand over the past 30,000 years. Institute of Geological and Nuclear Sciences Science Report SR2005/07 (includes large-format poster). Available at www.paleoclimate.org.nz.

Beanland, S., Berryman, K.R., 1989. Style and episodicity of late Quaternary activity on the Pisa-Grandview Fault Zone, Central Otago, New Zealand. New Zealand Journal of Geology and Geophysics 32: 451-461.

Benn, D.I., 1995. Subglacial and subaqueous processes near a grounding line: Sedimentological evidence from a former ice –damed lake, Achnasheen, Scotland. Boreas. 25(1): 23-36.

Berger, G.W., Tonkin, P.J., Pillans, B.J. 1996. Thermoluminescence ages of post-glacial loess, Rakaia River, South Island, New Zealand. Quaternary International 34-36: 177-181.

Berger, G.W., Almond, P.C. and Pillans, B.J., 2001. Luminescence dating and glacial stratigraphy in Westland, New Zealand. New Zealand Journal of Geology and Geophysics, 44(1): 25-35

Berger, G.W.; Pillans, B.J.; Tonkin, P.J. 2001: Luminescence chronology of loess-paleosol sequences from Canterbury, South Island, New Zealand. New Zealand Journal of Geology and Geophysics 44(4): 501-516.

Birkeland, P.W., 1982. Subdivision of Holocene glacial deposits, Ben Ohau Range, New Zealand, using relative-dating methods. Geological Society of America Bulletin 93: 433-449.

Blick, G.H., Read, S.A.L., Hall, P.T., 1989. Deformation monitoring of the Ostler fault zone, South Island, New Zealand. Tectonophysics 167: 329-339.

Brown, L.J. and Wilson, D.D. 1988. Stratigraphy of the late Quaternary deposits of the northern Canterbury Plains, New Zealand. New Zealand Journal of Geology and Geophysics 31:305-355.

Browne, G.H., Barrell, D.J.A., 2002. Gravel clast size variations in the Tasman River, Mt Cook, New Zealand. Institute of Geological and Nuclear Sciences science report 2002/12. Institute of Geological and Nuclear Sciences, Wellington, New Zealand.

Browne, G. and Naish, T. 2003. Facies development and sequence architecture of a late Quaternary fluvial marine transition. Sedimentary Geology 158:57-86.

Bull, W.B. and Cooper, A.F., 1986. Uplifted Marine Terraces Along the Alpine Fault, New Zealand. Science, 234(4781): 1225-1228.

Burge, P.I. and Shulmeister, J. 2007. Re-envisioning the structure of New Zealand vegetation during the last glaciation using beetle fossils. Quaternary Research 68: 121-132.

Burrows, C.J., 1989. Aranuian radiocarbon dates from moraines in the Mount Cook region. New Zealand Journal of Geology and Geophysics 32: 205-216.

Chappell, J. and Shackleton, N.J., 1986. Oxygen isotopes and sea level. Nature, 324: 137-140.

Clayton, L.S., 1968. Late Pleistocene glaciations of the Waiau Valleys, North Canterbury. New Zealand Journal of Geology and Geophysics 11: 753-767.

Cooper, A.F. and Norris, R.J., 1990. Estimates for the timing of the last coseismic displacement on the Alpine Fault, northern Fiordland, New Zealand. New Zealand Journal of Geology and Geophysics, 33: 303-307.

Cooper, A.F. and Kostro, F., 2006. A tectonically uplifted marine shoreline deposit, Knights Point, Westland, New Zealand. New Zealand Journal of Geology and Geophysics, 49: 203-216.

Cowan, H.A., 1991. The north Canterbury earthquake of September 1, 1888. Journal of the Royal Society of New Zealand 21(1): 1-12.

Cox, S.C.; Barrell, D.J.A. (compilers) in press 2007: Geology of the Aoraki area. GNS Science 1:250 000 geological map 15. Lower Hutt, New Zealand. Institute of Geological and Nuclear Sciences Limited.

Cullen, L.E., Duncan, R.P., Wells, A. and Stewart, G.H., 2003. Floodplain and regional scale variation in earthquake effects on forests, Westland, New Zealand. Journal of the Royal Society of New Zealand, 33(4): 693-701.

Davis, K., Burbank, D.W., Fisher, D., Wallace, S., Nobes, D., 2005. Thrust-fault growth and segment linkage in the active Ostler fault zone, New Zealand. Journal of Structural Geology 27: 1528-1546.

Davies, T. R. H. and O. Korup 2007. "Persistent alluvial fanhead trenching resulting from large, infrequent sediment inputs." Earth Surface Processes and Landforms 32(5): 725-742.

Denton, G.H. and Hendy, C.H., 1994. Younger Dryas age advance of Franz Josef glacier in the Southern Alps of New Zealand. Science, 264: 1434-1437.

Dickson, M., 1972. Palynology of a late Oturi interglacial and early Otira glacial sequence from Sunday Creek (S51), Westland, New Zealand. New Zealand Journal of Geology and Geophysics, 15(4): 590-598.

Forsyth, J., 2001. Geology of the Waitaki area. Institute of Geological and Nuclear Sciences 1:250 000 geological map 19, Lower Hutt, New Zealand, 1 sheet + 64 pp.

Gage, M., 1958. Late Pleistocene glaciations of the Waimakariri Valley, Canterbury, New Zealand., New Zealand Journal of Geology and Geophysics 1: 123-155.

Gellatly, A.F., 1984: The use of rock weathering rind thickness to re-date moraines in Mt Cook National Park, New Zealand. Arctic and Alpine Research 16: 225-232.

Gellatly, A.F., Chinn, T.J.H., Röthlisberger, F., 1988. Holocene glacier variations in New Zealand: a review. Quaternary Science Reviews 7: 227-242.

Grant-Taylor, T.L. and Rafter, T.A., 1971. New Zealand radiocarbon age measurements–6. New Zealand Journal of Geology and Geophysics, 14: 364–402.

Gregg, D.R., 1964. Geological Map of New Zealand, 1: 250 000, Sheet 18 – Hurunui, Department of Industrial and Scientific Research, Wellington.

Griffiths, G.A., 1979. High sediment yields from major rivers of the western Southern Alps, New Zealand. Nature, 282: 61-63.

Hancox, G. T., M. J. McSaveney, Manville, V.R. and Davies, T.R., 2005. The October 1999 Mt Adams rock avalanche and subsequent landslide dam-break flood and effects in Poerua Valley, Westland New Zealand. New Zealand Journal of Geology and Geophysics 48: 683-705.

Hart, J.K., 1996. Proglacial glaciotectonic deformation associated with glaciolacustrine sedimentation, Lake Pukaki, New Zealand. Journal of Quaternary Science 11: 149-160.

Henderson, R.D., Thompson, S.M., 1999. Extreme rainfalls in the Southern Alps of New Zealand. Journal of Hydrology (New Zealand) 38: 309-330.

Hochstein, M.P., Claridge, D., Henrys, S.A., Pyne, A., Nobes, D.C., Leary, S.F., 1995. Downwasting of the Tasman Glacier terminus, South Island, New Zealand: changes in the terminus region between 1971 and 1993. New Zealand Journal of Geology and Geophysics 38: 1-16.

Hooker, B.L. and Fitzharris, B.B., 1999. The correlation between climatic parameters and the retreat and advance of Franz Josef Glacier, New Zealand. Global and Planetary Change, 22(1-4): 39-48.

Hovius, N., Stark, C.P. and Allen, P.A., 1997. Sediment flux from a mountain belt derived by landslide mapping. Geology, 25(3): 231-234.

Irwin, J., Pickrill, R.A., 1983. Sedimentation in glacial-fed natural lakes: implications for hydro-electric storage lakes. Transactions of the Institution of Professional Engineers of New Zealand 10: 84-92.

Kirkbride, M.P. 1993. The temporal significance of transitions from melting to calving termini of glaciers in central Southern Alps. The Holocene 3:232-240.

Kirkbride, M.P. and Warren, C.R. 1999. Tasman Glacier, New Zealand; 20th-century thinning and predicted calving retreat. Global and Planetary Change 22:11-28.

Langdale, S.; Stern, T.A. 1998: Late Tertiary deformation in Cannington Basin, South Canterbury, New Zealand: evidence from seismic and gravity data. New Zealand Journal of Geology and Geophysics 41 (3): 247-257.

Leckie, D.A. 1994: Canterbury Plains, New Zealand: implications for sequence stratigraphic models. American Association of Petroleum Geologists Bulletin 78(8): 1240-1256.

Lowell, T.V., Heusser, C.J., Andersen, B.G., Moreno, P.I., Hauser, A., Denton, G.H., Heusser, L.E., Schluchter, C., Marchant, D.R., 1995. Interhemispheric symmetry of paleoclimatic events during the last glaciation. Science 269, 1541–1544.

Lowell, T.V., Schoenenberger, K. Deddens, J.A., Denton, G.H., Smith, C., Black, J., Hendy, C.H. 2005. Rhizocarpon calibration curve for the Aoraki/Mount Cook area of New Zealand. Journal of Quaternary Science 20: 313-325.

Mabin, M.C.G. 1980: The glacial sequences in the Rangitata and Ashburton valleys, South Island, New Zealand. Ph.D thesis, University of Canterbury, Christchurch.

Mabin, M.C.G. 1984: Late Pleistocene glacial sequence in the Lake Heron basin, mid Canterbury. New Zealand Journal of Geology and Geophysics 27(2): 191-202.

Mabin, M.C.G. 1995. Age of the Waiho Loop glacial event: Comment. Science, 271:868.

Maizels, J.K. 1989: Differentiation of late Pleistocene terrace outwash deposits using geomorphic criteria: Tekapo valley, South Island, New Zealand. New Zealand Journal of Geology and Geophysics 32: 225-242.

Mager, S., Fitzsimons, S., 2007. Formation of glaciolacustrine Late Pleistocene end moraines in the Tasman Valley, New Zealand. Quaternary Science Reviews 26: 743-758

Mansergh, G.D., Read, S.A.L., 1973. The Ostler Fault Zone (S109) – Ground movement near the Ohau A powerhouse site. Unpublished New Zealand Geological Survey engineering geology report EG151.

McGlone, M.S., 1996. Lateglacial landscape and vegetation change and the Younger Dryas climatic oscillation in New Zealand. Quaternary Science Reviews 14: 867-881.

McGlone, M.S., Moar, N.T., 1998. Dryland Holocene vegetation history, Central Otago and the Mackenzie Basin, South Island, New Zealand. New Zealand Journal of Botany 36: 91-111.

McKellar, I.C., 1960. Pleistocene deposits of the upper Clutha valley, Otago, New Zealand. New Zealand Journal of Geology and Geophysics 3: 432-460.

McSaveney, M.J., Thomson, R., Turnbull, I.M., 1992. Timing of relief and large landslides in central Otago. Pp. 1451-1456 in Bell, D.H. ed: Sixth international symposium on large landslides, Christchurch. Landslides glissements de terrain.

Rotterdam, Balkema.

Mercer, J.H. 1988. The age of the Waiho Loop terminal moraine, Franz Josef Glacier, Westland. New Zealand Journal of Geology and Geophysics. 31: 95-100.

Mew, G., 1983. Applications of the term 'pakihi' in New Zealand—a review. Journal of the Royal Society of New Zealand 13, 175–198.

`MfE 2003: Planning for Development of Land assist resource management planners in New Zealand. Ministry for the Environment, July 2003. (http:// www.mfe.govt.nz/publications/rma/active-faults-jul03/index.html)

Moar, N.T. and Suggate, R.P., 1973. Pollen analysis of late Otiran and Aranuian sediments at Blue Spur Road, (S51), North Westland. New Zealand Journal of Geology and Geophysics, 16(3): 333-344.

Moar, N. T. & Suggate, R. P., 1979. Contributions to the Quaternary history of the New Zealand flora 8. Interglacial and glacial vegetation in the Westport District, South Island. New Zealand Journal of Botany 17, 361-387.

Moar, N.T., 1980. Late Otiran and early Aranuian grassland in central South Island. New Zealand Journal of Ecology 3: 4-14.

Moar, N.T. and Suggate, R.P., 1996. Vegetation history from the Kaihinu (Last) Interglacial to the present, West Coast, South Island, New Zealand. Quaternary Science Reviews, 15: 521-547.

Nathan, S., Rattenbury, M.S. and Suggate, R.P., 2002. Geology of the Greymouth area. Institute of Geological and Nuclear Sciences 1:250 000 geological map 12, Lower Hutt, New Zealand, 1 sheet + 58 pp.

Newnham, R.M. and Lowe, D.J., 2000. Fine-resolution pollen record of late-glacial climate reversal from New Zealand. Geology, 28(8): 759-762.

Newnham R.M., Vandergoes M.J., Hendy C.H., Lowe D.J., Preusser F. 2007. A terrestrial palynological record for the last two glacial cycles from southwestern New Zealand. Quaternary Science Reviews 26: 517-535.

Norris, R.J., Cooper, A.F., 2001. Late Quaternary slip rates and slip partitioning on the Alpine Fault, New Zealand. Journal of Structural Geology 23: 507–520.

Oliver, P.J.; Keene, H.W. 1990: Clearwater - Sheet J36 BD and part Sheet J35. Geological Map of New Zealand 1:50,000. Wellington, Department of Scientific and Industrial Research.

Porter, S.C., 1975. Equilibrium-line altitudes of late Quaternary glaciers in the Southern Alps, New Zealand. Quaternary Research 5: 27-47.

Porter, S.C., 2000. Onset of Neoglaciation in the Southern Hemisphere. Journal of Quaternary Science 15: 95-408.

Preusser, F., Andersen, B.G., Denton, G.H. and Schluchter, C., 2005. Luminescence chronology of Late Pleistocene glacial deposits in North Westland, New Zealand. Quaternary Science Reviews, 24(20-21): 2207-2227.

Rattenbury, M.S., Townsend, D.B. and Johnston, M.R., 2006. Geology of the Kaikoura area. Institute of Geological and Nuclear Sciences 1:250 000 geological map 13, Lower Hutt, New Zealand, 1 sheet + 70 pp.

Read, S.A.L., 1976. Upper Waitaki Power Development Scheme. Pukaki Lake Control. Engineering geological completion report. Unpublished New Zealand Geological Survey Engineering Geology report EG276.

Read, S.A.L. 1984: The Ostler Fault Zone. In P.R. Wood (compiler): Guidebook to the South Island Scientific Excursions (Part 2: Greymouth to Christchurch). International Symposium on Recent Crustal Movements of the Pacific Region (Wellington, NZ, February 1984). Royal Society of New Zealand Miscellaneous Series 9: 121-134.

Richardson, S.J., Peltzer, D.A., Allen, R.B., Mcglone, M.S. and Parfitt, R.L., 2004. Rapid Development of Phosphorus Limitation in Temperate Rainforest Along the Franz Josef Soil Chronosequence. Oecologia. 139(2): 267276.

Roehl, K. 2003. Thermal regime of an ice-contact lake and its implication for glacier retreat. Ice in the Environment: Proceedings of the 16th IAHR International Symposium on Ice, Dunedin, New Zealand, 2–6 December 2002. 304–312.

Roehl, K. 2005. Behaviour of lake-terminating glacier margins. Unpublished PhD thesis, in Geography, at the University of Otago, New Zealand. 390 pp.

Rother, H., Late Pleistocene glacial geology of the Hope-Waiau valley system in North Canterbury, New Zealand. Unpublished Ph.D. thesis, University of Canterbury, New Zealand, 344p.

Rother, H. and J. Shulmeister. 2006. Synoptic climate change as a driver of late Quaternary glaciations in the mid-latitudes of the Southern Hemisphere. Climate of the Past 2:11-19. 1814-9359/cpd/2005-1-1.

Rother, H. Jol, H.M. and J. Shulmeister. 2007. Tectonic and climatic implications of Late Pleistocene valley fill in the lower Hope Valley, Canterbury, South Island, New Zealand. in: Baker, G.S., Jol, H.M., (Ed.) Stratigraphic analyses using ground penetrating radar (GPR), *Geological Society of America Special Paper* 432 : xxx-xxx, doi: 10.1130/2007.2432(11).

Ross, C.W., Mew, G. and Searle, P.L., 1977. Soil sequences on two terrace systems in north Westland area, New Zealand. New Zealand Journal of Science, 20: 231-244.

Schaefer, J.M., Denton, G.H., Barrell, D.J.A., Ivy-Ochs, S., Kubik, P.W., Andersen, B.G., Phillips, F.M., Lowell, T.V., Schlüchter, C., 2006. Near-synchronous interhemispheric termination of the Last Glacial Maximum in mid-latitudes. Science 312: 1510-1513.

Shulmeister, J., Goodwin, I., Renwick, J., Harle, K., Armand, L., McGlone, M.S., Cook, E., Dodson, J., Hesse, P.P., Mayewski, P. and Curran, M., 2004. The Southern Hemisphere westerlies in the Australasian sector over the last glacial cycle: a synthesis. Quaternary International, 118-119: 23-53.

Shulmeister, J., Fink, D. and Augustinus, P.C. 2005. A cosmogenic nuclide chronology of the last glacial transition in North-West Nelson, New Zealand - new insights in Southern Hemisphere climate

forcing during the last deglaciation. Earth and Planetary Science Letters. 233:455-466.

Smith, S.M. and Lee, W.G., 1984. Vegetation and soil development on a Holocene river terrace sequence, Arawata Valley, south Westland, New Zealand. New Zealand Journal of Science, 27: 187-196.

Soil Survey Staff, 1999. Soil taxonomy : a basic system of soil classification for making and interpreting soil surveys, 2nd Edition. U.S. Dept. of Agriculture Natural Resources Conservation Service, Washington, DC, 869 pp.

Soons, J.M. 1963. The glacial sequence in part of the Rakaia Valley, Canterbury, New Zealand. New Zealand Journal of Geology and Geophysics, 6:735-756.

Soons, J.M and Gullentops, F.W. 1973. Glacial advances in the Rakaia Valley, New Zealand. New Zealand Journal of Geology and Geophysics, 16:425-438.

Soons, J.M. and Selby, M.J., 1982. Landforms of New Zealand. Longman Paul, Auckland, N.Z., ISBN 0582717868 (pbk.), x, 392 p. pp.

Sowden, J.R., 1986. Plant succession and soil development, Wanganui River catchment, South Westland, New Zealand : a thesis submitted in fulfilment of the requirements for the degree of Master of Applied Science in the University of Canterbury [Lincoln College]. M Appl Sc Thesis, University of Canterbury, 1986., 266 pp.

Speight, J.G., 1963. Late Pleistocene historical geomorphology of the Lake Pukaki area, New Zealand. New Zealand Journal of Geology and Geophysics 6: 160-188.

Stevens, P.R., 1963. A chronosequence of soils and vegetation near the Franz Josef Glacier : a thesis submitted in partial fulfilment of the requirements for the degree of Master of Agricultural Science with Honours in the University of Canterbury [Lincoln College]. M Agr Sc (Hons) Thesis, University of Canterbury, 1963., 143 pp.

Stevens, P.R., 1968a. A chronosequence of soils near Franz Josef glacier. Unpubl. PhD Thesis, Lincoln College, University of Canterbury, New Zealand.

Stevens, P.R., 1968b. A chronosequence of soils near the Franz Josef Glacier : a thesis submitted in partial fulfilment of the requirements for the degree of Doctor of Philosophy in the University of Canterbury. Ph D Thesis, Lincoln College, 1968., 2 v. 389 pp.

Suggate, R.P. 1963: The fan surfaces of the central Canterbury Plain. New Zealand Journal of Geology and Geophysics 6(2): 281-287.

Suggate, R.P. 1965: Late Pleistocene geology of the northern part of the South Island, New Zealand. New Zealand Geological Survey Bulletin 77. 91 p.

Suggate, R.P. 1973: Sheet 21 – Christchurch. 2nd Edition. Geological Map of New Zealand 1:250 000. Wellington, Department of Scientific and Industrial Research.

Suggate, R.P., 1987. Active folding in north Westland, New Zealand. New Zealand Journal of Geology and Geophysics, 30: 169-174.

Suggate, R.P., 1989. The postglacial shorelines and tectonic development of the Barrytown coastal lowland, North Westland, New Zealand. New Zealand Journal of Geology and Geophysics, 32(4): 443-450.

Suggate, R.P., 1990. Late Pliocene and Quaternary glaciations of New Zealand. Quaternary Science Reviews 9: 175-197.

Suggate, R.P. and Waight, T.E., 1999. Geology of the Kumara-Moana Area. Institute of Geological and Nuclear Sciences Geological Map 24 (1:50,000), Lower Hutt, New Zealand, 1 map plus 124 pp.

Suggate, R.P. and Almond, P.C., 2005. The Last Glacial Maximum (LGM) in western South Island, New Zealand: implications for the global LGM and MIS 2. Quaternary Science Reviews, 24(16-17): 1923-1940.

Sutherland, R. and Norris, R., 1995. Late Quaternary displacement rate, paleoseismicity, and geomorphic evolution of the Alpine Fault: evidence from Hokuri Creek, South Westland, New Zealand. New Zealand Journal of Geology and Geophysics. 38(8): 419-430.

Sutherland, R., Kim, K., Zondervan, A. and McSaveney, M., 2007. Orbital forcing of mid-latitude Southern Hemisphere glaciation since 100 ka inferred from cosmogenic nuclide ages of moraine boulders from the Cascade Plateau, southwest New Zealand. Geological Society of America Bulletin, 119(3): 443-451.

Tonkin, P.J. and Basher, L.R., 1990. Soil stratigraphic techniques in the study of soil and landform evolution across the Southern Alps, New Zealand. Geomorphology, 3: 547-575.

Turnbull, I.M. (compiler), 2000. Geology of the Wakatipu area. Institute of Geological and Nuclear Sciences 1:250 000 geological map 18. Lower Hutt, Institute of Geological and Nuclear Sciences Ltd. 1 sheet + 72 p.

Turney, C.S.M., McGlone, M.S. and Wilmshurst, J.M., 2003. Asynchronous climate change between New Zealand and the North Atlantic during the last deglaciation. Geology, 31(3): 223-226.

Vandergoes, M.J., Newnham, R.M., Preusser, F., Hendy, C.H., Lowell, T.V., Fitzsimons, S.J., Hogg, A.G., Kasper, H.U. and Schluchter, C., 2005. Regional insolation forcing of late Quaternary climate change in the Southern Hemisphere. Nature, 436(7048): 242-245.

Van Dissen, R.J., Hull, A.G., Read, S.A.L., 1993. Timing of some large Holocene earthquakes on the Ostler Fault, New Zealand. In Proceedings of the Eighth International Symposium on Recent Crustal Movements (CRCM '93), December 6-11 1993, Kobe, Japan. Pp. 381-386.

Van Dissen, R.J., Berryman, K.R., Webb, T.H., Stirling, M.W., Villamor, P., Wood, P.R., Nathan, S., Nicol, A., Begg, J.G., Barrell, D.J.A., McVerry, G.H., Langridge, R.M., Litchfield, N.J., Pace, B., 2003a. An interim classification of New Zealand's active faults for the mitigation of surface rupture hazard. 8 p. In: Proceedings of the 2003 Pacific Conference on Earthquake Engineering, 13-15 February 2003, Christchurch, New Zealand. New Zealand Society for Earthquake Engineering.

Van Dissen, R.J., Wood, P.R., Berryman, K.R., Nathan, S., 2003b. Illustrations of historic and pre-historic surface rupture of active faults in New Zealand. 8 p.

In: Proceedings of the 2003 Pacific Conference on Earthquake Engineering, 13-15 February 2003, Christchurch, New Zealand. New Zealand Society for Earthquake Engineering.

Walker, T.W. and Syers, J.K., 1976. The fate of phosphorous during pedogenesis. Geoderma, 15: 1-19.

Warren, C.R. and Kirkbride, M.P. 1998. Temperature and bathymetry of ice-contact lakes in Mount Cook National Park, New Zealand. NZ Journal of Geology and Geophysics 41: 133-143.

Ward, C., 1988. New Zealand marine terraces: uplift rate (comment). Science, 240: 803-804.

Wardle, P., 1973. Variations of the glaciers of Westland National Park and the Hooker Range, New Zealand. New Zealand Journal of Botany, 11: 349-388.

Wardle, P., 1980. Primary succession in Westland National Park and its vicinity, New Zealand. New Zealand Journal of Botany, 18: 221-232.

Wellman, H.W., Wilson, A.T., 1964. Notes on the geology and archaeology of the Martins Bay District. New Zealand Journal of Geology and Geophysics 7: 702–721.

Wells, A., Duncan, R.P. and Stewart, G.H., 2001. Forest dynamics in Westland, New Zealand: the importance of large, infrequent earthquake-induced disturbance. Journal of Ecology, 89(6): 1006-1018.

Wells, A. and Goff, J., 2006. Coastal dune ridge systems as chronological markers of palaeoseismic activity: a 650-yr record from southwest New Zealand. The Holocene, 16(4): 543-550.

Wells, A., Stewart, G.H. and Duncan, R.P., 1998. Evidence of widespread, synchronous, disturbance-initiated establishment in New Zealand. Journal of the Royal Society of New Zealand, 28(2): 333-345.

Williams, P.A., Courtney, S., Glenny, D., Hall, G., Mew, G., 1990. Pakihi and surrounding vegetation in North Westland, South Island. Journal of the Royal Society of New Zealand 20, 179–203.

Wilson, D.D. 1989: Quaternary geology of the northwestern Canterbury Plains - Sheet L35 and part Sheets L36, M35 and M36. New Zealand Geological Survey miscellaneous series map 14, 1:100 000. Wellington, Department of Scientific and Industrial Research.

Winkler, S., 2000. The ‘Little Ice Age’ maximum in the Southern Alps: preliminary results at Mueller Glacier. The Holocene 10: 643-647.

Winkler, S., 2004. Lichenometric dating of the ‘Little Ice Age’ maximum in Mt Cook National Park, Southern Alps, New Zealand. The Holocene 14: 911-920.

Yetton, M.D., Wells, A. and Traylen, N.J., 1998. Probability and consequences of the next Alpine Fault earthquake. EQC Research Report 95/193, New Zealand, 161 pp.